

IAEA HUMAN HEALTH SERIES

No. 41

Clinical Applications of SPECT-CT



IAEA
International Atomic Energy Agency

IAEA HUMAN HEALTH SERIES PUBLICATIONS

The mandate of the IAEA human health programme originates from Article II of its Statute, which states that the “Agency shall seek to accelerate and enlarge the contribution of atomic energy to peace, health and prosperity throughout the world”. The main objective of the human health programme is to enhance the capabilities of IAEA Member States in addressing issues related to the prevention, diagnosis and treatment of health problems through the development and application of nuclear techniques, within a framework of quality assurance.

Publications in the IAEA Human Health Series provide information in the areas of: radiation medicine, including diagnostic radiology, diagnostic and therapeutic nuclear medicine, and radiation therapy; dosimetry and medical radiation physics; and stable isotope techniques and other nuclear applications in nutrition. The publications have a broad readership and are aimed at medical practitioners, researchers and other professionals. International experts assist the IAEA Secretariat in drafting and reviewing these publications. Some of the publications in this series may also be endorsed or co-sponsored by international organizations and professional societies active in the relevant fields.

There are two categories of publications in this series:

IAEA HUMAN HEALTH SERIES

Publications in this category present analyses or provide information of an advisory nature, for example guidelines, codes and standards of practice, and quality assurance manuals. Monographs and high level educational material, such as graduate texts, are also published in this series.

IAEA HUMAN HEALTH REPORTS

Human Health Reports complement information published in the IAEA Human Health Series in areas of radiation medicine, dosimetry and medical radiation physics, and nutrition. These publications include reports of technical meetings, the results of IAEA coordinated research projects, interim reports on IAEA projects, and educational material compiled for IAEA training courses dealing with human health related subjects. In some cases, these reports may provide supporting material relating to publications issued in the IAEA Human Health Series.

All of these publications can be downloaded cost free from the IAEA web site:

<http://www.iaea.org/Publications/index.html>

Further information is available from:

Marketing and Sales Unit
International Atomic Energy Agency
Vienna International Centre
PO Box 100
1400 Vienna, Austria

Readers are invited to provide their impressions on these publications. Information may be provided via the IAEA web site, by mail at the address given above, or by email to:

Official.Mail@iaea.org

CLINICAL APPLICATIONS
OF SPECT-CT

The following States are Members of the International Atomic Energy Agency:

AFGHANISTAN	GERMANY	PALAU
ALBANIA	GHANA	PANAMA
ALGERIA	GREECE	PAPUA NEW GUINEA
ANGOLA	GRENADA	PARAGUAY
ANTIGUA AND BARBUDA	GUATEMALA	PERU
ARGENTINA	GUYANA	PHILIPPINES
ARMENIA	HAITI	POLAND
AUSTRALIA	HOLY SEE	PORTUGAL
AUSTRIA	HONDURAS	QATAR
AZERBAIJAN	HUNGARY	REPUBLIC OF MOLDOVA
BAHAMAS	ICELAND	ROMANIA
BAHRAIN	INDIA	RUSSIAN FEDERATION
BANGLADESH	INDONESIA	RWANDA
BARBADOS	IRAN, ISLAMIC REPUBLIC OF	SAINT KITTS AND NEVIS
BELARUS	IRAQ	SAINT LUCIA
BELGIUM	IRELAND	SAINT VINCENT AND THE GRENADINES
BELIZE	ISRAEL	SAMOA
BENIN	ITALY	SAN MARINO
BOLIVIA, PLURINATIONAL STATE OF	JAMAICA	SAUDI ARABIA
BOSNIA AND HERZEGOVINA	JAPAN	SENEGAL
BOTSWANA	JORDAN	SERBIA
BRAZIL	KAZAKHSTAN	SEYCHELLES
BRUNEI DARUSSALAM	KENYA	SIERRA LEONE
BULGARIA	KOREA, REPUBLIC OF	SINGAPORE
BURKINA FASO	KUWAIT	SLOVAKIA
BURUNDI	KYRGYZSTAN	SLOVENIA
CAMBODIA	LAO PEOPLE'S DEMOCRATIC REPUBLIC	SOUTH AFRICA
CAMEROON	LATVIA	SPAIN
CANADA	LEBANON	SRI LANKA
CENTRAL AFRICAN REPUBLIC	LESOTHO	SUDAN
CHAD	LIBERIA	SWEDEN
CHILE	LIBYA	SWITZERLAND
CHINA	LIECHTENSTEIN	SYRIAN ARAB REPUBLIC
COLOMBIA	LITHUANIA	TAJIKISTAN
COMOROS	LUXEMBOURG	THAILAND
CONGO	MADAGASCAR	TOGO
COSTA RICA	MALAWI	TONGA
CÔTE D'IVOIRE	MALAYSIA	TRINIDAD AND TOBAGO
CROATIA	MALI	TUNISIA
CUBA	MALTA	TÜRKIYE
CYPRUS	MARSHALL ISLANDS	TURKMENISTAN
CZECH REPUBLIC	MAURITANIA	UGANDA
DEMOCRATIC REPUBLIC OF THE CONGO	MAURITIUS	UKRAINE
DENMARK	MEXICO	UNITED ARAB EMIRATES
DJIBOUTI	MONACO	UNITED KINGDOM OF GREAT BRITAIN AND NORTHERN IRELAND
DOMINICA	MONGOLIA	UNITED REPUBLIC OF TANZANIA
DOMINICAN REPUBLIC	MONTENEGRO	UNITED STATES OF AMERICA
ECUADOR	MOROCCO	URUGUAY
EGYPT	MOZAMBIQUE	UZBEKISTAN
EL SALVADOR	MYANMAR	VANUATU
ERITREA	NAMIBIA	VENEZUELA, BOLIVARIAN REPUBLIC OF
ESTONIA	NEPAL	VIET NAM
ESWATINI	NETHERLANDS	YEMEN
ETHIOPIA	NEW ZEALAND	ZAMBIA
FIJI	NICARAGUA	ZIMBABWE
FINLAND	NIGER	
FRANCE	NIGERIA	
GABON	NORTH MACEDONIA	
GEORGIA	NORWAY	
	OMAN	
	PAKISTAN	

The Agency's Statute was approved on 23 October 1956 by the Conference on the Statute of the IAEA held at United Nations Headquarters, New York; it entered into force on 29 July 1957. The Headquarters of the Agency are situated in Vienna. Its principal objective is "to accelerate and enlarge the contribution of atomic energy to peace, health and prosperity throughout the world".

IAEA HUMAN HEALTH SERIES No. 41

CLINICAL APPLICATIONS OF SPECT-CT

INTERNATIONAL ATOMIC ENERGY AGENCY
VIENNA, 2023

COPYRIGHT NOTICE

All IAEA scientific and technical publications are protected by the terms of the Universal Copyright Convention as adopted in 1952 (Berne) and as revised in 1972 (Paris). The copyright has since been extended by the World Intellectual Property Organization (Geneva) to include electronic and virtual intellectual property. Permission to use whole or parts of texts contained in IAEA publications in printed or electronic form must be obtained and is usually subject to royalty agreements. Proposals for non-commercial reproductions and translations are welcomed and considered on a case-by-case basis. Enquiries should be addressed to the IAEA Publishing Section at:

Marketing and Sales Unit, Publishing Section
International Atomic Energy Agency
Vienna International Centre
PO Box 100
1400 Vienna, Austria
fax: +43 1 26007 22529
tel.: +43 1 2600 22417
email: sales.publications@iaea.org
www.iaea.org/publications

© IAEA, 2023

Printed by the IAEA in Austria

January 2023

STI/PUB/1971

IAEA Library Cataloguing in Publication Data

Names: International Atomic Energy Agency.

Title: Clinical applications of SPECT-CT / International Atomic Energy Agency.

Description: Vienna : International Atomic Energy Agency, 2023. | Series: IAEA human health series, ISSN 2075-3772 ; no. 41 | Includes bibliographical references.

Identifiers: IAEAL 22-01494 | ISBN 978-92-0-111522-5 (paperback : alk. paper) | ISBN 978-92-0-111722-9 (pdf) | ISBN 978-92-0-111622-2 (epub)

Subjects: LCSH: Single-photon emission computed tomography. | Diagnostic imaging. | Tomography. | Nuclear medicine.

Classification: UDC 616-073 | STI/PUB/1971

FOREWORD

More than two decades after the advent of positron emission tomography–computed tomography (PET–CT), a new era of revived interest in conventional nuclear medicine imaging is being witnessed. So-called ‘hybrid imaging’ refers not only to PET–CT (or PET combined with magnetic resonance imaging (MRI)), but also to the combination of single photon emission computed tomography (SPECT) with CT. SPECT–CT shares with PET–CT the possibility of accurate anatomical localization of areas of increased uptake, as well as — more importantly — the benefits and advantages deriving from the ability to directly translate molecular or metabolic information into an immediate clinical impact on the widest possible range of diseases. Indeed, SPECT–CT has demonstrated significant improvements for patient management in a variety of clinical indications, including both oncologic and non-oncologic diseases. Of course, this changing scenario has also raised new issues and continuing debate on the optimal modalities of managing the wealth of clinical information that can be retrieved by hybrid imaging.

In 2008, the IAEA published a technical document on the clinical advantages of SPECT–CT toward improved staging, prognosis and treatment monitoring for a wide variety of conditions, at a time when the technique was just coming out of its infancy. Since then, tremendous advances in technology have taken place; furthermore, the amount of clinical evidence that has accumulated worldwide is impressive. An up-to-date review of the current uses of SPECT–CT has therefore been undertaken in this publication, addressing its application both as a problem-solving approach (for which it was often initially used after its introduction into clinical practice) and as, above all, a systematic clinical practice that is fully integrated into the routine diagnostic approach to a series of disease conditions.

In this review, the complex technological and radiochemistry issues involved in the application of SPECT–CT imaging, such as gamma camera hardware, image acquisition protocols (including specific cardiac aspects and whole body SPECT–CT), quantitation and dosimetry, radiation exposure, novel single photon emitting radiopharmaceuticals, artefacts and pitfalls were deliberately not addressed. This matter is worthy of a separate initiative, which will be undertaken in the near future.

The IAEA wishes to thank the contributors to the drafting and review of this book for contributing their knowledge, time and effort. The IAEA officers responsible for this publication were F. Giammarile and D. Paez of the Division of Human Health.

EDITORIAL NOTE

Although great care has been taken to maintain the accuracy of information contained in this publication, neither the IAEA nor its Member States assume any responsibility for consequences which may arise from its use.

This publication does not address questions of responsibility, legal or otherwise, for acts or omissions on the part of any person.

Guidance provided here, describing good practices, represents expert opinion but does not constitute recommendations made on the basis of a consensus of Member States.

The use of particular designations of countries or territories does not imply any judgement by the publisher, the IAEA, as to the legal status of such countries or territories, of their authorities and institutions or of the delimitation of their boundaries.

The mention of names of specific companies or products (whether or not indicated as registered) does not imply any intention to infringe proprietary rights, nor should it be construed as an endorsement or recommendation on the part of the IAEA.

The IAEA has no responsibility for the persistence or accuracy of URLs for external or third party Internet web sites referred to in this book and does not guarantee that any content on such web sites is, or will remain, accurate or appropriate.

CONTENTS

1.	INTRODUCTION.....	1
1.1.	Background	1
1.2.	Scope	2
1.3.	Objective	2
1.4.	Structure	2
2.	GENERAL PRINCIPLES	3
2.1.	Appropriateness of imaging procedures based on the use of ionizing radiation	5
2.2.	Education/training of the imaging specialist	5
2.3.	Radiation dosimetry for hybrid SPECT–CT imaging	6
	References to Section 2	8
3.	CLINICAL APPLICATIONS	11
3.1.	SPECT–CT in neurology	11
3.2.	SPECT–CT in endocrinology.....	12
3.3.	SPECT–CT in cardiology.....	15
3.4.	SPECT–CT in pneumology	19
3.5.	SPECT–CT in orthopaedics	24
3.6.	SPECT–CT in inflammation	33
3.7.	SPECT–CT in oncology.....	37
3.8.	Gastroenterology	50
3.9.	Paediatrics	52
	References to Section 3	54
4.	INCIDENTAL FINDINGS ON CT.....	90
	References to Section 4	92
	ABBREVIATIONS	95
	CONTRIBUTORS TO DRAFTING AND REVIEW	97

1. INTRODUCTION

1.1. BACKGROUND

Nuclear medicine techniques create images of functional processes by using radioactive tracers and photon detectors. Tomographic imaging with radionuclides began in the 1960s and pre-dates computed tomography (CT). Single photon emission computed tomography (SPECT) is a mainstay in nuclear medicine and has been used in routine diagnostic applications and research since the 1980s. In 1996, the first model of a combined SPECT–CT design, which comprised a clinical SPECT gamma camera in tandem with a clinical single slice CT, was produced. Since then, SPECT–CT has advanced rapidly, and several commercial systems are available today employing various designs of CT and dual head SPECT configurations. There are numerous advantages of an integrated, functional and morphological imaging device, including the following:

- (a) A single examination can provide comprehensive functional and anatomical information on the state of a disease;
- (b) Patients can be scheduled for only one instead of two or multiple examinations;
- (c) Experts in radiology and nuclear medicine can review the complementary image sets together and integrate their interpretation into a single report.

Similarly to positron emission tomography (PET)–CT, the ability of SPECT–CT to provide, in a single image session, detailed anatomical and functional or metabolic information — a synergistic effect greater than the sum of the information from the two individual techniques — has established SPECT–CT as an indispensable imaging procedure for an increasing number of pathologies. In addition, it has a significant advantage over PET–CT, namely the use of a radiotracer widely available in all nuclear medicine departments: 99m-technetium (^{99m}Tc). As a result, an increasing number of SPECT–CT systems are being installed by Member States, thus making it essential that capacities are built and strengthened in SPECT–CT for many nuclear medicine and imaging departments, particularly in countries that are just embarking on this imaging modality.

1.2. SCOPE

Hybrid imaging, including SPECT–CT, has experienced significant developments and improvements that have had positive impacts in recent years, and it now has an important place in several procedural guidelines. The technology has matured and more data are available to appraise its clinical role.

This publication was thus developed to emphasize classical indications in SPECT–CT imaging and highlight new fields in which SPECT–CT is being adopted while providing relevant information with regard to patient management.

1.3. OBJECTIVE

This publication is intended to support nuclear medicine physicians, radiologists and clinical practitioners in their clinical decision making process when allocating resources dedicated to the health care system. This is a critical issue that is especially important for the development of nuclear medicine in developing countries.

Medical imaging is an integral part of patient management; the objective of this publication is to provide a list of the most common indications of SPECT–CT in clinical practice. The IAEA hopes that this publication will be of help for medical professionals and staff working with SPECT–CT for personal learning, training, and teaching purposes. Guidance provided here, describing good practices, represents expert opinion but does not constitute recommendations made on the basis of a consensus of Member States.

1.4. STRUCTURE

The structure of this publication is adapted to the applications of SPECT–CT in nine different clinical scenarios, namely neurology; endocrinology; cardiology; orthopaedics; oncology; respiratory, infectious and gastrointestinal diseases; and paediatrics. A final chapter describes the clinical impact of incidental findings observed in the CT component of the scan.

2. GENERAL PRINCIPLES

There are several tokens by which one can identify the events or discoveries that have revolutionized the practice of medicine throughout history. No consensus exists on what to consider the most important of ‘modern’ medicine’s achievements, some of which have induced dramatic paradigm shifts in patient management [2.1]. Candidates vary widely [2.2] and include tools specifically related to therapy (e.g. vaccines, the hypodermic needle, antibiotics and antiviral drugs, germ theory and antiseptics, anaesthesia, haemodialysis, prosthetic implants, cardiac pacemakers, organ transplantation and the cardiac defibrillator) and diagnostic methods (e.g. the stethoscope, the thermometer, X rays and medical imaging in general, and the electrocardiogram), as well as procedures that aim to have a more general impact on medical science (e.g. controlled clinical trials and artificial intelligence) [2.3].

For investigators and clinicians working in the field — and increasingly for the whole medical community — nuclear medicine represents a crucial turning point because it provides an interface or bridge between physiology and clinical medicine. This intrinsic feature of both diagnostic and therapeutic nuclear medicine has led to the coining of the term ‘molecular imaging’ or, more appropriately, ‘molecular targeting’. Molecular targeting “may be defined as the specific concentration of a diagnostic tracer or therapeutic agent by virtue of its interaction with a molecular species that is distinctly present or absent in a disease state” [2.4]. Although intrinsic to nuclear medicine since its earliest inception, this feature has been heightened by the development of PET imaging (and especially hybrid PET–CT, or, more recently, PET combined with magnetic resonance imaging (MRI)), which has revolutionized diagnostic nuclear medicine and revived its long standing position as a crucial approach to theranostics [2.5–2.15].

The excitement and expectation that the advent of PET–CT raised in the nuclear medicine community and in the diagnostic imaging community at large led to speculation in 2008 that, the availability of a complete armamentarium of PET radiopharmaceuticals would eventually replace virtually all single photon agents [2.16]. This would therefore result in the impending and irreversible obsolescence of single photon planar and tomographic imaging, so-called ‘conventional’ nuclear medicine imaging. Such a dismal forecast for conventional nuclear medicine imaging is actually proving not to be true, especially after the development and clinical availability of hybrid SPECT–CT scanners SPECT–CT [2.17]. In fact, this form of hybrid imaging has revived interest in single photon imaging, since SPECT–CT shares with PET–CT the benefits and advantages deriving from the ability to directly translate molecular or metabolic

information into an immediate clinical impact on the widest possible range of diseases. Thus, nowadays, hybrid imaging constitutes a more general approach by which the nuclear medicine specialist makes a fundamental contribution to improved health care by tailoring clinical interventions to the individual patient's needs according to the best principles of personalized medicine. Of course, this changing scenario has also raised new issues and continuing debate on the optimal management of the wealth of clinical information that can be retrieved by hybrid imaging, based on incidental, unanticipated findings in the CT component of the study [2.18].

The continuing evolution of technology and knowledge in the field of nuclear medicine takes advantage of the cooperation between SPECT and PET [2.19]. The speed of development is reflected in trends in the sales of new equipment for nuclear medicine, where installations of hybrid SPECT–CT gamma cameras have exhibited a steep surge both worldwide [2.20] and on a country level [2.21]. On a global level, a market size of \$1.41 billion was estimated for SPECT and SPECT–CT scanners in 2018, with a forecast of growth to approximately \$1.934 billion in 2025 at a compound annual growth rate of approximately 4.64% between 2019 and 2025 [2.22]. Within the United States of America alone, SPECT and SPECT–CT equipment constitutes the major share (approximately 55–60%) of the market size in nuclear medicine, with a clear forecast for growth for the next five years at least.

Technetium-99m (Tc-99m) is used in about 85% of nuclear medicine diagnostic procedures worldwide with over 30 million patients examined on a yearly basis [2.22]. The overall good performance of SPECT–CT stems from its established clinical advantages in terms of improved staging, prognosis and treatment monitoring for a wide variety of both oncologic and non-oncologic diseases. The clinical evidence regarding such advantages as reported in the literature published up to 2008–2009 was initially reviewed SPECT–CT in Mariani et al. [2.23] when SPECT–CT was just coming out of its infancy. This comprehensive review was updated 10 years later in Israel et al. [2.24], when it was deemed appropriate to re-evaluate the uses of SPECT–CT not just as a case based problem-solving technique (as applied early in the introduction of SPECT–CT into clinical practice), but rather as a systematic clinical practice fully integrated into the routine diagnostic approach to a series of disease conditions, with due consideration of the tremendous advances in technology that had taken place in the meantime.

Some important considerations have emerged from this optimistic scenario, however, fuelling debate as to the optimal way to take full advantage of the diagnostic value of hybrid imaging in terms of not only the functional or metabolic information deriving from the radionuclide component of the scan, but also the predominantly anatomical information deriving from the CT (or MRI, in the case of hybrid PET–MRI) component of the study. These issues relate to the

optimization of the diagnostic pathways using those imaging modalities that are most frequently associated with a certain radiation burden that must be minimized as much as possible. Three main avenues for improvement branch out from this issue as they relate to (a) the appropriateness of any imaging procedure involving exposure of the patient to ionizing radiation, (b) adequate education/training of the imaging specialist for the best benefit to patients and (c) the radiation dose deriving from the CT component in addition to the radiation dose intrinsically associated with the radionuclide component of the hybrid test.

2.1. APPROPRIATENESS OF IMAGING PROCEDURES BASED ON THE USE OF IONIZING RADIATION

As it is a diagnostic procedure that involves exposing patients to ionizing radiation, the preliminary step for referring patients to SPECT-CT (as well as for a PET-CT study) must take into account the appropriate clinical indications for the diagnostic investigation according to Radiation Protection and Safety of Radiation Sources: International Basic Safety Standards, IAEA Safety Standards Series No. GSR Part 3 [2.25].

2.2. EDUCATION/TRAINING OF THE IMAGING SPECIALIST

Education and training are currently issues causing the liveliest debate and controversy within the imaging community with reference to hybrid imaging [2.26]. There are at least two facets to this topic. The first is how to interpret and report the incidental discovery in the ‘radiological’ portion of the hybrid scans (SPECT-CT, PET-CT or PET-MRI) of unexpected lesions outside the primary area of interest for the radionuclide investigation. The issues involved include both the competence and expertise of the nuclear medicine specialist to read and interpret radiological findings, and the binding legal value of such medical reports. The second is how to derive maximum benefit in terms of sensitivity and specificity from the concomitant radiological studies (CT or MRI) when interpreting the radionuclide based images (SPECT or PET). These issues have raised debate concerning the optimal education and training of imaging specialists [2.27–2.29]. In recent years various scenarios have been proposed, and considerable heterogeneity is currently found worldwide concerning the core curriculum for imaging specialists. In some countries, the disciplines of nuclear medicine and radiology are completely independent specialities (the majority of cases, especially in Europe), whereas in others, a single speciality encompasses both types of competence (which is mainly the case in the USA) [2.30–2.34]. The

prevailing trend appears now to favour the highest possible interaction between the two disciplines (whether as a single postgraduate speciality or two separate specialities), with the goal of the maximum benefit to patients [2.35–2.38]. In this regard, the IAEA has recently issued a detailed Training Curriculum for Nuclear Medicine Physicians (IAEA-TECDOC-1883), endorsed by the European Association of Nuclear Medicine, the European Union of Medical Specialists, the World Federation of Nuclear Medicine and Biology, the African Association of Nuclear Medicine, the Arab Society of Nuclear Medicine, the Asia and Oceania Federation of Nuclear Medicine and Biology, the Asian Regional Cooperative Council for Nuclear Medicine and the Latin American Association of Societies of Nuclear Medicine and Biology [2.39].

2.3. RADIATION DOSIMETRY FOR HYBRID SPECT–CT IMAGING

The added diagnostic value of SPECT–CT over planar scintigraphy and stand-alone SPECT, as increasingly evident in the routine clinical applications of SPECT–CT, must be counterbalanced with the additional burden of ionizing radiation associated with the CT component of the scan. In particular, during hybrid imaging with either PET–CT or SPECT–CT, the total effective dose delivered to patients is the sum of the internal radiation associated with administration of the specific radiopharmaceutical and the radiation associated with the use of an external X ray source for the CT portion of the investigation.

The radiation burden due to the CT component depends heavily on the acquisition parameters used, which include the X ray tube potential (kVp), the X ray current (mAs), the pitch and the beam width. A study in which an anthropomorphic phantom was utilized to measure CT dose index volume to various organs compared with calculated values [2.40] revealed several discrepancies between calculated and measured values for different regions or organs, the measured values being in general greater than the a priori calculated values. Such discrepancies range from ‘minor’ to ‘non-negligible’ differences. Furthermore, there was an approximate fortyfold increase in radiation doses when increasing the X ray tube parameters from 90 kVp and 25 mAs to 140 kVp and 300 mAs.

According to an extensive review published by Ferrari et al. [2.41], the percentage increase in effective dose per field of view due to the addition of the CT study to the standard SPECT acquisition varies according to the type of radionuclide investigation, as follows:

- (a) 10–23% for ^{67}Ga -citrate SPECT–CT;
- (b) 18.8–65.1% for $^{99\text{m}}\text{Tc}$ -sestamibi parathyroid SPECT–CT;

- (c) 30.6–58.3% for ^{111}In -octreotide SPECT–CT;
- (d) 60.3–102.4% for $^{99\text{m}}\text{Tc}$ -methylene diphosphonate ($^{99\text{m}}\text{Tc}$ -MDP) bone SPECT–CT.

These data, listed in detail in Table 2.1, show that the lowest percentage increases in values are observed for radionuclide investigations involving an intrinsically higher radiation dosimetry.

An important variable in radiation dosimetry associated with the use of an external X ray source is related to the fact that during hybrid SPECT–CT, the CT portion of the study is generally limited to a single field of view (the region

TABLE 2.1. EFFECTIVE DOSES DELIVERED TO PATIENTS DURING SOME COMMON SPECT–CT EXAMINATIONS
(as derived from published literature and summarized by Ferrari et al. [2.41])

Study type	Author	Effective dose from radiopharmaceuticals (mSv)	Effective dose from CT component (mSv)	Increase due to CT (%)
Ga-67-citrate	Larkin [2.42]	37	8.5	23.0
	Montes [2.43]	26.5 ^a	2.6 ^a	9.8 ^a
	Montes [2.43]	18.9 ^b	2.6 ^b	13.7 ^b
Tc-99m-sestamibi ^c	Larkin [2.42]	8.3	5.4	65.1
	Montes [2.43]	6.4	1.6	25.0
	Sharma [2.44]	6.4	1.2	18.8
In-111-octreotide	Larkin [2.42]	12	7.0	58.3
	Montes [2.43]	8.5	2.6	30.6
Tc-99m-MDP	Larkin [2.42]	6.3	3.8	60.3
	Sharma [2.44]	4.1	4.2	102

^a Lymphoma.

^b Infection.

^c Parathyroid disease.

of interest), whereas during PET–CT imaging the CT covers the whole body. Therefore, the total radiation burden due to the CT portion is generally much lower for SPECT–CT than for a PET–CT scan.

In current generation SPECT–CT scanners, the modern CT component is equipped with current modulation technology, which optimizes the radiation exposure according to the body habitus of each individual patient being examined. Nuclear medicine centres are recommended to adopt such optimization technology whenever acquiring a SPECT–CT study in order to keep the radiation burden to patients as low as possible, both for the radionuclide component per se and for the CT component, according to the ‘as low as reasonably achievable’ (ALARA) principle. Recommendations have been issued to deliver more comparable international radiation doses for administered activity and CT doses across centres employing PET–CT and SPECT–CT imaging [2.45].

REFERENCES TO SECTION 2

- [2.1] THOMSON, A., The three revolutions in medicine, *Br. Med. J.* **2** (1959) 130–134.
- [2.2] CHILDS, D., KANSAGRA, S., Ten health advances that changed the world, ABC News Medical Unit (2007),
<https://abcnews.go.com/Health/TenWays/story?id=3605442&page=1>
- [2.3] CHATURVEDI, R., VERMA, N., The next revolution in medicine — Are we ready? *JOMA* **1** (2018) 1–4.
- [2.4] BRITZ-CUNNINGHAM, S.H., ADELSTEIN, S.J., Molecular targeting with radionuclides: State of the science, *J. Nucl. Med.* **44** (2003) 1945–1961.
- [2.5] MAZZIOTTA, J.C., et al., Relating structure to function in vivo with tomographic imaging, *Ciba. Found. Symp.* **163** (1991) 93–101.
- [2.6] LARSON, S.M., Molecular imaging in oncology: The diagnostic imaging ‘revolution’, *Clin. Cancer Res.* **6** (2000) 2125.
- [2.7] ALAVI, A., KUNG, J.W., ZHUANG, H., Implications of PET based molecular imaging on the current and future practice of medicine, *Semin. Nucl. Med.* **34** (2004) 56–69.
- [2.8] ALAVI, A., LAKHANI, P., MAVI, A., KUNG, J., ZHUANG, H., PET: A revolution in medical imaging, *Radiol. Clin. North Am.* **42** (2004) 983–1001.
- [2.9] SCHILLACI, O., SIMONETTI, G., Fusion imaging in nuclear medicine — Applications of dual-modality systems in oncology, *Cancer Biother. Radiopharm.* **19** (2004) 1–10.
- [2.10] BEYER, T., PICHLER, B., A decade of combined imaging: From a PET attached to a CT to a PET inside an MR, *Eur. J. Nucl. Med. Mol. Imaging* **36** Suppl. 1 (2009) S1–S2.
- [2.11] BASU, S., From pure research imaging tool to PET-guided personalized medicine in oncology: A true revolution in modern medicine, *Indian J. Cancer* **47** (2010) 98–99.

- [2.12] MANSI, L., CIARMIELLO, A., CUCCURULLO, V., PET/MRI and the revolution of the third eye, *Eur. J. Nucl. Med. Mol. Imaging* **39** (2012) 1519–1524.
- [2.13] VERBURG, F.A., et al., Nothing new under the nuclear sun: Towards 80 years of theranostics in nuclear medicine, *Eur. J. Nucl. Med. Mol. Imaging* **41** (2014) 199–201.
- [2.14] HERMANN, K., LARSON, S.M., WEBER, W.A., Theranostic concepts: More than just a fashion trend — introduction and overview, *J. Nucl. Med.* **58** Suppl. 2 (2017) 1S–2S.
- [2.15] YORDANOVA, A., et al., Theranostics in nuclear medicine practice, *OncoTargets Ther.* **10** (2017) 4821–4828.
- [2.16] ALAVI, A., BASU, S., Planar and SPECT imaging in the era of PET and PET–CT: Can it survive the test of time? *Eur. J. Nucl. Med. Mol. Imaging* **35** (2008) 1554–1559.
- [2.17] HUTTON, B.F., The origins of SPECT and SPECT–CT, *Eur. J. Nucl. Med. Mol. Imaging* **41** Suppl. 1 (2014) S3–S16.
- [2.18] GOETZE, S., PANNU, H.K., WAHL, R.L., Clinically significant abnormal findings on the ‘nondiagnostic’ CT portion of low-amperage-CT attenuation-corrected myocardial perfusion SPECT–CT studies, *J. Nucl. Med.* **47** (2006) 1312–1318.
- [2.19] MARIANI, G., STRAUSS, H.W., Positron emission and single-photon emission imaging: Synergy rather than competition, *Eur. J. Nucl. Med. Mol. Imaging* **38** (2011) 1189–1190.
- [2.20] KASHYAP, R., DONDI, M., PAEZ, D., MARIANI, G., Hybrid imaging worldwide — challenges and opportunities for the developing world: A report of a technical meeting organized by IAEA, *Semin. Nucl. Med.* **43** (2013) 208–223.
- [2.21] NISHIYAMA, Y., et al., Nuclear medicine practice in Japan: A report of the eighth nationwide survey in 2017, *Ann. Nucl. Med.* **33** (2019) 725–732.
- [2.22] OECD/NEA, The Supply of Medical Isotopes: An Economic Diagnosis and Possible Solutions, OECD Publishing, Paris (2019), <https://doi.org/10.1787/9b326195-en>
- [2.23] MARIANI, G., et al., A review on the clinical uses of SPECT–CT, *Eur. J. Nucl. Med. Mol. Imaging* **37** (2010) 1959–1985.
- [2.24] ISRAEL, O., et al., Two decades of SPECT–CT — the coming of age of a technology: An updated review of literature evidence, *Eur. J. Nucl. Med. Mol. Imaging* **46** (2019) 1990–2012.
- [2.25] INTERNATIONAL ATOMIC ENERGY AGENCY, Radiation Protection and Safety of Radiation Sources: International Basic Safety Standards, IAEA Safety Standards Series No. GSR Part 3, IAEA, Vienna (2014).
- [2.26] BISCHOF DELALOYE, A., et al., White paper of the European Association of Nuclear Medicine (EANM) and the European Society of Radiology (ESR) on multimodality imaging, *Eur. J. Nucl. Med. Mol. Imaging* **34** (2007) 1147–1151.
- [2.27] BEYER, T., HICKS, R., BRUN, C., ANTOCH, G., FREUDENBERG, L., An international survey on hybrid imaging: Do technology advances preempt our training and education efforts? *Cancer Imaging* **18** (2018) 15.
- [2.28] STEGGER, L., SCHÄFERS, M., WECKESSER, M., SCHOBER, O., EANM-ESR white paper on multimodality imaging, *Eur. J. Nucl. Med. Mol. Imaging* **35** (2008) 677–680.

- [2.29] GUIBERTEAU, M.J., GRAHAM, M.M., ACR-SNM task force on nuclear medicine training: Report of the task force, *J. Nucl. Med.* **52** (2011) 998–1002.
- [2.30] DELBEKE, D., ROYAL, H.D., FREY, K.A., GRAHAM, M.M., SEGALL, G.M., SNMMI/ABNM joint position statement on optimizing training in nuclear medicine in the era of hybrid imaging, *J. Nucl. Med.* **53** (2012) 1490–1494.
- [2.31] PRIGENT, A. HUSTINX, R., COSTA, D.C., Nuclear medicine training in the European Union: 2015 update, *Eur. J. Nucl. Med. Mol. Imaging* **43** (2016) 583–596.
- [2.32] MANKOFF, D., PRYMA, D.A., Nuclear medicine training: What now? *J. Nucl. Med.* **58** (2017) 1536–1538.
- [2.33] SEGALL, G.M., GRADY, E.E., FAIR, J.R., GHESANI, M.V., GORDON, L., Nuclear medicine training in the United States, *J. Nucl. Med.* **58** (2017) 1733–1734.
- [2.34] MUYLLE, K., MAFFIOLI, L., Nuclear medicine training in Europe: ‘All for one, one for all’, *J. Nucl. Med.* **58** (2017) 1904–1905.
- [2.35] BIERSACK, H.J., Nuclear medicine training: Two different pathways? *J. Nucl. Med.* **59** (2018) 1335.
- [2.36] FRANGOS, S., et al., The future of the past is the present: The role of the UEMS/EBNM in the current challenge of educating nuclear medicine specialists, *J. Nucl. Med.* **59** (2018) 396–398.
- [2.37] KIM, S.Y., et al., Radiologists and nuclear medicine physicians are looking forward to a cross-curricular training, *Eur. Radiol.* **29** (2019) 4803–4811.
- [2.38] CHITI, A., MENU, Y., Radiology and nuclear medicine: Advancing together in the era of precision medicine, *Eur. J. Nucl. Med. Mol. Imaging* **47** (2020) 517–518.
- [2.39] INTERNATIONAL ATOMIC ENERGY AGENCY, Training Curriculum for Nuclear Medicine Physicians, IAEA-TECDOC-1883, IAEA, Vienna (2019).
- [2.40] HARA, N., et al., Assessment of patient exposure to X-radiation from SPECT–CT scanners, *J. Nucl. Med. Technol.* **38** (2010) 138–148.
- [2.41] FERRARI, M., DE MARCO, P., ORIGGI, D., PEDROLI, G., SPECT–CT radiation dosimetry, *Clin. Transl. Imaging* **2** (2014) 557–569.
- [2.42] LARKIN, A.M., SERULLE, Y., WAGNER, S., NOZ, M., FRIEDMAN, K., Quantifying the increase in radiation exposure associated with SPECT–CT compared to SPECT alone for routine nuclear medicine examinations, *Int. J. Mol. Imaging* **2011** (2011) 897202.
- [2.43] MONTES, C., et al., Estimation of the total effective dose from low-dose CT scans and radiopharmaceutical administrations delivered to patients undergoing SPECT–CT explorations, *Ann. Nucl. Med.* **27** (2013) 610–617.
- [2.44] SHARMA, P., et al., SPECT–CT in routine clinical practice: Increase in patient radiation dose compared with SPECT alone, *Nucl. Med. Commun.* **33** (2012) 926–932.
- [2.45] ALKHYBARI, E.M., et al., Determining and updating PET–CT and SPECT–CT diagnostic reference levels: A systematic review, *Radiat. Prot. Dosimetry* **182** (2018) 532–545.

3. CLINICAL APPLICATIONS

3.1. SPECT–CT IN NEUROLOGY

SPECT imaging of the brain is a well-established tool in the diagnostic workup of dementia, epilepsy, parkinsonism and some other cerebral diseases. In contrast to other indications, the addition of CT to SPECT has not led to a breakthrough in brain imaging. One of the major reasons for this is that CT is not the imaging procedure of choice for the brain; MRI is superior to CT in resolving cerebral structures. Therefore, only a small number of publications have investigated the diagnostic gain of acquiring SPECT and CT images in one examination [3.1–3.12].

Technetium-99m-tetrofosmin can be used to differentiate between radiation necrosis and recurrence of gliomas. This radiopharmaceutical does not accumulate in normal brain tissue but concentrates in the skull and the choroid plexus. Filippi et al. showed that in 13 of 30 cases SPECT–CT pathological uptake by glioma recurrence could only be reliably differentiated from physiological uptake with fused SPECT–CT datasets [3.1]. Three years later, the authors confirmed their initial findings in a group of 40 patients [3.2].

Due to the neurodegenerative process occurring in diseases of the basal ganglia, striatal tracer uptake will heterogeneously decrease in this structure, with its posterior parts being involved earlier than its anterior ones. This renders the definition of striatal regions of interest, ideally covering the whole structure, on stand-alone ^{123}I - ω -fluoropropyl-2 β -carbomethoxy-3 β -(4-iodophenyl)nortropane (^{123}I -FP-CIT) SPECT images difficult. Hsu et al. demonstrated that CT-guided region of interest definition of the basal ganglia in SPECT–CT datasets might be highly reproducible and that the semiquantitative data derived from these regions of interest correlate well with MRI-guided data [3.6].

When voxelwise comparison to age-matched healthy controls is desired to obtain a more accurate diagnosis of brain diseases, the use of anatomical information from CT to obtain a more robust spatial normalization of SPECT data can be helpful. SPECT–CT has therefore been integrated into commercially available software tools, such as NeuroGam, allowing for three dimensional (3-D) evaluation of regional cerebral blood flow as used by Lou et al. in Moyamoya disease [3.11]. However, a review of the literature yields only one publication that has demonstrated a benefit of CT integration into such an analysis tool: Yokoyama et al. employed statistical parametric mapping with anatomical standardization that uses the exponentiated Lie algebra algorithm in ^{123}I -FP-CIT-SPECT–CT scans to differentiate between Parkinson’s disease and

non-parkinsonian disorders [3.9]. Their CT-guided method showed the greatest power of discrimination between the studied patient groups.

Some evidence shows that SPECT–CT offers a more accurate attenuation correction of SPECT images than the conventionally used Chang approach [3.4]. Kato et al. [3.7] and Farid et al. [3.3, 3.5] demonstrated, in small patient groups, a gain in diagnostic accuracy when using CT based attenuation correction compared with Chang’s method. However, a systematic analysis of how this tool performs in larger groups of patients is still outstanding. Furthermore, for ^{123}I -FP-CIT SPECT, the diagnostic accuracy for the differentiation between Parkinson’s disease and essential tremor was shown not to be dependent on the attenuation correction method employed, even if preliminary correlation analyses suggested that striatal binding potential estimates derived from CT based attenuation correction were a superior biomarker of nigrostriatal integrity [3.10].

The potential value of SPECT–CT to quantify regional tissue radioactivity concentration constitutes an interesting option for brain imaging. Welz et al. reported that global cerebral uptake of $^{99\text{m}}\text{Tc}$ -hexamethylpropylenoxime as expressed in absolute units correlated significantly with the minimal-state examination score in 65 patients with cognitive impairment [3.8]. However, in ^{123}I -FP-CIT-SPECT, determining the standardized uptake values (SUVs) of striatal binding of the tracer did not provide a higher diagnostic accuracy than calculating ratios of uptake to differentiate between neurodegenerative diseases [3.12].

3.2. SPECT–CT IN ENDOCRINOLOGY

3.2.1. Parathyroid disease

Functional imaging has a major impact on the workup of patients with hyperparathyroidism (HPT). Initially, planar and SPECT $^{99\text{m}}\text{Tc}$ -sestamibi (Tc-MIBI) were used for the diagnosis of parathyroid adenoma (PTA), at times in combination with thyroid scintigraphy using radiotracers such as $^{99\text{m}}\text{Tc}$ -pertechnetate or ^{123}I . The dual-phase Tc-MIBI scintigraphy protocol is based on the increased presence of mitochondria in PTA cells with subsequent higher radiotracer uptake, as well as the reduced expression of P-glycoprotein leading to slower washout from PTAs than from thyroid tissues (Table 3.1).

SPECT–CT has improved the detectability rate for the diagnosis and accuracy of localization of PTAs in comparison with planar and SPECT stand-alone imaging, even in combination with ultrasound. The reported detectability rate of SPECT–CT for PTAs ranges between 90 and 96% [3.13–3.15]. SPECT–CT is particularly helpful in cases with small PTAs,

TABLE 3.1. SUMMARY OF LITERATURE TOPICS RELATED TO SPECT–CT IN PATIENTS WITH HYPERPARATHYROIDISM

SPECT–CT indications	No. papers (2008–2019)
Localization of PTA (pre-operative)	7
Diagnosis of PTA	6
Diagnosis and localization	4
Comparison with other imaging tests (ultrasound, 4-D CT, F-18-choline PET–CT)	7
Diagnosis and localization in secondary HPT	5
Cost effective studies	2

below 10 mm in diameter [3.14, 3.16] or weighing less than 210 mg [3.17]. There is a good correlation between Tc-MIBI SPECT–CT findings and serum parathyroid hormone and calcium levels [3.18, 3.19]. Recently, a new technique of quantitative SPECT–CT has measured maximum standardized Tc-MIBI uptake values and has calculated tracer washout rates in PTAs and thyroid tissue. The early tracer uptake was found to be higher and the washout of Tc-MIBI was slower in PTAs than in the normal thyroid, supporting the two hypotheses proposed as explanations for the success of Tc-MIBI for parathyroid imaging: increased mitochondrial binding and reduced P-glycoprotein expression. Quantitative SPECT–CT is suggested as a powerful tool for improving the diagnostic accuracy in equivocal parathyroid lesions [3.20].

In recent decades there have been significant advances in the treatment of PTAs, in particular, the introduction of minimally invasive surgery. The use of this surgical approach underscores the need for the precise anatomical and functional topographic information that can be provided by SPECT–CT. The main current clinical indication for parathyroid imaging is accurate pre-operative localization of PTAs. SPECT–CT has been shown to improve localization of PTAs in 8–39% of patients [3.21, 3.22]. Studies including large numbers of patients, although mainly retrospective, provide evidence on the high performance indices of Tc-MIBI SPECT–CT for localization of PTAs, with sensitivity of 83–97%, specificity of 89–96%, positive predictive value (PPV) of 94–97% and negative predictive value (NPV) of 85% [3.15, 3.17, 3.23–3.26]. In particular, SPECT–CT is highly valuable for correctly localizing ectopic PTAs, as well as in patients

with distorted anatomy following prior neck surgery that had previously failed to identify the adenoma [3.22].

The ability of SPECT–CT to localize a PTA was found to be superior to that of both stand-alone SPECT and ultrasound [3.13, 3.16, 3.17, 3.23, 3.25]. Sensitivity, specificity and accuracy for pre-surgical PTA localization were highest using a combined protocol of Tc-MIBI SPECT–CT and ultrasound (87%, 71% and 85%, respectively) and lowest for stand-alone ultrasound [3.27, 3.28]. The addition of contrast-enhanced CT significantly increased the sensitivity, from 81% to 90% for localization mainly of small PTAs, with no significant change in specificity [3.29]. Four dimensional (4-D) CT provides additional information in a small number of patients, mainly those with non-MIBI-avid adenomas, as well as in cases with a suspicion of ectopic lesions [3.30–3.32]. The combination of Tc-MIBI SPECT–CT with both ultrasound and 4-D CT resulted in the highest sensitivity for precise PTA localization, in particular to a specific quadrant [3.31, 3.33, 3.34]

PET–CT using ^{18}F -fluorocholine (FCH) has also been used for the detection of PTAs in patients with primary HPT and compared with SPECT–CT performed with $^{99\text{m}}\text{Tc}$ -labelled radiotracers. Pre-operative FCH–PET–CT had a high sensitivity and PPV for lesion localization in cases with negative or inconclusive Tc-MIBI SPECT–CT and ultrasound, mainly in patients with small PTAs [3.35, 3.36]

Reporting SPECT–CT makes it possible to apply anatomy based nomenclature, also known as Perrier classification, that is routinely used by surgeons and is associated with better interspeciality communication [3.37]. Following the use of Tc-MIBI SPECT–CT, there was a reported decrease in time of surgery of up to 50% [3.14, 3.24, 3.25]. Positive SPECT–CT is a good criterion to define the eligibility of patients for surgical removal of PTAs [3.38] and is also helpful in planning the surgical procedure, particularly in patients with associated thyroid pathology such as multinodular goitre [3.24].

A cost effectiveness analysis performed in Canada assessed differences in sensitivity between SPECT and SPECT–CT and indicated that costs related to hybrid imaging in patients with known or suspected PTAs were 30% higher when compared with stand-alone SPECT [3.39]. However, another study performed in Italy suggested that while performing SPECT–CT in patients with PTA led to a 4% increase in direct costs, the mean savings related to further patient management, including surgery, were of approximately €98.7 per patient [3.26].

Secondary HPT is a complication occurring in patients with end-stage renal disease on dialysis, frequently associated with hyperplasia and multigland parathyroid disease. In severe cases that are resistant to medical treatment, patients are referred to parathyroidectomy, with variable rates of success. Pre-operative Tc-MIBI SPECT–CT imaging has improved the results of surgery

in this clinical setting as well [3.40]. SPECT–CT has been shown to detect more PTAs, mainly smaller lesions, as well as more ectopic PTAs than stand-alone SPECT [3.41–3.43], with a reported sensitivity of around 75% [3.42, 3.44].

While Tc-MIBI SPECT–CT constitutes at present an important part of the pre-operative workup of patients with HPT, it should be mentioned that varying imaging protocols are used in different centres. These protocols include options such as single tracer dual-phase studies, subtraction imaging following the injection of a thyroid imaging tracer (^{99m}Tc pertechnetate or ^{123}I), timing the SPECT–CT so that it is used either during the early or late phase of imaging, or using it twice [3.15, 3.18, 3.26, 3.45].

3.2.2. Benign thyroid disease

Since their introduction, nuclear medicine techniques have always been involved in both the diagnosis and treatment of benign thyroid diseases. Thyroid uptake and scans are used in differential diagnosis in patients presenting with abnormal thyroid hormone serum levels. In the case of biological signs of hyperthyroidism, elevated radiotracer uptake suggests toxic nodular goitre or Graves' disease, whereas very low thyroid uptake is related to thyroiditis. Conversely, in the case of hypothyroidism, scintigraphy may be used to identify thyroid agenesis or ectopia.

SPECT–CT is not commonly used to image benign thyroid diseases. A review of the literature evidenced a total of 12 articles about SPECT–CT and benign thyroid diseases, with six of them addressing the search for ectopic thyroid tissue. While the total number of patients described was limited (less than 30), scintigraphy with SPECT–CT is suggested as a reliable method for the diagnosis of ectopic thyroid tissue [3.46]. Quantitative SPECT–CT was also used to evaluate Graves' disease in four studies [3.47–3.50].

3.3. SPECT–CT IN CARDIOLOGY

Cardiovascular diseases are the leading cause of death worldwide, and coronary artery disease (CAD) is the number one cause of cardiovascular morbidity and mortality. Current European and US guidelines for the assessment of stable CAD recommend that, depending on the pre-test probability, patients with low probability should have cardiac computed tomography angiography (CCTA), which has a high NPV, while patients with high probability should be referred to invasive coronary angiography. The intermediate risk group, comprising most patients, needs further non-invasive tests. Defining the haemodynamic significance and quantifying ischaemia in addition to assessing

the degree of stenosis are of great importance, thus the role of non-invasive functional testing in the management of patients with intermediate risk for CAD.

Myocardial perfusion imaging (MPI) with SPECT using tracers, such as ^{99m}Tc labelled sestamibi, tetrofosmin and thallium-201 (^{201}Tl) chloride, has been validated for diagnosis, risk stratification and prognosis of patients with known or suspected CAD [3.51]. MPI assesses the physiological significance of angiographically borderline stenosis and the presence of viable, but dysfunctional, hypoperfused myocardium. SPECT is limited by photon attenuation (i.e. the interaction and absorption of gamma rays with tissues resulting in decreased photon detection). In addition, the need for collimation causes reduced spatial resolution and lower efficiency of photon detection. All this leads to a reduced specificity of MPI-SPECT.

The diagnostic accuracy of MPI can be further affected by respiratory and cardiac motion causing approximately 15–20 mm displacement of the heart and leading to the appearance of false, artefactual defects. Furthermore, men are prone to artefacts involving the inferior wall, due to attenuation by subdiaphragmatic structures, as can also be the case in obese women. Anterior wall artefacts are more frequent in women due to shifting breast tissue, but can also be seen in men with large chest circumferences.

The development of attenuation correction algorithms utilizing CT, as well as iterative techniques for image reconstruction, have resulted in improved image quality, with evidence pointing towards higher diagnostic accuracy [3.52]. The performance indices of SPECT with and without attenuation correction had a sensitivity of 89% and 87% and a specificity of 81% vs 73%, respectively [3.53]. Artefacts causing soft tissue attenuation and thus leading to false positive results are corrected with the help of the CT component of the SPECT–CT study. The diagnostic performance of gated and CT-attenuation correction (CT-AC) MPI studies was compared and referenced to coronary angiography for diagnosis of CAD. Gated MPI performed better than non-attenuation correction studies, mainly in overweight male patients and specifically in the territory of the right coronary artery. When compared with CT-AC, gated studies had a higher specificity but similar sensitivity. These results indicate that both attenuation correction examinations and gated MPI can improve the performance indices of MPI for diagnosis of CAD [3.54].

In the routine imaging protocol, the rest SPECT study is followed by a low dose CT (2.5 mA, 140 keV) acquisition performed only over the area of the heart and further used for attenuation correction of the scintigraphic data. SPECT–CT for attenuation correction has been shown to increase diagnostic confidence in the interpretation of stress-only MPI studies, thus leading to a reduction in patient exposure to radiation following the implementation of this imaging protocol [3.55]. Additional solutions to reduce patient radiation exposure

related to MPI-SPECT-CT have been proposed. Studies comparing filtered back projection processing at full dose and ordered-subset expectation maximization iterative reconstruction at a quarter dose were associated with similar diagnostic performance for detection of cardiac perfusion defects. Based on these results, lower radiotracer doses can be recommended in future cardiac SPECT-CT imaging protocols [3.56]. Furthermore, attenuation correction obtained from ultra-low dose CT components using 70 kVp and 80 kVp tube voltage provides similar MPI study image quality and clinical results to attenuation maps obtained with standard CT, while at the same time reducing patient radiation exposure [3.57].

CT-AC can be combined with CT examinations intended to take calcium score measurements without significantly increasing the radiation exposure of the patients. Calcium scanning performed on SPECT-CT devices is therefore becoming a routine part of MPI with paramount diagnostic and prognostic value [3.58, 3.59]. The presence and progression of coronary artery calcification (CAC) is an indicator of coronary atherosclerosis and predicts the risk for CAD, irrespective of the presence or absence of other cardiovascular risk factors [3.60–3.63]. Calcifications are identified as areas of hyperattenuation of at least 1 mm² measuring more than 130 Hounsfield units (HU). The CAC score is obtained using highly reproducible semiautomatic computer methods based on the product of the calcified plaque area multiplied by the coefficient of its density, with the peak HU categorized as 1 for 131–199 HU, 2 for 200–299 HU, 3 for 300–399 HU and 4 for over 400 HU. Visually, coronary calcifications can be defined as minimal (1–10), mild (11–99), moderate (100–399) or severe (above 400). While CAC measurements have downsides, in particular cost and downstream testing following incidental findings, this parameter can improve the diagnostic and prognostic value of MPI. The combination of CAC measurements with MPI findings is of value, especially in cases with a potentially high rate of false positive results. In addition, in view of current efforts to reduce radiation exposure, in stress-first protocols, the availability of the CAC score helps in selecting those patients who will also require a rest SPECT acquisition.

CCTA has a high diagnostic accuracy for assessment of the presence of stenosis in native coronary arteries, with a sensitivity of 85–99% and an NPV of 83–99% [3.64–3.66]. This reaches even higher values with the use of modern dual source technology, up to a sensitivity of 93–100% and NPV of 94–100% [3.67–3.69]. Although CCTA has a high NPV, image quality is lower in a substantial number of patients because of extensive calcifications or motion artefacts. In a study aiming to test an algorithm for sequential non-invasive CCTA and SPECT, half of the patients still required MPI following initial CCTA [3.70]. Hybrid SPECT-CT systems equipped with components that allow sufficient resolution to perform CCTA are available. Current literature

data have demonstrated an improvement in sensitivity and PPV, as well as better localization of coronary stenosis in comparison with either invasive coronary angiography or the analysis of both image sets when done separately. One study reported a sensitivity of 96%, specificity of 95%, PPV of 77% and NPV of 99% for detecting haemodynamically significant stenosis [3.71], followed by additional studies with similar values [3.72, 3.73]. Hybrid SPECT/CCTA led to the same patient management when compared with the gold standard of invasive coronary angiography [3.74].

When MPI is combined with a CT scan for AC, CAC or CCTA, the patient is exposed to additional radiation. This varies from 0.5 mSv to 1.0 mSv for CT-AC. Absorbed doses from the CT component for performing CAC and CCTA depend on the imaging system and protocol used. For CAC measurements, these are estimated to be below 1 mSv. The absorbed dose for CCTA is estimated at 2–5 mSv using commonly available single source 64-slice CT scanners with a prospectively electrocardiogram triggered step-and-shoot acquisition protocol. The latest generation dual source or 256- and 320-slice single source CT scanners enable even lower absorbed doses of less than 1 mSv [3.75, 3.76].

Following the use of diagnostic CT components as part of the cardiac SPECT–CT study, detection of clinically significant incidental findings such as pulmonary arterial dilatation has been reported. These findings can provide an explanation for the patient’s symptomatology, unrelated to CAD [3.77].

New tests have been recently introduced in nuclear cardiology, addressing a number of clinical indications other than CAD. Technetium-99m-labelled 3,3-diphosphono-1,2-propanodicarboxylic acid (DPD) scintigraphy can provide a reliable diagnosis of transthyretin related cardiac amyloidosis (ATTR). While visual assessment of ^{99m}Tc -DPD uptake in comparison with the intensity of tracer activity in the skeleton is used as a rule, a quantitative approach can potentially provide a more precise tool for diagnosis, risk stratification and therapy evaluation. Myocardial ^{99m}Tc -DPD SUV_{max} and SUV_{peak} were measured using SPECT–CT of the thorax and showed a good correlation with the visual assessment score. Quantitative SPECT–CT also allowed a good separation of cardiac ^{99m}Tc -DPD uptake values between normal subjects and patients with ATTR amyloidosis [3.77, 3.78]. A promising new indication, still evaluated mainly in research projects, is the use of cardiac SPECT–CT with ^{123}I -metaiodobenzylguanidine (^{123}I -mIBG) to identify ganglionated plexi prior to ablation in patients with paroxysmal atrial fibrillation [3.79] An additional novel approach uses SPECT–CT with ^{123}I -mIBG to assess and quantify right ventricular sympathetic dysfunction in patients diagnosed with arrhythmogenic cardiomyopathy [3.80] (Table 3.2).

TABLE 3.2. SUMMARY OF CARDIAC SPECT–CT LITERATURE

SPECT–CT indications	No. papers (2008–2019)
Diagnosis of CAD	3
Value of attenuation correction	5
CT parameters for cardiac SPECT–CT	9
Calcium score	3
CCTA	6
Quantitation	5
Cardiac I-123-mIBG uptake	3
Cardiac amyloidosis assessment	2
Novel technology assessment	6
CZT devices	4
New collimation	1
Respiratory motion correction	1
Radiation exposure reduction	4
Incidental CT findings	1

CAD — coronary artery disease; CCTA — cardiac computed tomography angiography; CZT — cadmium-zinc-telluride.

3.4. SPECT–CT IN PNEUMOLOGY

3.4.1. Pulmonary embolism

3.4.1.1. Acute pulmonary embolism

Lung perfusion (Q) or combined ventilation and perfusion (V/Q) scintigraphy is a popular scan in the workup of patients with suspected acute pulmonary embolism [3.81–3.84]. However, on conventional planar imaging (2-D) there is overlapping of information originating at different depth levels within the lungs. Distinguishing between anatomical segments is challenging and it is therefore difficult to determine the extent of embolic involvement, even if oblique views are used to better define the lung lobes or segments with V/Q abnormalities [3.85, 3.86]. Furthermore, in the traditional Prospective

Investigation of Pulmonary Embolism Diagnosis (PIOPED) approach, planar V/Q scans are reported with a probabilistic approach with a relatively high rate of indeterminate cases [3.87–3.89], which may not be helpful for decision making in the emergency setting of acute pulmonary embolism [3.90, 3.91].

Following the development and wide availability of multidetector CT technology, also in the emergency setting, contrast CT pulmonary angiography (CTPA) has started to gradually replace planar V/Q scans as the modality of choice for diagnosis of pulmonary embolism worldwide. Literature data have shown that CTPA has a high sensitivity associated with sufficient specificity for pulmonary embolism [3.92]. In addition to its overall satisfactory diagnostic performance, the ability to also use CTPA in emergency settings explains a declining trend that was observed between the years 2000 and 2008 in the use of pulmonary scintigraphy as the first-line diagnostic test in patients with clinical suspicion of acute pulmonary embolism [3.93]. Many nuclear medicine centres are not equipped to perform pulmonary scintigraphy ‘after hours’ on a 7 days a week, 24 hours a day basis.

However, CTPA suffers from some limitations, including technical artefacts (motion artefacts, image noise due to body habitus, etc.), contrast allergy, contraindication in patients with poor renal function and radiation dose (of particular concern in younger women) [3.94, 3.95]. Furthermore, concern is rising about possible overdiagnosis and overtreatment of pulmonary embolism, with the associated risk of adverse side effects, in patients in whom CTPA detects subsegmental pulmonary embolism that in several instances is not clinically relevant [3.96–3.99].

V/Q SPECT is reported to be useful particularly because 3-D imaging overcomes problems of segmental overlaps and shinethrough effects while accurately defining the location and size of perfusion defects [3.100]. These features have considerably enhanced the diagnostic accuracy of the V/Q scan, most likely because of the favourable results that can be obtained by radionuclide tomographic imaging in the intrathoracic space, a body region characterized by a relative paucity of anatomical structures (excluding the mediastinum). SPECT has higher sensitivity, specificity and interobserved agreement than planar scintigraphy [3.101, 3.102]. A preclinical study in an animal model of acute pulmonary embolism in a pig showed that V/Q SPECT has higher sensitivity and specificity (100% and 96%, respectively) than planar imaging (85% and 78%, respectively) [3.103]. Nonetheless, V/Q SPECT still has lower specificity than CTPA [3.104–3.106]. The advantages of employing V/Q SPECT rather than planar scintigraphy and/or CTPA for the diagnosis of acute pulmonary embolism have been confirmed by a number of investigators [3.101, 3.107, 3.108].

For application in benign pulmonary disorders, the CT component of a SPECT–CT scan is typically ‘low dose’ as it serves for attenuation correction and

for anatomical localization purposes [3.109, 3.110]. Nonetheless, even a CT scan that would be considered technically ‘non-diagnostic’ according to radiological standards increases the specificity of the V/Q scan, since it can satisfactorily characterize lung comorbidities and can thus clarify the source of abnormalities seen on the radionuclide component of the study [3.106–3.108], providing alternative diagnoses justifying the signs or symptoms that had raised the clinical suspicion of acute pulmonary embolism.

Clinical interest in lung scintigraphy (including SPECT–CT), despite the competition of CTPA, is demonstrated also by the data shown in Fig. 3.1, which plots the number of yearly downloads through PubMed of articles dealing with the use of V/Q scintigraphy for diagnosing pulmonary embolism. In this regard, it must be noted that, after the peak reached in 1999, an obvious decline can be observed — most likely associated with the growing use of CTPA in the clinical emergency setting. Nonetheless, this declining trend has subsequently plateaued and even risen moderately since 2015, when virtually all publications on V/Q scintigraphy concerned the use of either V/Q SPECT–CT or (even more often) stand-alone V/Q SPECT. The overall excellent diagnostic performance of V/Q SPECT or V/Q SPECT–CT also justifies their use in the emergency setting of suspected acute pulmonary embolism, as recommended by guidelines issued by the European Association of Nuclear Medicine in 2009 [3.105, 3.106] and updated in 2019 [3.111].

A systematic review and meta-analysis published in 2016 concluded that the diagnostic performance of V/Q SPECT–CT is superior in most clinical settings to that of CTPA, planar scintigraphy and stand-alone V/Q SPECT [3.112]. In particular, the pooled sensitivity of V/Q SPECT–CT for diagnosing acute



FIG. 3.1. Plot of the number of yearly downloads versus time in the period 1965–2020 for articles describing V/Q scintigraphy in patients with pulmonary embolism.

pulmonary embolism was 97.6%, with a 95.9% specificity, 93% PPV, 98.6% NPV and 96.5% overall diagnostic accuracy. Shortly afterwards, a cost effectiveness modelling study based on prior literature quantified the potential economic value of V/Q SPECT–CT versus CTPA, planar V/Q scintigraphy and V/Q scintigraphy with stand-alone SPECT. The authors concluded that SPECT–CT confers superior economic value versus the other imaging modalities, thanks primarily to improved sensitivity and specificity as well as to lower rates of non-diagnostic scans [3.113]. Recent data further confirm the clinical advantages of V/Q SPECT–CT in patients with suspected acute pulmonary embolism [3.114–3.118].

3.4.1.2. Chronic pulmonary embolism

Chronic thromboembolic disease is the most frequent cause of pulmonary hypertension, a clinical condition that, if undetected and untreated, can severely impair the quality of life of patients and is burdened with a high rate of complications, not rarely leading to premature death [3.119]. The diagnosis of this condition remains challenging, primarily because of the lack of early clinical signs and because of the overlap with signs and symptoms suggesting other cardiopulmonary conditions [3.120]. In this scenario, the use of CTPA alone is not optimal for patient management, both because lung scintigraphy is more accurate for detecting segmental or subsegmental perfusion defects [3.121–3.123] and because follow-up of the condition during treatment is based on repeat evaluations during treatment — a procedure that would direct unnecessarily high radiation doses to the patient if performed with repeat CTPA. A recent study based on the use of state of the art contemporary CT scanners has reported that, although reduced with respect to earlier generation CT scanners, the radiation dose to the breast during CTPA is still over five times higher than that delivered during a V/Q SPECT scan, with a total effective dose that is approximately 20% higher for CTPA than for V/Q scans [3.124].

The most recent studies published on the use of V/Q SPECT–CT in patients with pulmonary hypertension caused by chronic thromboembolic disease [3.125–3.128] showed the overall superiority of the hybrid imaging procedure versus CTPA. It is to be noted that, even when the main focus of the study is optimization of various CT based techniques, the V/Q SPECT–CT scan is considered the ‘gold standard’.

3.4.2. Non-embolic diseases

Perfusion only or V/Q scans are often used in several non-pulmonary embolism applications [3.107] in order to:

- (a) Optimize radiotherapy fields in lung cancer patients so as to minimize radiation damage to normal pulmonary parenchyma;
- (b) Provide pre-operative quantification of lung function (adult and paediatric patients);
- (c) Assess inhomogeneity of ventilation in patients with emphysema;
- (d) Assess regional changes in asthma;
- (e) Estimate regional lung function, with particular attention to interstitial pulmonary disease.

External beam radiation therapy is reported to improve survival in lung cancer. However, the normal lung is highly sensitive to radiation, and radiotherapy often leads to radiation pneumonitis and fibrosis. The dose administered to the tumour in order to spare the surrounding normal parenchyma therefore needs to be limited [3.129–3.132]. There is a relative decrease in lung function post-radiotherapy, often dose dependent, reported to peak around 12–18 months after treatment [3.133, 3.134]. A baseline perfusion and/or ventilation scan is useful in identifying areas of either preserved or reduced function. The ventilation scan can also be used to plan therapy [3.135]. Experience with the use of SPECT–CT for radiotherapy planning in patients with lung cancer builds upon the vast evidence gathered with the use of perfusion and/or ventilation stand-alone SPECT in this scenario. Bucknell et al. published in 2018 a systematic review and meta-analysis of the role of functional lung imaging with perfusion and/or ventilation/perfusion scintigraphy for radiation therapy planning in patients with lung cancer [3.136]. The authors analysed a total of 114 publications in which methods of identifying functional lung volumes included CT, MRI, SPECT and PET to assess ventilation and/or perfusion. They concluded that, despite significant heterogeneity in approaches and reporting, functional lung imaging with any of the above methods (including, especially, perfusion and/or ventilation SPECT) has the potential of optimizing radiation therapy planning and delivery. Among more recent studies on the use of SPECT–CT in diagnosing lung cancer, Lee et al. reported that anatomical and functional data derived from perfusion SPECT–CT were useful to explain differences in outcome (i.e. to discriminate between patients with and without radiation pneumonitis, respectively, especially when combined with a PET–CT scan using ^{18}F fluorodeoxyglucose (FDG)) PET–CT[3.137]. Thomas et al. employed serial perfusion SPECT–CT to characterize the dose-perfusion response in two groups of patients submitted

to radiation therapy and treated with and without a functional lung avoidance technique, respectively. This study suggested that in selected patients radiotherapy planning based on the functional lung avoidance approach promotes increased post-radiotherapy perfusion to low dose regions [3.138]. In a somewhat different clinical scenario, Liss et al. used attenuation-corrected SPECT–CT to quantify changes in lung perfusion following radiation therapy of the breast/chest wall in patients with breast cancer. Perfusion SPECT–CT demonstrated that radiation therapy decreased lung perfusion with a clear dose–effect relationship [3.139].

In patients undergoing lung reduction surgery, perfusion imaging can be used to assess function and to estimate the potential impact of surgery on residual pulmonary function. Although planar V/Q scans have traditionally been used to assess the contribution of each region, this approach is not optimal, both because of overlapping of pulmonary lobes and segments, and because of the fact that the anatomy might differ between patients. Recently, perfusion and/or ventilation SPECT–CT were used to assess regional pulmonary function with a 3-D mode approach that helps in identifying and delineating the lung segments more accurately [3.140–3.146]. All such studies confirm the accuracy of SPECT–CT imaging for delineating the functional anatomy of the lungs, on a segmental and subsegmental basis, as a predictor of residual pulmonary function after lung reduction surgery.

Finally, in the case of miscellaneous pulmonary conditions, SPECT–CT often serves as the reference gold standard to validate other imaging techniques [3.147–3.150].

3.5. SPECT–CT IN ORTHOPAEDICS

3.5.1. Benign bone diseases

The musculoskeletal system is affected by various benign and malignant conditions. In general, patients present with intermittent or chronic pain. Conventional radiological imaging modalities such as ultrasound, MRI and CT are used in the assessment of pain in symptomatic patients. MRI provides useful information related to soft tissues, CT provides excellent anatomical details of the skeleton and ultrasound is useful to assess superficial structures and small effusions. However, these techniques are often prone to artefacts (e.g. magnetic susceptibility artefacts in MRI or beam-hardening artefacts in CT) [3.151, 3.152]. There are several hardware and software based artefact reduction solutions available that improve image quality [3.152].

Bone SPECT–CT with ^{99m}Tc -MDP is reported as useful in the assessment of musculoskeletal pathology both in pre- and post-operative scenarios. Current

evidence favours its use in chronic settings and in cases when cross-sectional imaging techniques are indeterminate [3.151–3.154]. Bone SPECT–CT provides valuable information, such as localization and characterization of bone abnormalities, and in most cases identifies the potential pain generators. The addition of arthrography to SPECT–CT of wrist, ankle and knee joints has been shown to provide useful supplementary information for the detection of lesions in cartilage, ligaments, the triangular fibrocartilage complex, the meniscus or loose bodies [3.155]. Quantitative bone SPECT–CT is evolving, and several reports have suggested that it is a promising objective tool in the assessment of arthropathies [3.156].

The common indications for bone SPECT–CT include evaluation of symptomatic joints in the pre-operative scenario, as well as localization, characterization and assessment of post-operative complications. Bone SPECT–CT plays a complementary role, in most cases with equivocal MRI findings.

3.5.1.1. Bone SPECT–CT of the spine

Lower back pain is common and increases in frequency and severity with age. The treatment of back pain often depends on clinical presentation. Imaging of patients with lower back pain in pre- and post-operative scenarios includes both conventional radiological and scintigraphic techniques. The understanding of the tracer uptake pattern of physiological and post-operative remodelling is always challenging, in part because of complex pathophysiology. In patients with lower back pain, bone SPECT–CT is useful in the localization and characterization of degenerative disease such as facet joint arthropathy or disc degeneration. In patients with chronic lower back pain, SPECT–CT is useful (a) for accurate localization of metabolically active facet joints, (b) to localize alternate metabolically active sites in the spine [3.157–3.159], (c) as a supporting tool in the clinical workup/diagnosis and (d) to guide therapy [3.160]. In general, imaging plays an important role in the assessment of patients after spine surgery. Post-operative imaging helps in the assessment of (a) position of implants, (b) status of implants, (c) bone fusion progression/integration, (d) adequacy of implant, (e) new sites of disease, (f) disease progression and (g) complications [3.161].

The current evidence regarding the use of bone SPECT–CT in the assessment of post-operative back pain is limited but evolving [3.152]. Bone SPECT–CT is useful in the assessment of complications related to spine surgery, such as hardware failure, pseudoarthrosis (non-union), adjacent segment degeneration (e.g. facet joint or endplate degeneration), instability, spondylolisthesis or infection [3.162–3.164]. Recurrent pain after lumbar spine surgery is due to multiple causes. Identifying the pain generator on imaging

studies is challenging. Furthermore, not all structural and functional changes can be translated into clinical symptoms or pathology. In a retrospective study of patients with recurrent back pain following lumbar arthrodesis, bone SPECT-CT is reported to be sensitive and specific for the confirmation or exclusion of screw loosening [3.165]. In patients with pelvic girdle pain, bone SPECT-CT has shown altered metabolic activity around the sacroiliac joint in patients with sacroiliac joint dysfunction, and a diagnosis of sacroiliac joint incompetence was made with a sensitivity, specificity, PPV and NPV of 95%, 99%, 99% and 94%, respectively [3.166]. The presence of non-specific tracer uptake in pseudoarthrosis is challenging. It is often seen secondary to healing or remodelling. The increased tracer uptake at the site of intervention might persist for 3–6 months post-surgery [3.167]. Based on serial bone scans, Gates et al. have reported a steady decrease in tracer activity at around three months after surgery [3.168]. Further reports suggest that the highest tracer uptake is often seen up to one month after surgery, and that it generally plateaus around two months. However, the tracer uptake might persist for several years after an intervention [3.169]. In the post-operative scenario, persistent tracer uptake beyond one year favours the diagnosis of pseudoarthrosis. Lucency with increased metabolic activity on bone SPECT-CT scans suggests loosening. Bone SPECT-CT is reported to have a sensitivity of 90% and specificity of 100% in detecting screw loosening [3.170]. Lastly, it is important to check SPECT and CT image co-registration to avoid misdiagnosis of the site of altered metabolic activity (facet joints vs uptake in the screws) [3.152]. Bone SPECT-CT is useful in both pre-operative and post-operative back pain and should be used routinely as an adjunct to conventional imaging techniques, especially in symptomatic patients with indeterminate findings on cross-sectional imaging.

3.5.1.2. Bone SPECT-CT in wrist and hand

Accurate diagnosis of the cause of wrist and hand pain is challenging because of the complex regional anatomy. The advantages of using bone SPECT-CT include localizing altered or abnormal sites of metabolic activity and detecting post-traumatic bone remodelling and occult fractures [3.171]. Bone SPECT-CT is reported to be useful in the detection of occult fractures compared with CT alone [3.172]. Bone SPECT-CT has also been shown to be of value in the visualization of the scapholunate and lunotriquetral ligaments, triangular fibrocartilage complex and articular cartilages when SPECT-CT is combined with CT arthrography [3.173]. Bone SPECT-CT provided higher lesion detection rates compared with X ray and planar scintigraphy [3.174]. In addition, the specificity of SPECT-CT was found to be relatively higher than MRI in patients with non-specific pain of the hand and wrist [3.175].

3.5.1.3. *Bone SPECT–CT in hip and knee*

Patients often experience pain in the hip or knee after the respective joint replacement. Detecting the source of pain in post-operative joints is always challenging. In general, X ray is the first and most common method used to assess complications. The conventional two- or three-phase bone scan is requested to confirm or refute septic or aseptic loosening in these patients. If there is a suspicion of infection on a two- or three-phase bone scan, assessment is often supplemented with a radiolabelled white blood cell scan and ^{99m}Tc -sulphur colloid bone marrow scans for confirmation. It is not always easy to interpret the scans in binary fashion, and the non-specific tracer activity on a bone scan (planar or SPECT) is a limitation. The CT component of SPECT–CT can be helpful in localizing the potential pain generators (e.g. osteolysis, fracture, calcification, ossifications or joint effusion). The different patterns of tracer uptake on bone SPECT–CT in both symptomatic and asymptomatic patients with total hip arthroplasty were evaluated by Schweizer et al., who reported the presence of increased tracer uptake that significantly correlates with symptoms [3.176].

Bone SPECT–CT is also used in the evaluation of bone viability and compared with MRI findings. MRI and bone SPECT–CT have been shown to be complementary and allow reliable differentiation between viable and non-viable bone tissue [3.177]. Barthassat et al. evaluated patients with painful total hip arthroplasty using a novel SPECT–CT localization scheme and a semiquantitative 3-D volumetric quantification method for the assessment of bone tracer uptake. The localization scheme had a high inter- and intra-observer reliability [3.178]. In patients with knee pain following knee replacement, bone SPECT–CT was found to be useful for evaluating patello-femoral disorders [3.179]. Bone SPECT–CT was used to evaluate patients with symptomatic and asymptomatic knees after bilateral total knee arthroplasty (TKA) and it identified typical tracer uptake patterns in both groups, which was helpful in accurately assessing their symptoms in order to provide optimal management [3.180]. In symptomatic patients after anterior cruciate ligament reconstruction, bone SPECT–CT provided additional information related to bone remodelling, graft incorporation or insufficiency [3.181, 3.182]. In patients with contraindications to MRI, bone SPECT–CT arthrography could be a promising alternative technique to assess internal derangement of joints [3.183].

In patients with pain, swelling or stiffness after TKA, bone SPECT–CT changed the clinical diagnosis and final treatment in 65% of cases [3.184]. In a recent study, blood pool SPECT is reported to outperform the planar assessment of painful knee replacement. Distinct uptake patterns have been reported to be used as a biomarker in the assessment of prosthesis survival and biomechanical functioning. Blood pool SPECT has improved the prognostic value of late phase

SPECT–CT for the assessment of the medial tibial region [3.185]. Overall, bone SPECT–CT is useful and increases the diagnostic accuracy in assessing aseptic and septic loosening of hip and knee prostheses when compared with conventional three-phase bone scans and SPECT [3.186–3.188]. In addition, bone SPECT–CT is also useful in the follow-up of patients after realignment procedures, osteotomies, de-loader devices or insoles, as it reflects the specific loading pattern of the knee with regard to its alignment [3.189]. In the assessment of bone viability, SPECT–CT has been found to be reliable in differentiating viable and non-viable bone tissue with a sensitivity and specificity of 90% and 94%, respectively [3.190].

Overall, bone SPECT–CT is reported to be a cost-saving test when compared with CT or metal artefact reduction sequence magnetic resonance imaging (MARS-MRI) in patients with recurrent and persistent knee pain after TKA. Out of 1000 TKA patients, diagnostic bone SPECT–CT was expected to lead to three year cost savings of up to \$1 867 695 versus CT (or \$622.6 per patient per year) and \$1 723 435 versus MARS-MRI (or \$574.5 per patient per year) [3.191]. Therefore, bone SPECT–CT should be used in the assessment of patients with knee pain after TKA.

3.5.1.4. Bone SPECT–CT in foot and ankle

Accurate assessment of foot and ankle pain is often challenging because of the complex anatomy of small bone and joint structures. In general, clinical evaluation and radiological imaging are limited in localizing the pain generators. Patients present with pain one year after foot surgery in approximately 20% (at rest) and 40% (during walking) of cases [3.192]. Plain X ray and CT are routinely used but are insufficient to assess persistent pain after foot and ankle surgery. In the post-operative scenario, MRI provides insufficient image quality secondary to metallic artefacts. Nathan et al. have reported a change in management of nearly 75% of cases following the use of SPECT–CT to assess pain [3.193]. Bone SPECT–CT is useful for the localization and characterization of abnormal increased metabolic activity in patients with foot and ankle pain in both pre- and post-operative scenarios, including cases such as fractures, infection, non-union, accessory sesamoids and tarsal coalition [3.194]. Ha et al. compared the diagnostic role of SPECT–CT and MRI in patients with ankle and foot pain to assess lesion types, and found SPECT–CT and MRI to provide comparable diagnostic accuracy for symptomatic lesions. These two modalities can be used as complementary imaging methods to further improve the specificity [3.195]. Bone SPECT–CT was found to be useful in localizing and characterizing impingement syndromes and soft tissue pathology in patients with ankle or foot pain [3.196]. Singh et al. reported modification of the treatment

plan in most patients when bone SPECT–CT was used to assess foot and ankle pain [3.197]. Bone SPECT–CT is reported to be useful in assessing the varus and valgus maligned hind foot [3.198].

3.5.1.5. Bone SPECT–CT in shoulders and elbow

Bone SPECT–CT might be useful in the assessment of mechanical complications following shoulder surgery, such as glenoiditis after hemiarthroplasty, glenoidal loosening after total shoulder arthroplasty and scapular notching after reverse shoulder arthroplasty. However, the evidence for the role of SPECT–CT in post-operative shoulder is limited and is evolving [3.154, 3.199, 3.200].

The advantages of bone SPECT–CT include accurate localization of the altered metabolic activity, characterization of hypermetabolic foci, improved sensitivity and specificity, accurate diagnosis, localization of alternate pain generators, decrease in the number of equivocal results and higher reporting confidence. The limitations include additional radiation, lack of standardized acquisition protocols, limited structured imaging pathway and lack of structured training.

In summary, bone SPECT–CT is useful in the assessment of painful conditions related to benign bone diseases in both pre- and post-operative scenarios. However, it is important to get good clinical details. Close collaboration with referring physicians is vital in setting up a diagnostic pathway. Understanding and recognizing normal variants and documenting relevant abnormal findings can improve patient outcomes and boost the confidence of referring clinicians to use bone SPECT–CT in their clinical practice.

3.5.2. Malignant bone disease

Bone metastases occur frequently in breast, prostate, lung and renal carcinomas, and they reduce survival rates significantly (for reviews, see Refs [3.201, 3.202]). Their occurrence depends on some risk factors and, in particular, on tumour stage. Although less than 2.6% of patients affected by low stage breast cancer harbour bone metastases, those with higher stages have a risk between 16.8% and 40.5% [3.201, 3.202]. Roughly 16% of men suffering from prostate cancer with prostate specific antigen serum levels higher than 10 ng/ml or a Gleason score greater than or equal to 8 carry osseous deposits [3.201, 3.202]. Bone pain is considered a risk factor for skeletal metastases in cancer patients.

Bone scintigraphy is suboptimal in detecting purely lytic metastases, such as in renal cancer or lymphoma. Typical indications for bone scintigraphy are breast and prostate cancer, as well as primary bone tumours such as Ewing

sarcoma or osteosarcoma. In bronchial carcinoma, PET with ^{18}F -FDG has replaced bone scintigraphy in most countries at present. The development of radiopharmaceuticals binding to the prostate specific membrane antigen (PSMA) might replace bone scintigraphy in this entity, as PSMA-SPECT-CT has been reported to have a higher accuracy in staging prostate cancer [3.203].

Most studies investigating the accuracy of bone scintigraphy lack a gold standard. Its sensitivity ranges between 85% and 96%, higher in prostate than in breast cancer (for reviews, see Refs [3.202, 3.204, 3.205]). A recent meta-analysis compared literature sensitivity and specificity values for planar bone scintigraphy, bone SPECT, FDG-PET and MRI in detecting vertebral bone metastases [3.206]. In this analysis, the pooled per-patient sensitivity and specificity of SPECT were 90.3% and 86%, respectively. Its sensitivity was not markedly different from that of FDG-PET and MRI, but was significantly higher than that of CT and planar bone scintigraphy. The per-patient specificity of SPECT was significantly higher than that of FDG-PET, but significantly lower than that of planar bone scan, CT and MRI, which did not differ significantly.

The spatial resolution of planar and/or SPECT cameras is limited, between 7 mm and 15 mm, and reduces the sensitivity of bone scintigraphy (for a review, see Ref. [3.207]). Very small osseous metastases may, therefore, escape detection by bone scintigraphy. However, it is not only the size that counts, but also the signal-to-noise ratio. In the case of very high uptake occurring (e.g. in osteoblastic metastases of prostate cancer), deposits smaller than 1 cm in diameter may be visualized by bone scintigraphy, whereas metastases with low metabolic activity, such as predominantly osteolytic metastases of breast cancer, may elude detection, even when larger than 1 cm. Lytic processes are, on the other hand, well visualized on the CT images of SPECT-CT, thus increasing the sensitivity of this hybrid imaging method in comparison with stand-alone scintigraphy. However, thorough research investigating this issue is absent to date.

Bone marrow infiltration is the first step in osseous involvement. When the neoplastic cells infiltrating bone marrow also invade the osseous tissue, bone metabolism increases. Only then may they be diagnosed by skeletal scintigraphy. CT visualizes osseous metastases only when considerable amounts of osseous tissue have been destroyed. MRI and scintigraphy using tumour specific radiotracers focus on visualizing the neoplastic lesions specifically and are thus, at least in theory, more sensitive than bone scintigraphy and CT [3.203, 3.206, 3.208].

Bone scintigraphy has a rather low specificity to detect bone metastases (for a review, see [3.209]), as a variety of benign conditions are accompanied by hypermetabolism. In particular, in older patients, degenerative diseases of the skeleton such as spinal osteochondrosis and facet joint osteoarthritis are quite frequent. Contrary to metastases, hypermetabolic foci due to degenerative

processes are joint related and also have a typical morphology on CT. This explains why bone scintigraphy for staging malignant disease gains considerably by the addition of CT. Further benign differential diagnoses of a hypermetabolic focus are vertebral fractures or benign bone tumours, which, in their majority, can also be readily diagnosed on CT images.

Since the advent of SPECT–CT, some evidence has been published on its utility for staging. A PubMed search (2008–2019) using the keywords ‘SPECT–CT bone metastases’ yielded 413 hits. Many hits corresponded to publications using planar bone scan and stand-alone SPECT, reviews and case reports or studies performed with tracers other than radiolabelled polyphosphonates. For this review, 39 original articles actually reporting on the value of skeletal SPECT–CT in cancer patients were selected.

At least 17 papers analysed how many of the unclear lesions seen on stand-alone planar/SPECT imaging could be elucidated by SPECT–CT [3.208, 3.210–3.226]. The studies have some methodological heterogeneities. Despite this, the results obtained are remarkably consistent. SPECT–CT allows for a definitive diagnosis of 66.7% to 100% of lesions deemed equivocal on conventional nuclear medical imaging. Weighted by the number of equivocal lesions, the average rate of precise characterization was enabled in 87.6% of the total 1183 lesions studied. Utsunomiya et al. also reported a higher diagnostic confidence for fused SPECT–CT image datasets than for side by side viewing of images from SPECT and CT [3.227].

Furthermore, these and several additional publications provide data on the sensitivity and specificity of stand-alone nuclear medicine procedures and compare them to those of SPECT–CT and some other imaging modalities [3.208, 3.213, 3.215, 3. 219, 3.223, 3.224, 3.226, 3.228–3.233]. With the exception of the findings in Fonager et al. [3.230], the diagnostic accuracy of SPECT–CT is higher than that achieved by stand-alone nuclear medicine imaging. As expected, and already discussed above, the performance of SPECT–CT was inferior to that of whole body MRI in the one study that compared them [3.208]. Interestingly, the two studies comparing SPECT–CT with ¹⁸F-fluoride-PET–CT had contradictory results [3.208, 3.230].

A new perspective for skeletal scintigraphy is whole body SPECT–CT substituting for planar whole body imaging. At least four publications compared the diagnostic yield of whole body or two bed position SPECT–CT to that of whole body scintigraphy accompanied by single position SPECT–CT. Guezennec et al. found only a limited incremental diagnostic value of double bed SPECT–CT over single bed SPECT–CT [3.221]. Whole body SPECT outperformed whole body scintigraphy in a publication by Abikhzer et al. [3.234]. Weissinger et al. reported that their SPECT–CT-only protocol involving three bed positions did not prolong acquisition time significantly compared with the standard approach

and was able to detect more lesions than planar acquisition in a group of 50 patients with high risk prostate cancer [3.235]. In 212 consecutive patients with a history of cancer, whole body SPECT–CT had a significantly higher sensitivity than targeted SPECT–CT and whole body planar bone scintigraphy, but similar specificity [3.236]. On the whole, it thus seems sensible to substitute in the future skeletal whole body planar scans by a SPECT or SPECT–CT based approach, in particular, when fast acquisition protocols become available [3.237].

A further perspective is quantitative SPECT–CT (i.e. the ability of this technology to quantify tissue radioactivity concentration in absolute units). Its technical performance and its value for staging malignant disease using skeletal scintigraphy was reviewed in 2017 [3.237]. Using a research protocol [3.238], Cachovan et al. measured the radioactivity concentration in spongy bone of the vertebral bodies of women referred to bone scintigraphy and found an average value of 48.15 kBq/mL [3.239]. They reported a significant correlation between skeletal SUVs with the X ray densities of the vertebral bodies. This establishes an association between the osseous uptake of the polyphosphonates and the amount of metabolically active bone tissue. Fluorine-18-fluoride-PET–CT was shown to have SUVs in normal bony tissues similar to those reported by skeletal SPECT–CT, with a significant correlation [3.240]. This illustrates that quantitative skeletal SPECT yields information on bone metabolism similarly to ¹⁸F-fluoride PET.

As yet, normal ranges for skeletal uptake on bone SPECT–CT have not been established in the literature. In addition, discussion on standardization of the procedures involved is needed to establish threshold SUVs for clinical use. Nevertheless, some papers have used SUV values of bone SPECT–CT to distinguish benign from malignant skeletal lesions. In a multicentre study, the clinical performance of quantitative SPECT–CT to characterize hypermetabolic foci has been investigated [3.241]. Patient data from 72 subjects from three US and two German institutions were pooled and analysed by ten physicians independently. The gold standard was a final consensus read. For non-joint lesions greater than 6 mm in size, the diagnostic accuracy was high when using SUV thresholds of 9.28 or 9.68, depending on the type of reconstruction. Kuji et al. showed in 170 patients with prostate cancer that maximal SUVs measured in metastases, 40.9 ± 33.46 , were significantly higher than those measured in degenerative lesions (16.73 ± 6.74 [3.242]). Malignant foci could be distinguished from benign lesions with high diagnostic accuracy. In 264 bone metastases of prostate cancer, Tabotta et al. reported SUVs of 34.6 ± 24.6 , significantly higher than those measured in benign osteoarthritic lesions amounting to 14.2 ± 3.8 [3.243]. Using a SUV_{max} threshold of 19.5, these authors found a sensitivity and specificity of 87% and 92%, respectively, to differentiate benign from malignant foci. Also, in prostate cancer, Rohani et al. reported an SUV_{max}

of 20 as the discrimination threshold to achieve a sensitivity and specificity of 73.8% and 85.4% to differentiate degenerative from neoplastic foci [3.244]. It should, nevertheless, be noted that the evidence summarized above pertains to osseous metastases of prostate cancer only. It cannot readily be extrapolated to other tumours such as breast cancer, because those metastatic deposits might not engender uptake values of the same magnitude as prostate neoplasms.

Quantitative SPECT–CT has also been used to determine total tumour load with the intention of creating a variable facilitating monitoring skeletal involvement under therapy. Umeda et al. used an SUV threshold of 7 to segment metastatically involved bone [3.245]. Fiz et al. developed an analogous approach and showed that the calculated segmentation based tumour load correlated with radiological and laboratory indices reflecting tumour expansion [3.246]. The behaviour of bone metastases is difficult to assess longitudinally by medical imaging for the following reasons. The size of osteolytic lesions is difficult to measure on CT or MRI as their borders are usually ill defined. Using these modalities, it is also not possible to reliably diagnose the viability of blastic foci, since sclerosis is also a sign of bone healing. Bone scintigraphy is, in principle, suited to provide information on at least the regression of malignant skeletal foci, but changes in activity are difficult to assess by visual interpretation only. Beck et al. showed in a small group of subjects that errors in assessing the activity of metastases occurred in every third patient when visual evaluation was compared with quantitative SPECT–CT as the reference standard [3.241]. When monitoring osseous metastases with bone scintigraphy, the so-called flare phenomenon also has to be considered. This represents a transient increase in uptake due to healing of a metastasis, which could be misinterpreted as disease progression or non-response to therapy [3.247]. No paper has as yet correlated SUV changes determined by quantitative SPECT–CT with clinical response to therapy or patient survival. However, a prospective study using ¹⁸F-fluoride-PET–CT for this purpose in metastatic prostate cancer disclosed a highly significant correlation of PET response with progression free survival [3.248]. This suggests that skeletal SPECT–CT also bears considerable potential in this regard.

3.6. SPECT–CT IN INFLAMMATION

Infectious diseases are a major health care issue. While diagnosis of an infectious process is based on clinical and laboratory data, localization of disease foci can be difficult. Over the years various infection-seeking radiotracers, including many single photon emitting radioisotopes, have been developed. SPECT tracers applied in patients with known or suspected infectious processes include, first and foremost, autologous leukocytes (WBCs) labelled

with either ^{99m}Tc - or ^{111}In -oxine [3.249], and, to a lesser extent, radiolabelled antibiotics [3.250], antibodies [3.251, 3.252] and ^{99m}Tc -ubiquitin [3.253]. Gallium-67-citrate is still being used in some countries [3.254–3.257]. Over the last decades SPECT–CT has been applied in imaging of infection, combining functional studies with structural CT images. This enables both diagnosis of infectious processes, even in the early phases of the disease, as well as their precise localization. While scintigraphy is characterized by an inherent high sensitivity and NPV, further enhanced by SPECT, fused images improve the specificity, PPV and diagnostic accuracy. Although there has been a trend over the last decade in the direction of shifting hybrid imaging procedures for assessment of infection towards FDG-PET–CT [3.258], SPECT–CT is still a valid alternative.

Diagnosis of clinically suspected musculoskeletal infections and precise localization of known disease processes are optimized by the addition of anatomical landmarks. This is of value in cases when osseous involvement has to be proven or excluded in the presence of an adjacent soft tissue infection. The addition of CT can clarify the presence, localization and extent of the disease process in an area of complex anatomy, as well as in sites showing structural alterations following fractures, surgery or implants of medical devices. Initial studies with mixed patient populations have assessed the contribution of SPECT–CT with ^{111}In - or ^{99m}Tc -labelled WBCs or ^{67}Ga -citrate and have demonstrated an incremental value for hybrid imaging with higher performance indices than stand-alone procedures in up to one third of cases [3.251, 3.254, 3.259–3.261]. Technetium-99m-UBI 29-41 was also used in a mixed series of patients with musculoskeletal pathologies with a sensitivity, specificity, PPV, NPV and accuracy of 99%, 94%, 93%, 99% and 95%, respectively, for diagnosis of infection [3.253]. Subsequent studies have evaluated the role of SPECT–CT in particularly challenging clinical subgroups of patients with musculoskeletal pathologies.

Osteomyelitis has to be considered in any diabetic patient with a chronic, non-healing wound, occurring mainly in the feet. Labelled WBCs will identify the presence of infectious foci but lack the ability to diagnose osteomyelitis. SPECT–CT has made a significant impact in this patient group by confirming or excluding bone involvement in the presence of a known infectious process in adjacent soft tissues in over half of patients with diabetic foot [3.262–3.264], increasing mainly the specificity and PPV [3.265, 3.266]. Various imaging protocols, occasionally combining labelled WBC and bone SPECT–CT techniques [3.263, 3.264], and attempts to improve the prognostic value by quantification [3.266] have been advocated. Labelled WBC-SPECT–CT has been compared with and found to be superior to FDG-PET–CT [3.262], while similar to MRI [3.267], in assessing the diabetic foot. SPECT–CT has also been

used to monitor response to treatment, with high sensitivity and NPV but lower specificity and PPV for predicting the response of the infectious process at the end of antibiotic therapy [3.268, 3.269].

Diagnosis of spondylodiscitis is difficult and is often delayed or missed. Nuclear medicine procedures are used as an adjunct to MRI in this clinical setting. When available, FDG imaging is used successfully. Gallium-67-citrate remains the main SPECT tracer in spite of its known limitations. In combination with bone scintigraphy, ^{67}Ga SPECT–CT improves diagnostic accuracy in suspected spondylodiscitis, similar to MRI [3.256] but inferior to FDG-PET–CT [3.255]. Indium-111-biotin SPECT–CT was also found to be of value for localizing foci of spinal infection and for tailoring the therapeutic approach [3.250].

Differentiating aseptic loosening of a prosthetic joint from infection is important in order to define the correct treatment strategy. Technetium-WBC-SPECT–CT provided accurate anatomical localization of all infected knee and hip prosthetic joints and had high performance indices, with sensitivity, specificity, NPV and PPV of 100%, 90%, 100% and 88%, respectively. While the diagnostic accuracy of SPECT–CT using Tc-WBC reached up to 93%, it was somewhat lower using Tc-labelled antigranulocyte antibodies [3.252, 3.270, 3.271].

Diagnosis of osteomyelitis of the jaw [3.272] or skull [3.273] is more accurate with the use of SPECT–CT. Foci of infection could be localized to a specific bone in the base of the skull in half of the patients [3.273] and osteomyelitis could be diagnosed in cases with malignant otitis externa [3.274]. Dual isotope Tc-MDP bone and In-WBC-SPECT–CT were associated with a high diagnostic confidence to define the presence and depth of infected pelvic pressure sores [3.275].

Assessment of soft tissue infections is an additional important field where the use of radiotracers and hybrid imaging, specifically SPECT–CT, make a significant clinical impact. Soft tissue infections can have a challenging, non-specific clinical presentation, thus requiring extensive imaging, laboratory and invasive diagnostic procedures. As for musculoskeletal infections, the main single photon emitting tracers used for the assessment of soft tissue infections are WBCs labelled with either $^{99\text{m}}\text{Tc}$ or ^{111}In , and, to a lesser extent at present, ^{67}Ga [3.254]. SPECT–CT improves the diagnostic certainty by excluding the presence of clinically significant findings as the cause for equivocal foci of uptake detected on scintigraphy. For example, sites of WBC accumulation near major vessels or bowel loops can be differentiated from infectious foci in patients with suspected vascular graft, cardiac or abdominal infections, and abdominal ^{67}Ga activity can be easily identified as physiological bowel uptake, thus shortening time to diagnosis.

Vascular graft infection, although a relatively rare complication following stent implantation, is associated with significant morbidity. While CT angiography confirms the presence of vascular graft infection, scintigraphy using labelled WBCs plays a role in equivocal cases, in the early phases of the infection and in low grade processes. While scintigraphy can confirm or exclude the presence of infection, SPECT–CT will demonstrate whether a vascular graft is indeed involved or if the infectious process is limited to adjacent surrounding tissues, in particular in areas with crowded, complex anatomy and/or in the presence of post-surgical distortions [3.254, 3.276–3.278]. SPECT–CT reduced the number of false positive findings in 37% of patients and had a sensitivity and specificity of 100% as compared with 85% and 63%, respectively, for stand-alone SPECT [3.278]. Fluorodeoxyglucose-PET–CT and Tc-WBC-SPECT–CT were compared in patients on haemodialysis with suspected arteriovenous graft infection, a pathological entity that requires early treatment in order to avoid later removal of the infected stent. Early on, at approximately 10 weeks after graft implantation, the presence of abnormal FDG uptake foci had the highest diagnostic accuracy. At 20–30 weeks post-graft insertion, FDG and Tc-WBC imaging performed similarly, while later, at 40–50 weeks after surgery, the foci of Tc-WBC accumulation had a slightly higher diagnostic value than FDG abnormalities [3.279].

Scintigraphy is used in the assessment of patients with suspected infectious endocarditis and equivocal echocardiography. Hybrid imaging (SPECT–CT with Tc-WBC and FDG-PET–CT) allows for an accurate diagnosis and localization of cardiac and potential extracardiac sites of disease. These modalities are currently being performed routinely as part of the diagnostic workup [3.280, 3.281]. Technetium-WBC-SPECT–CT had high performance indices for diagnosis of infectious endocarditis, with a sensitivity of 90%, NPV of 94% and specificity and PPV of 100% [3.282]. It had, however, lower clinical utility scores for detecting extracardiac complications than FDG-PET–CT [3.281].

While the incidence of infections involving cardiac implantable electronic devices (CIEDs) is relatively low, they are also associated with significant morbidity and mortality. Technetium-WBC-SPECT–CT plays an incremental role in confirming or excluding the presence of disease in patients with suspected or known CIED infection, and furthermore in assessing its extent [3.282, 3.283]. WBC-SPECT–CT had a high sensitivity and NPV for diagnosis of CIED and determined whether the disease process was limited to either the pocket or leads, or if it involved both components [3.282]. SPECT–CT detected additional sites of previously unsuspected extracardiac foci of infection in up to 23% of patients and provided relevant information for tailoring the further therapeutic strategy [3.282, 3.283]. A study comparing PET–CT with labelled WBC-SPECT–CT in patients with suspected CIED infection demonstrated higher sensitivity and NPV but

lower specificity and PPV for FDG imaging [3.284]. In an additional study, both FDG-PET-CT and WBC-SPECT-CT showed high performance indices in patients with a final diagnosis of left ventricular assist devices. However, because of its higher sensitivity and easy logistics, FDG-PET-CT has been suggested as the first-line nuclear medicine procedure in this clinical scenario [3.285].

Additional radiotracers have been evaluated for the assessment of cardiovascular infections. Gallium-67 SPECT-CT has been used for the diagnosis of percutaneous driveline infection in patients with left ventricular assist devices. Increased tracer uptake was associated with higher one year event rates, including surgical interventions and hospital readmissions [3.286]. The performance of labelled granulocyte imaging was investigated in patients with suspected endocarditis. Technetium-99m-besilesomab-SPECT-CT had a sensitivity of 86–100% and a specificity of 100%, being of particular value in difficult cases with prosthetic valves or cardiac devices, as well as in patients with inconclusive echocardiography results, by identifying and localizing abnormal tracer uptake to a certain valve, prosthesis or device cable [3.287].

Following multiple case reports, a few series of studies have assessed the role of SPECT-CT in additional infectious processes. Gallium-67 SPECT-CT has been used to evaluate patients with fever of unknown origin, providing clinically significant information in over 40% of cases [3.254]. It had a sensitivity of 79% but was associated with a relatively high false negative rate, probably due to technical limitations related to the physical characteristics of this radiotracer [3.288]. In an additional study, ⁶⁷Ga SPECT-CT was contributory in 80% of patients with end-stage renal failure and in one third of patients after renal transplant, not only by diagnosing and localizing the infectious process, but also by correctly characterizing sites of physiological tracer activity [3.289].

These data from the literature, although still limited, demonstrate that SPECT-CT is an extremely important, clinically relevant tool for the early diagnosis and precise localization of infectious processes and can play an important role in patient management and changing outcomes (Table 3.3).

3.7. SPECT-CT IN ONCOLOGY

3.7.1. Thyroid cancer

The guidelines issued in 2015 by the American Thyroid Association [3.290] have revived the debate about the optimal modalities for managing differentiated thyroid cancer, in particular with respect to the selection of patients to whom to offer radioiodine ablation of post-surgical thyroid remnants according

TABLE 3.3. SUMMARY OF SPECT–CT IN MUSCULOSKELETAL, SOFT TISSUE AND VISCERAL INFECTIONS

SPECT–CT indications	No. papers (2008–2019)
<i>Musculoskeletal infections</i>	25
Mixed case population	6
Diabetic foot	9
Spondylodiscitis	3
Skull osteomyelitis	3
Infected joint prosthesis	2
Joint infection	1
Pelvic pressure sore	1
<i>Soft tissue infections</i>	16
Mixed case population	1
Vascular graft infection	5
Infective endocarditis	3
Cardiac devices	5
Fever of unknown origin	1
Renal transplant	1

to their risk stratification level based on clinical and histopathological information [3.291–3.294].

Although addressing this issue is outside the scope of this work, it must be emphasized that the information that whole body scintigraphy with radioiodine provides, particularly if performed at the completion of the ablation procedure (usually 3–7 days after administration of ¹³¹I-iodide), can indeed change the risk stratification level of patients as compared with that obtained using the clinical information available before ablation. This will thus directly influence the patient management strategy [3.291–3.295]. It is therefore increasingly recognized that SPECT–CT imaging provides crucial information and has an incremental diagnostic value over planar whole body scintigraphy (WBS) [3.296].

As with other types of scintigraphy with single photon emitting agents [3.297], the lack of anatomical landmarks and ill-defined body contour on planar WBS, and even more so on stand-alone SPECT, makes precise

identification of the location and aetiology of abnormal radioiodine uptake difficult. Therefore, there remains a substantial fraction of studies in which planar imaging alone yields difficult to interpret findings — the so-called ‘cryptic’ foci of radioiodine uptake [3.298]. SPECT–CT clarifies most of these equivocal cases, as it makes it possible to more precisely characterize ‘abnormal’ foci of uptake, considering that there are several possible causes of false positive radioiodine uptake, including benign processes, physiological variants, artefacts, contamination and non-thyroidal malignant lesions [3.299].

The added value of SPECT–CT for the management of patients with differentiated thyroid cancer after surgery has been explored through different approaches: (a) in the diagnostic pre-ablation setting, (b) during scintigraphy performed after administration of radioiodine for ablation of post-surgical remnants, (c) in the diagnostic setting to verify the success of ablation and (d) during scintigraphy performed after radioiodine therapy for recurrent/metastatic disease.

Besides occasional case reports, seven studies have been published on the added value of SPECT–CT imaging over planar WBS after administration of a diagnostic ^{131}I -iodide activity prior to the ablative dose of radioiodine [3.300–3.306], four of which come from the Ann Arbor group (Michigan, USA). The results of these studies consistently demonstrate the high incremental value of SPECT–CT over planar WBS, with the detection of unexpected neck lymph node metastases in approximately 30–44% of patients and distant metastases in approximately 4–10% of patients. These findings led to changes in intended management in 30–60% of patients, mostly consisting of the administration of radioiodine doses for ablation that were greater than those planned after risk stratification based on clinical or surgical data.

As expected, most studies (the majority of them including quite large patient groups) on the incremental value of SPECT–CT imaging over planar WBS have focused on the post-ablation scan, which is generally acquired 3–7 days after administration of radioiodine. A few of these studies focused on specific, limited issues of the post-ablation scan (i.e. on radiation dosimetry estimates [3.307–3.309] and on the identification of remnants of the thyroglossal duct as a cause of radioiodine uptake in the neck [3.310–3.311]). Mínguez et al., in particular, reported that the radiation burden to the thyroid remnants based on whole-volume estimates were 12–15% higher than those based on maximum-voxel estimates, both derived from SPECT–CT imaging [3.307]. The same group of investigators subsequently confirmed and validated the superior accuracy of SPECT–CT for radiation dosimetry purposes in patients treated with different activity levels of ^{131}I -iodide, depending on risk stratification [3.309]. Similarly, Hong et al. demonstrated a significantly higher accuracy of radiodosimetric estimates (retention rates and effective half-times in post-surgical

remnants) based on SPECT–CT versus those based on planar WBS [3.308]. On the other hand, Kairemo et al. used SPECT–CT data as the reference standard for validation of radiodosimetric estimates derived by external counting with a probe detector [3.312].

Thyroglossal duct remnants were observed in almost 50% of patients and SPECT–CT contributed to unequivocal interpretation in most cases, thus avoiding additional procedures to clarify doubtful images on planar WBS [3.310–3.311].

Similarly, in post-ablation scans, SPECT–CT has demonstrated incremental value(s) over planar WBS [3.313–3.329]. On average, SPECT–CT correctly characterized >90% of all cryptic/equivocal sites of radioiodine uptake observed on planar WBS, while it detected unexpected sites of either neck lymph node or distant metastases in almost one out of four patients (with a range of approximately 9% to 40% of cases). These findings led to changing the TNM stage in an average of 10% of patients (excluding the high 59% value reported by Zilioli et al. [3.326] in a selected subgroup of patients with equivocal findings on planar WBS). SPECT–CT also led to a change in the risk category in approximately 35% of patients and a change in intended management in approximately 15% of patients. It is interesting to note, for risk stratification, that SPECT–CT was more accurate than either unstimulated or thyroid-stimulating hormone stimulated serum thyroglobulin for detecting either local recurrence or distant metastatic disease, and for predicting long term disease relapse.

When evaluating patients for possible recurrence of differentiated thyroid cancer after primary treatment with surgery and radioiodine ablation of thyroid remnants, ^{123}I -iodide rather than ^{131}I -iodide can be used in order to minimize the risk of the so-called ‘stunning’ effect on subsequent administration of the ablative dose. In order to verify the success of ablation 6 months after treatment, Barwick et al. [3.330] assessed the added value of SPECT–CT over planar WBS and stand-alone SPECT in 79 patients after administration of 350–400 MBq ^{123}I -iodide. They found that SPECT–CT was significantly more specific than either planar WBS and WBS plus stand-alone SPECT ($P = 0.016$), a definite 42% incremental value of SPECT–CT being observed in 36 out of 85 scans (Fig. 3.2).

There is only one study reporting specifically on the incremental value of SPECT–CT in patients treated with radioiodine therapy because of recurrent or metastatic disease after primary treatment of differentiated thyroid cancer (i.e. surgery and ablation of post-surgical remnants). Chen et al. [3.331] evaluated 66 patients with equivocal findings on the planar WBS acquired after therapeutic level radioiodine was administered because of advanced or metastatic disease. They found that SPECT–CT imaging provided conclusive information in 73.9% of such patients, clarifying approximately 84% of the cryptic or equivocal foci of uptake. Furthermore, the SPECT–CT findings led to a change in management strategy for 47.1% of the patients.

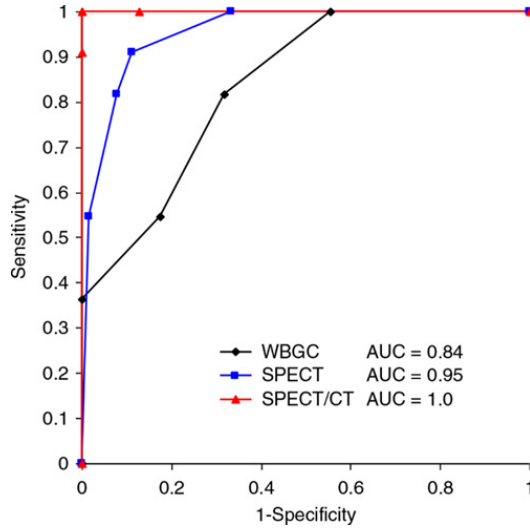


FIG. 3.2. Receiver operating characteristic curves of whole body gamma camera (WBGC) imaging (black) compared with WBGC+SPECT imaging (blue) and WBGC+SPECT-CT imaging (red) (patients with non-radioiodine-avid disease excluded). AUC denotes the area under the curve (adapted from Ref. [3.330]).

Several of the studies published on the incremental value of SPECT-CT imaging over planar WBS actually include mixed populations (i.e. patients on whom the scan was performed after administering radioiodine for ablation of post-surgical remnants and patients treated with radioiodine therapy because of recurrent or metastatic disease after primary treatment of differentiated thyroid cancer). At least three reports are worthy of separate mention. Out of an overall population of 3367 patients, Shen et al. [3.332] selected 71 patients with a positive post-ablation scintigraphy but with negative serum thyroglobulin and no interfering anti-thyroglobulin autoantibodies. Of the 71 patients, SPECT-CT detected unexpected neck lymph node metastases in 59 patients (83.1%), lung metastases in 11 patients (15.5%) and bone metastases in 2 patients (2.8%). A study by Ruhlman et al. [3.333] focused on a comparison between pre-treatment ^{124}I -iodide PET-CT and SPECT-CT acquired post-ablation ($n = 106$) or post-therapy ($n = 31$). Agreement between the two modalities was found in 97% of the lesions, leading the authors to conclude that pre-treatment ^{124}I -PET-CT is equally as effective as post-therapy ^{131}I -SPECT-CT in patients with differentiated thyroid cancer. Finally, Oh et al. [3.334] compared the diagnostic performances of pre-treatment ^{18}F -FDG-PET-CT with those of planar WBS and SPECT-CT acquired post-ablation ($n = 101$) or post-therapy ($n = 39$). They found that, on a lesion based analysis, post-ablation SPECT-CT performed better than either

planar WBS or ^{18}F -FDG-PET-CT ($P < 0.001$), while post-therapy SPECT-CT performed better than planar WBS but worse than ^{18}F -FDG-PET-CT ($P = 0.013$).

Overall, SPECT-CT had a definite diagnostic impact in an average of 57% of patients with well differentiated thyroid cancer, correctly characterizing approximately 84% of the cryptic or equivocal sites of radioiodine uptake observed on planar WBS [3.335–3.344]. It detected unexpected sites of either neck lymph node or distant metastases in more than one out of four patients, leading to up- or down-staging of the disease in over 20% of patients and to a change in intended management in approximately 25% of patients.

3.7.2. Neuroendocrine neoplasms

Neuroendocrine neoplasms (NENs) are a heterogeneous group of tumours that originate from neuroendocrine cells located in many different organs, most frequently in the gastrointestinal tract and the lungs. Less common locations include the thymus and other organs with endocrine function, such as the adrenal medulla, pituitary, parathyroid and thyroid.

NENs are a diagnostic and therapeutic challenge, as their clinical presentation is non-specific. Imaging plays a fundamental role in diagnosis, staging, treatment selection and follow-up. Current diagnostic modalities include morphological (CT, MRI, ultrasound) and molecular imaging techniques.

The majority of gastroenteropancreatic neuroendocrine tumours (GEP-NETs) express somatostatin receptors that can be used as targets for radionuclide imaging and therapy. Scintigraphy with radiolabelled somatostatin analogues (SSAs), first with ^{123}I followed by ^{111}In and $^{99\text{m}}\text{Tc}$ labelling, has been effectively used for the workup of somatostatin receptor-positive NEN patients with detection rates between 50% and 100% in different studies [3.345–3.347]. More recently, PET with ^{68}Ga -labelled SSAs has been proposed. Conversely, in adrenal tumours (i.e. pheochromocytoma and neuroblastoma), catecholamine metabolism is usually imaged with ^{123}I -mIBG, ^{18}F -dihydroxyphenylalanine (DOPA) and, more rarely, ^{11}C -5-hydroxytryptophan (HTP) [3.348–3.350]. It is important to note that ^{18}F -FDG-PET-CT has a prognostic role in NENs [3.351, 3.352].

The role of SPECT-CT in NENs is of particular importance, not only on a clinical basis, if we consider the existence of available PET radiopharmaceuticals, but also in dosimetry during theranostic procedures [3.353, 3.354].

In comparison with planar imaging, a review of the literature evidence, both in GEP-NETs [3.355–3.366] and adrenal tumours [3.360, 3.367], showed that SPECT-CT improved lesion localization and increased inter-reader agreement in more than two thirds of cases, and changed lesion classification, with subsequent up- or down-staging of the disease, in approximately one third

of patients, thus resulting in better patient management. Moreover, in comparison with stand-alone SPECT, the detection rate dramatically increased on a patient and lesion basis [3.368]. Finally, Nakamoto et al. showed the possibility of a precise quantification with SPECT–CT in adrenal tumours [3.369].

Similar results were found when comparing SPECT–CT and conventional imaging (including CT and/or MRI), both in GEP-NETs [3.370–3.374] and adrenal tumours [3.375–3.377]. More recently, Senica et al. proposed a glucagon-like peptide-1 (GLP-1) receptor agonist labelled with ^{99m}Tc for pre-operative localization of an occult insulinoma, which surpasses conventional imaging methods [3.378].

Finally, SPECT–CT has been compared with PET–CT:

- In GEP-NETs, ^{111}In and/or ^{99m}Tc labelled octreotide has been compared with ^{68}Ga -labelled SSAs [3.379–3.385];
- In adrenal tumours, ^{123}I -mIBG has been compared with ^{18}F -DOPA [3.386, 3.387] or ^{68}Ga -labelled SSAs [3.388, 3.389].

In all cases, the correlation was significantly in favour of PET–CT. However, the impact of PET–CT in radionuclide therapy management, the very definition of the Krenning score, is still a matter of debate [3.385].

3.7.3. Sentinel lymph node

The term ‘sentinel lymph node’ (SLN) indicates the first lymph node encountered by lymphatic vessels draining the primary tumour or the first lymph node upon which a lymph vessel originating in the tumour drains directly. This definition does not always correspond to the lymph node nearest to the tumour, as the route of the lymphatic vessels is often tortuous and unpredictable. There may be different lymphatic pathways draining certain tumour sites, leading to different SLNs; each of them should therefore be investigated for the presence of metastasis. Lymphoscintigraphy following interstitial radiocolloid injection is critical to precisely visualize sequential lymphatic drainage of the radiopharmaceutical. The presence or absence of SLN metastasis has a significant impact on further planning the therapeutic strategy. In patients with early cancer, if the SLN does not contain metastasis, the surgical approach should aim at removing the primary tumour and avoiding unnecessary regional node dissection. The likelihood that other nodes contain metastasis is extremely low, thus making extensive dissection unnecessary. Patients whose SLN contains metastasis usually require dissection of regional lymph nodes.

In the last few years, radio-guided surgical applications have rapidly expanded to perform SLN biopsy, in particular in patients with breast cancer and cutaneous melanoma.

Recent data obtained with SPECT–CT emphasize the importance of this hybrid imaging technique for accurate lymph node mapping, thus enabling the implementation of a more personalized surgical approach.

3.7.3.1. *Breast carcinoma*

Breast cancer is the most frequent cancer diagnosed in women worldwide. Accurate lymph node staging is essential for both prognosis (of early stage disease) and treatment (for regional control of disease) in patients with breast cancer.

SLN mapping and biopsy have become routine techniques in breast cancer management, contributing to the development of less invasive surgical procedures. The use of SPECT–CT-aided nodal mapping is correlated with a higher detection rate of SLNs due to a better anatomical localization and identification of SLNs not seen on planar scintigraphy [3.390–3.405].

3.7.3.2. *Melanoma*

Melanoma is one of the most aggressive and therapy resistant cancers. Its incidence is currently increasing worldwide. Diagnosis of metastatic lymph node involvement is of the utmost importance for prognosis in patients with intermediate thickness melanoma. Other prognostic factors include tumour thickness, presence of ulceration and mitotic rate. Radio-guided surgery has a prominent role in the treatment of melanoma, because the SLN approach is, nowadays, a choice procedure for regional lymphatic staging of these patients.

No imaging modality is accurate enough to detect lymph node metastases, but SLN biopsy is a highly reliable method for screening and for identifying metastatic and micrometastatic disease in regional lymphatic nodes.

SPECT–CT imaging increases the SLN identification rate and overcomes some of the limitations of planar imaging [3.398, 3.400, 3.406–3.419].

3.7.3.3. *Head and neck squamous cell carcinoma*

SLN biopsy is increasingly being used in early stage oral cancer, as well as in head and neck squamous cell cancer, in order to exclude occult lymph node metastases, a condition that has a definitive impact on treatment planning [3.420–3.426]. However, optimal patient management remains controversial, varying from watchful waiting to SLN biopsy or elective neck

dissection. SLN biopsy is generally associated with less morbidity and superior functional outcome, since up to 80% of T1 and T2 head and neck squamous cell carcinomas and clinically negative necks are overtreated with routine elective neck dissection [3.427]. SLN biopsy is fraught with a somewhat limited sensitivity, especially when performing planar lymphoscintigraphy only. In a recent study on oral squamous cell carcinoma, the addition of SPECT–CT to planar/dynamic scintigraphy revealed additional SLNs in 22% of patients and thus significantly increased the diagnostic accuracy [3.428]. The combination of dynamic scan with SPECT–CT demonstrated the best results [3.429]. Furthermore, SPECT–CT revealed additional anatomical information in 3% of patients and the overall detection rate of the combined approach was 98% [3.428]. When compared with the gold standard of intraoperative gamma ray detection probe, a high diagnostic accuracy (90.8%) was observed in another retrospective study [3.430].

3.7.3.4. Cancers of the reproductive tract

The nodal metastatic status constitutes the most important factor for therapy and prognosis in cervical cancer. Because of the fact that the presence of lymph node metastases significantly decreases survival rates, the introduction of radical lymphadenectomy was advocated. Since lymphatic drainage from the uterus is ramified and complex, accurate pre-surgical SLN detection is highly desirable in order to prevent systematic lymphadenectomy, which is commonly associated with higher morbidity.

Scintigraphic mapping and biopsy of SLNs is increasingly being performed in cervical cancer, whereas it remains a matter of clinical investigation in endometrial cancer, which is associated with a low prevalence of lymph node metastases. The rationale of improved SLN detection by means of SPECT–CT is based on its higher spatial resolution and the availability of additional morphological information that also enables the detection of nodes located adjacent to the injection area.

In cervical [3.431–3.433] as well as in vulvar [3.434, 3.435] cancer, several studies revealed the superiority of SPECT–CT for SLN detection and better anatomical correlation compared with planar lymphoscintigraphy, thus improving intraoperative detection rates and facilitating intraoperative SLN biopsy — factors that all together confirmed the higher oncologic safety of the SLN concept.

In endometrial cancer, the SLN procedure is not used in clinical routine and the detection rate was shown to be lower when compared with breast cancer and melanoma. In addition, the detection rate can be hampered by the injection technique used [3.436–3.437]. Nevertheless, preliminary evidence revealed

that SPECT–CT localization of SLNs was anatomically accurate in 91% of cases [3.438] and thus feasible and reliable for patients with endometrial cancer.

Recently, one prospective study also demonstrated the additional value of SPECT–CT compared with planar imaging in penile cancer, because of a higher detection rate and a lower number of false positive findings versus planar SLN imaging [3.439].

3.7.4. Prostate cancer

PET radioligands binding to PSMA have brought a revolution to the diagnostic workup of patients with prostate cancer [3.440]. In parallel, PSMA binding radiopharmaceuticals labelled with ^{99m}Tc and thus suitable for SPECT imaging have been developed. They have been preclinically validated and their normal distribution in humans has been studied [3.441–3.445]. PSMA radioligands avidly concentrate in prostate cancer tissue, as well as physiologically in sympathetic ganglia, salivary and lacrimal glands, parts of the bowels and — to a somewhat lesser extent — in the liver. Many, but not all, of these ligands are excreted via the kidneys, and therefore, considerable uptake of these tracers in the urinary tract is usually found. Uptake in the rest of the body is more or less negligible, so that PET or SPECT images of their distribution within the body provide little anatomical information. Therefore, SPECT–CT and not stand-alone conventional nuclear medical scintigraphy is the standard for SPECT imaging of PSMA expression.

Analogously to PET–CT, one possible application of SPECT–CT imaging of PSMA expression is for pre-operative staging of patients with prostate carcinoma. Goffin et al. reported on a phase 2 clinical trial using ^{99m}Tc -MIP-1404-SPECT–CT in 105 patients with a high risk of pelvic lymph node involvement scheduled for radical prostatectomy and nodal dissection [3.446]. They were able to detect 94% of the primary tumours and 50% of involved lymph nodes with a specificity of 87%. They did not analyse their scans for distant spread. In a retrospective analysis of 93 newly diagnosed patients, Schmidkonz et al. found prostate uptake above background, indicative of malignancy in 97% of cases [3.447]. They detected 48 lymph node and 29 bone metastases in 16 and 9 patients, respectively. In both studies, tumour uptake significantly correlated with Gleason score. Therefore, one might hypothesize that PSMA-SPECT–CT can be useful to determine dedifferentiation of low grade tumours under active surveillance. The results of a phase 3 trial of this issue have at the time of writing not yet been published, so it might be too early to speculate on the utility of ^{99m}Tc -MIP-1404-SPECT–CT in this pretherapeutic setting. Whether pretherapeutic PSMA-SPECT–CT can significantly improve care for patients with higher grade prostate carcinomas is also still unclear. Demonstrating lymph node metastases at this early stage

could, in principle, prompt their surgical excision or irradiation, thus potentially leading to higher rates of cure. This issue was addressed by Su et al., who showed that pre-operative SPECT–CT led to the removal of more lymph node metastases than conventional imaging with, for example, MRI, and claimed that this delayed disease progression [3.448]. Detecting distant metastases at first staging might bear the consequence of systemic treatment. However, this has not as yet been systematically studied. The results published so far undoubtedly encourage further prospective clinical trials aiming to evaluate the potential clinical impact of primary staging with PSMA-SPECT–CT and its effect on the survival of patients.

Sometime after first ablative therapy of the primary cancer, patients may present again with a measurable or rising serum level of the prostate specific antigen (PSA), representing biochemical recurrence. Localizing recurrent or persisting tumour tissue in these patients has major clinical consequences. Local or lymph node recurrence might be best met by surgery or radiation treatment. In the case of distant spread (e.g. to the skeleton), systemic therapy such as antiandrogenic treatment has to be instituted or given in a modified regimen, and this often affects quality of life. An initial study of 60 subjects with biochemical recurrence reported detection rates of 91.4% and 40% at PSA levels above and below a threshold of 2 ng/ml, respectively [3.449]. In 78% of 50 patients affected by the same condition, SPECT–CT allowed the localization of the recurrence in a study by Su et al. [3.450]. Schmidkonz et al. detected tracer-positive lesions indicative of tumour tissue in 77% of 225 patients with biochemical recurrence. These authors found local recurrences in 25% of the patients, lymph node metastases in 25%, bone metastases in 27% and metastases to other organs in 7%, respectively. Detection rate correlated significantly with the PSA level, being 90% at PSA levels ≥ 2 ng/ml and 54% below that threshold. SPECT–CT findings were reported to lead to changes in treatment in 74% of the patients [3.451]. Liu et al., using ^{99m}Tc -HYNIC-PSMA, another tracer, reported a detection rate of 72.6% in their group of 208 subjects with biochemical relapse [3.452]. Furthermore, they confirmed the relationship between PSA level and detection rate and also demonstrated a similar correlation between detection rate and PSA doubling time. Detecting and localizing tumour recurrence in patients with low or very low PSA levels below 1 ng/ml, or even 0.5 ng/ml, has a significant clinical impact for planning curative radiotherapy. In a study by Schmidkonz et al. involving 25 patients with PSA levels between 0.5 ng/ml and 1 ng/ml and 25 subjects with PSA levels between 0.2 ng/ml and 0.5 ng/ml, detection rates were 56% and 44%, respectively [3.453].

The above-cited evidence is remarkably consistent in view of the heterogeneity prevailing in study design, as well as in the selection of patients, tracer and imaging hardware. As reported above, the detection rates reported for

PSA levels higher than 1 ng/ml or 2 ng/ml range between 77% and 91.4%, and those for lower PSA levels range between 44% and 54%. In principle, these figures advocate the clinical use of SPECT–CT imaging of PSMA expression in patients with biochemical recurrence of prostate cancer. PSMA-PET–CT, however, would be expected to outperform SPECT–CT for this purpose due to its better spatial resolution. This assumption has been confirmed by Lawal et al. [3.454], but not by Garcia-Perez et al. [3.455], both comparing ^{99m}Tc -HYNIC-PSMA-SPECT–CT with ^{68}Ga -PSMA-11-PET–CT. Nevertheless, already available evidence indicates that PSMA-SPECT–CT is superior to skeletal SPECT–CT for staging [3.456] and may thus have the potential to substitute for this method in the near future.

The better spatial resolution of PET–CT compared with SPECT–CT would be no shortcoming of the latter technology for monitoring disease activity in systemically treated patients, as these usually suffer from large-volume disease. In a first study of this issue, Schmidkonz et al. could indeed demonstrate a high rate of concordance between PSA response and changes in SUV values in a group of 28 patients [3.457]. In another publication of this group, a much better reproducibility of quantitative evaluation compared with visual assessment of therapy-induced changes in uptake was found [3.458], underlining the potential of quantitative SPECT–CT.

PET tracers of PSMA expression are labelled by either ^{68}Ga or ^{18}F , with short half-lives of approximately 1 h or 2 h, respectively. Using these radiopharmaceuticals for radio-guided surgery is, thus, difficult. This is also true in view of the high energy of the annihilation radiation inherent to positron emission, which for this purpose is unfavourable. Some evidence indicates that ^{99m}Tc -labelled PSMA tracers might be well suited to radio-guided lymph node dissection, and to robot-assisted surgical procedures [3.445, 3.459].

Within the past few years, ^{177}Lu -labelled radiopharmaceuticals have been introduced for PSMA based treatment of prostate cancer. Evidence shows that the tissue concentration of this radioisotope can be determined using SPECT–CT, capitalizing on the photons that this beta-emitter also releases. This paves the way to using quantitative SPECT–CT for the dosimetry of ^{177}Lu -based therapies, as initial research already demonstrates [3.460–3.462].

3.7.5. Breast cancer

Breast cancer is the most common non-skin cancer and the second leading cause of cancer mortality in women. Although PET–CT is becoming increasingly important in the management of patients with breast cancer, SPECT–CT may play an important role in a context of PET shortage. A review of the literature from 2008 to 2019 turned up a total of 31 articles about SPECT–CT and breast cancer, of which only three were still relevant, since the majority of the clinical

data are related to the development of new radiopharmaceuticals, mainly for research purposes, that are not available worldwide. The indications of MIBI SPECT–CT were essentially related to quantification aspects in therapy evaluation [3.463–3.465]. Due to the lack of clinical data, the usefulness of this indication on an evidence basis could not be demonstrated.

3.7.6. Liver transarterial radioembolization

The liver represents a frequent site for both primary cancer and metastatic disease. Primary liver cancers (i.e. hepatocellular carcinoma or cholangiocarcinoma) are becoming some of the most frequent cancers worldwide, with rapidly fatal liver failure in a large majority of patients. Curative therapy consists of surgery (i.e. resection or liver transplantation), but it is only possible to perform this in 10–20% of patients. Alternatively, a variety of palliative treatments, such as liver-directed therapies (cytoreduction via surgery) or in situ ablative techniques (chemo-embolization, radiofrequency ablation, tyrosine kinase inhibitors), may influence the natural history of the disease progression and improve clinical outcomes.

Colorectal cancer is the second most lethal cancer in Europe and liver metastases are prevalent either at diagnosis or during follow-up. These patients are usually treated by a sequence of surgery, chemotherapy and immunotherapy.

Transarterial radioembolization is a therapeutic approach that involves the injection of micrometre-sized embolic particles, known as microspheres, loaded with a radioisotope, namely ^{90}Y , by the use of percutaneous intra-arterial techniques. The rationale for this selective internal radiotherapy modality arises from the dual blood supply of the liver through the hepatic artery and the portal vein. Normal liver parenchyma draws more than 80% of blood from the portal vein. Tumours bigger than 2 cm in diameter draw more than 80% of their blood supply from the arterial rather than the portal hepatic circulation. Highly selective tumour uptake can thus be achieved by delivery of radioactive compounds into the hepatic artery, which represents the arterial supply to liver tumours almost exclusively. The therapeutic efficacy of the method derives essentially from the delivered radiation, as opposed to the ischaemia associated with chemoembolization or pure embolization. The radiobiological effect results from beta irradiation, which favours destruction of tumour cells surrounding microvessels containing a high radioactive ligand concentration.

The advantages of the use of these intra-arterial radioactive compounds include the ability to deliver high doses of radiation to small target volumes, the relatively low toxicity profile, the possibility to treat the whole liver, including microscopic disease, and the feasibility of combination with other therapy

modalities. The disadvantages are mainly due to the possibility of inadvertent delivery or shunting.

Typically, a pre-therapy angiographic evaluation combined with an intra-arterial ^{99m}Tc -labelled macroaggregated albumin (MAA) scan is mandatory to map the tumour feeding vessels, to quantify potential liver–lung shunting and to avoid the inadvertent deposition of microspheres in organs other than the liver (i.e. to exclude blood reflux to the bowel, stomach or pancreas).

Prior to administration of ^{99m}Tc -MAA, prophylactic coil embolization of the gastroduodenal artery is recommended to avoid extrahepatic deposition of the microspheres. SPECT–CT allows direct correlation of anatomical and functional information in patients with unresectable liver disease. SPECT–CT is recommended to assess intrahepatic distribution as well as extrahepatic gastrointestinal uptake in these patients. Pre-therapeutic SPECT–CT is an important component of treatment planning, including catheter positioning and dose definition. After ^{90}Y -microsphere administration, bremsstrahlung SPECT–CT scan or ^{90}Y PET should follow transarterial radioembolization to verify the distribution of the administered tracer. Post-therapy imaging enables better localization and definition of intrahepatic and possible extrahepatic sphere distribution, and to a certain degree allows post-treatment dosimetry.

A review of the literature evidenced a total of 74 articles about SPECT–CT and transarterial radioembolization, the majority of which were focused on dosimetric evaluation of the treatment [3.466–3.481].

3.8. GASTROENTEROLOGY

3.8.1. Gastrointestinal bleeding

Gastrointestinal (GI) bleeding, originating above or below the first jejunal loop and thus defined as upper or lower haemorrhage, can be due to a variety of benign or malignant causes. Diagnosis is made by contrast angiography or endoscopy. A positive test indicates the presence of an active process and will further guide local therapy. Technetium-99m labelled red blood cell (Tc-RBC) scintigraphy is a highly sensitive, non-invasive imaging modality that can detect intermittent bleeding on serial studies performed up to 24 h after injection of the radiotracer. An early positive scan indicates the presence of active bleeding and identifies patients who should be referred to immediate treatment, provided that the site of the bleeding is precisely localized [3.482]. A few publications report on the potential value of Tc-RBC SPECT–CT to identify the site of GI bleeding. SPECT–CT provided exact anatomical localization in most of a group of 27 patients, with GI bleeding changing the result reports of planar scintigraphy

in over one third of the cases while being misleading in a single case [3.483]. In a group of 56 patients who had pre-operative Tc-RBC scans, SPECT-CT detected the presence of lower GI bleeding in an additional two patients, as compared with 50 positive cases confirmed by planar studies, corresponding to a statistically non-significant increase in sensitivity from 89% to 93%, respectively. However, more importantly, the correct site of bleeding was identified by planar imaging in 31 patients, as compared with 48 by SPECT-CT, corresponding to a statistically significant increase ($p < 0.05$) in the positional accuracy from 74% to 92% [3.484]. A recent retrospective study in 20 patients compared SPECT-CT to planar scintigraphy and SPECT to accurately detect and to localize the sites of the GI bleeding. SPECT-CT added to planar studies showed a 100% sensitivity, specificity accuracy for diagnosis, as well as a 100% ability to localize the site of the GI bleeding [3.485].

The timing of SPECT-CT in studies performed with Tc-RBC for assessment of GI bleeding is debated. It is not clear whether SPECT-CT should be acquired routinely at 60–90 min after tracer administration, or following the initial detection of bleeding on planar images. There is also concern that the duration of SPECT-CT and motion of patients during the study may affect correct identification of the bleeding site because of bowel movements or potential artefacts [3.486, 3.487].

Gastrointestinal bleeding is common in children as well, with Meckel diverticulum being the most frequent cause of lower GI haemorrhage in previously healthy infants. Bleeding is due to the acid secretion of ectopic gastric mucosa present in up to 50% of the diverticula. These are located, as a rule, on the ileum, approximately 50–80 cm from the ileocaecal valve. Technetium-99m-pertechnetate scintigraphy is the imaging procedure that can detect the presence of gastric mucosa in Meckel's diverticulum with a sensitivity of 85%, specificity of 95% and accuracy of 90% [3.488]. The role of SPECT-CT to improve the diagnostic accuracy of scintigraphy for Meckel's diverticulum requires further assessment. A few case reports and small case series have indicated that hybrid imaging has the potential to improve the capability to correctly diagnose Meckel's diverticulum, to differentiate it from uptake in artefacts, as well as for localization of uncommon sites of ectopic gastric mucosa. Since SPECT-CT fusion adds a small amount of radiation, it is recommended to tailor the CT dose to the patient's size and age [3.487, 3.489].

3.8.2. Spleen

Nuclear medicine procedures may have a particular importance in the differential diagnosis of splenosis. Theoretically, planar scintigraphy with ^{99m}Tc -labelled colloids may benefit from the support of SPECT-CT, for the

precise identification and localization of ectopic splenic nodules. However, the review of the literature evidenced a total of five articles about SPECT–CT and splenosis, of which only two could be retained. Due to the lack of clinical data, the usefulness of this indication on an evidence basis could not be demonstrated [3.490, 3.491].

3.9. PAEDIATRICS

While children are not small adults, with respect to SPECT–CT and the indications described in the previous sections, one could similarly use this hybrid imaging modality in paediatric patients when clinically justified and applicable. The scientific literature, however, does not have an abundance of pure paediatric science to validate as compared with adults. In the more than 100 papers found on PubMed from 2008 to 2019 that include ‘SPECT–CT and child’, pure paediatric studies are few, and more studies that mention an inclusive paediatric age range and case reports are found. The earliest scientific paediatric paper explored the prospective use of SPECT–CT for children and found added value for renal, bone and oncology studies, allowing for the determination of the site of biopsy in 6 out of 15 cases [3.492].

Nevertheless, there are clear areas where SPECT–CT has been shown to be effective in the paediatric patient for specific disease entities, mainly in the areas of oncology and orthopaedics. More random but novel use of SPECT–CT is increasing for benign endocrinology conditions, GI indications and miscellaneous cases where SPECT–CT can improve the diagnostic conspicuity and certainty.

With the increasing use of hybrid imaging tools in the paediatric population to include SPECT–CT, PET–CT and now PET–MRI, one must consider the ‘cost’ of doing these studies relative to the administered dose, the increased radiation exposure by the addition of CT and, in many instances, the increased requirement for sedation and/or general anaesthesia. The principle of as low as reasonably achievable (ALARA) for paediatric CT should be applied to adult studies as well.

3.9.1. Neuroblastoma

Radioiodinated mIBG imaging in paediatric neural crest tumours is the standard of care where the requirement for semiquantitative evaluation of Curie or SIOOPEN score is needed at diagnosis and for response assessment. Although this semiquantitative assessment of disease and then response to treatment is made on planar imaging, the use of SPECT has been recommended [3.493]. The use of SPECT–CT is increasing but has limited validation. A total of five original papers, of which three have only paediatric subjects, address the added value of

SPECT–CT [3.377, 3.494–3.498]. The common conclusion of these papers is that SPECT–CT is superior to planar imaging or SPECT alone for lesion detectability, as well as for correct categorization of suspected abnormalities seen on planar imaging as physiological foci of uptake. Two papers compared ^{123}I -mIBG SPECT–CT to PET imaging with either ^{18}F -FDG or ^{18}F -DOPA [3.497, 3.498]. The prospective study [3.499] showed better detection of primary tumour, bone, bone marrow and soft tissue metastases with ^{18}F -DOPA compared with mIBG SPECT–CT at diagnosis and after chemotherapy. The comparison of ^{18}F -FDG with ^{123}I -mIBG SPECT–CT was similar for lesion detection. Current response assessments for paediatric treatment group clinical trials still use mIBG imaging for evaluation of response.

3.9.2. Lymphoscintigraphy

The value of lymphoscintigraphy with SPECT–CT compared with PET–CT has been evaluated in a prospective study of paediatric and adolescent sarcoma patients for detection of lymph node metastases at staging. Seven out of 28 patients had lymph node metastases detected on SPECT–CT lymphoscintigraphy, including three patients who had negative ^{18}F -FDG-PET studies [3.500]. In one additional paper, SPECT–CT lymphoscintigraphy helped determine the cause of lymphatic stasis in post-congenital cardiac surgery patients due to leak, reflux and obstruction [3.501].

3.9.3. Thyroid

Two paediatric based studies have confirmed the value of SPECT–CT for localization of neck disease after thyroidectomy in children with differentiated thyroid cancer. In the study by Kim et al. [3.502], all detected lesions were correctly localized by SPECT–CT. Liu et al. [3.503] correctly localized 20 metastatic lesions by SPECT–CT and determined that the correlation with stimulated thyroglobulin was significantly higher in patients with metastatic disease.

3.9.4. Musculoskeletal

As with adult indications, SPECT–CT in paediatric patients is often used to evaluate a cause of pain. Five combined adult and paediatric papers reviewed the use of SPECT–CT for evaluation of specific bone diagnoses. Two of the papers looked at newer techniques of quantitation, with one paper describing SUV measurement on SPECT–CT for evaluation of growth plate disturbances and the second paper evaluating focal activity in accessory navicular bone that might require surgical intervention [3.504, 3.505]. In a combined adult and

paediatric study of 200 patients assessing pathology of the spine and sacrum with SPECT–CT, a cause of pain that impacted management was found in 80% of cases [3.506]. Although MRI is now the study of choice for assessment of acute osteomyelitis in children, SPECT–CT was helpful in the diagnosis of osteomyelitis of the jaw in both adult and paediatric patients when compared with orthopantomogram and CT [3.272, 3.506, 3.507]. Also, SPECT–CT had 100% accuracy, sensitivity and specificity for diagnosis of osteoid osteoma compared with planar bone scan and CT in 31 patients [3.508].

3.9.5. Radiation dose consideration

All SPECT–CT studies increase the dose to the patient with the addition of CT over the scintigraphic study alone. However, the CT component of the exam is rarely performed with diagnostic intent, thus the CT dose used for attenuation correction and lesion localization is generally low.

Obviously, considerations to adhere to the ALARA principle are particularly important in the paediatric population. Two studies have looked at possible dosimetric implications of SPECT–CT. In a combined adult and paediatric study by Sharma et al. [3.509], 33% of the 357 patients were less than 25 years of age. For the CT parameters of SPECT–CT, 80 kVp was used for children less than 5 years of age and 110 kVp was used between ages 5 and 18. In addition, each exam was tailored to determine the need for CT after SPECT was performed. If indicated, the CT component was subsequently limited to an area of concern and not likely the entire SPECT acquisition. This tailored approach is a common technique known to those who routinely perform dedicated paediatric scintigraphic studies. Adherence to appropriate administered dose is also important, and should be weight based in paediatric examinations [3.510]. Hou et al. [3.511] referred to the practice of performing dosimetry studies when performing SPECT–CT for a specific radiotracer, and found that dosimetry values were 30% higher compared with adult dosimetry studies. With more targeted therapies being performed, many more centres are making such dosimetry calculations; however, these can be challenging to do in paediatric patients.

REFERENCES TO SECTION 3

- [3.1] FILIPPI, L., et al., Usefulness of SPECT–CT with a hybrid camera for the functional anatomical mapping of primary brain tumors by [Tc99m] tetrofosmin, *Cancer Biother. Radiopharm.* **21** (2006) 41–48.

- [3.2] FILIPPI, L., SANTONI, R., NICOLÌ, P., DANIELI, R., SCHILLACI, O., Intracranial tumors after radiation therapy: Role of ^{99m}Tc -tetrofosmin SPECT/CT with a hybrid camera, *Cancer Biother. Radiopharm.* **24** (2009) 229–235.
- [3.3] FARID, K., HABERT, M.-O., MARTINEAU, A., CAILLAT-VIGNERON, N., SIBON, I., CT nonuniform attenuation and TEW scatter corrections in brain Tc-99m ECD SPECT, *Clin. Nucl. Med.* **36** (2011) 665–668.
- [3.4] ISHII, K., et al., Impact of CT attenuation correction by SPECT–CT in brain perfusion images, *Ann. Nucl. Med.* **26** (2012) 241–247.
- [3.5] FARID, K., PETRAS, S., POULLIAS, X., CAILLAT-VIGNERON, N., Clinical impact of nonuniform CT-based attenuation correction in brain perfusion SPECT–CT using ^{99m}Tc -ECD, *Clin. Nucl. Med.* **39** (2014) e343–e345.
- [3.6] HSU, C.-C., et al., The feasibility of using CT-guided ROI for semiquantifying striatal dopamine transporter availability in a hybrid SPECT–CT system, *Sci. World. J.* **2014** (2014) 879497.
- [3.7] KATO, H., SHIMOSEGAWA, E., FUJINO, K., HATAZAWA, J., CT-based attenuation correction in brain SPECT–CT can improve the lesion detectability of voxel-based statistical analyses, *PLoS One* **11** (2016) e0159505.
- [3.8] WELZ, F., et al., Absolute SPECT–CT quantification of cerebral uptake of ^{99m}Tc -HMPAO for patients with neurocognitive disorders, *Nuklearmedizin* **55** (2016) 158–165.
- [3.9] YOKOYAMA, K., et al., Computed-tomography-guided anatomic standardization for quantitative assessment of dopamine transporter SPECT, *Eur. J. Nucl. Med. Mol. Imaging* **44** (2017) 366–372.
- [3.10] LAPA, C., et al., Influence of CT-based attenuation correction on dopamine transporter SPECT with [^{123}I] FP-CIT, *Amer. J. Nucl. Med. Mol. Imaging* **5** (2015) 278–286.
- [3.11] LOU, J., et al., Evaluation of ^{99m}Tc -ECD SPECT–CT brain imaging with NeuroGam analysis in Moyamoya disease after surgical revascularization, *Medicine* **98** (2019) e16525.
- [3.12] TORIIHARA, A., et al., Semiquantitative analysis using standardized uptake value in ^{123}I -FP-CIT SPECT–CT, *Clin. Imaging* **52** (2018) 57–61.
- [3.13] PATEL, C.N., SALAHUDEEN, H.M., LANSDOWN, M., SCARSBROOK, A.F., Clinical utility of ultrasound and ^{99m}Tc sestamibi SPECT–CT for preoperative localization of parathyroid adenoma in patients with primary hyperparathyroidism, *Clin. Radiol.* **65** (2010) 278–287.
- [3.14] TOKMAK, H., DEMIRKOL, M.O., ALAGÖL, F., TEZELMAN, S., TERZIOGLU, T., Clinical impact of SPECT-CT in the diagnosis and surgical management of hyper-parathyroidism, *Int. J. Clin. Exp. Med.* **7** (2014) 1028–1034.
- [3.15] WOODS, A.-M., et al., Dual-isotope subtraction SPECT-CT in parathyroid localization, *Nucl. Med. Commun.* **38** (2017) 1047–1054.
- [3.16] BURAL, G.G., MUTHUKRISHNAN, A., OBORSKI, M.J., MOUNTZ, J.M., Improved benefit of SPECT–CT compared to SPECT alone for the accurate localization of endocrine and neuroendocrine tumors, *Mol. Imaging Radionucl. Ther.* **21** (2012) 91–96.

- [3.17] SANDQVIST, P., NILSSON, I.-L., GRYBÄCK, P., SANCHEZ-CRESPO, A., SUNDIN, A., SPECT–CT’s advantage for preoperative localization of small parathyroid adenomas in primary hyperparathyroidism, *Clin. Nucl. Med.* **42** (2017) e109–e114.
- [3.18] CIAPPUCCINI, R., et al., Dual-phase ^{99m}Tc sestamibi scintigraphy with neck and thorax SPECT–CT in primary hyperparathyroidism: A single-institution experience, *Clin. Nucl. Med.* **37** (2012) 223–228.
- [3.19] KOBERSTEIN, W., FUNG, C., ROMANIUK, K., ABELE, J., Accuracy of dual phase single-photon emission computed tomography/computed tomography in primary hyperparathyroidism: Correlation with serum parathyroid hormone levels, *Can. Assoc. Radiol. J.* **7** (2016) 115–121.
- [3.20] ROBIN, P., et al., Quantitative analysis of technetium-99m-sestamibi uptake and washout in parathyroid scintigraphy supports dual mechanisms of lesion conspicuity, *Nucl. Med. Commun.* **40** (2019) 469–476.
- [3.21] GAYED, I.W., et al., The value of ^{99m}Tc-sestamibi SPECT–CT over conventional SPECT in the evaluation of parathyroid adenomas or hyperplasia, *J. Nucl. Med.* **46** (2005) 248–252.
- [3.22] KRAUSZ, Y., et al., Technetium-99m-MIBI SPECT–CT in primary hyperparathyroidism, *World J. Surg.* **30** (2006) 76–83.
- [3.23] NEUMANN, D.R., OBUCHOWSKI, N.A., DIFILIPPO, F.P., Preoperative ¹²³I/^{99m}Tc-sestamibi subtraction SPECT and SPECT–CT in primary hyperparathyroidism, *J. Nucl. Med.* **49** (2008) 2012–2017.
- [3.24] PATA, G., et al., Financial and clinical implications of low-energy CT combined with ^{99m}Tc-sestamibi SPECT for primary hyperparathyroidism, *Ann. Surg. Oncol.* **18** (2011) 2555–2563.
- [3.25] PATA, G., CASELLA, C., BESUZIO, S., MITTEMPERGER, F., SALERNI, B., Clinical appraisal of ^{99m}Tc-sestamibi SPECT–CT compared to conventional SPECT in patients with primary hyperparathyroidism and concomitant nodular goiter, *Thyroid* **20** (2010) 1121–1127.
- [3.26] MANDAL, R., MUTHUKRISHNAN, A., FERRIS, R.L., DE ALMEIDA, J.R., DUVVURI, U., Accuracy of early-phase versus dual-phase single-photon emission computed tomography/computed tomography in the localization of parathyroid disease, *Laryngoscope* **125** (2015) 1496–1501.
- [3.27] TAWFIK, A.I., KAMR, W.H., MAHMOUD, W., ABO SHADY, I.A., MOHAMED, M.H., Added value of ultrasonography and Tc-99m MIBI SPECT–CT combined protocol in preoperative evaluation of parathyroid adenoma, *Eur. J. Radiol. Open* **6** (2019) 336–342.
- [3.28] OKUDAN, B., SEVEN, B., COSKUN, N., ALBAYRAK, A., Comparison between single-photon emission computed tomography/computed tomography and ultrasound in preoperative detection of parathyroid adenoma: Retrospective review of an institutional experience, *Nucl. Med. Commun.* **40** (2019) 1211–1215.

- [3.29] SANDQVIST, P., NILSSON, I.-L., GRYBÄCK, P., SANCHEZ-CRESPO, A., SUNDIN, A., Multiphase iodine contrast-enhanced SPECT–CT outperforms nonenhanced SPECT–CT for preoperative localization of small parathyroid adenomas, *Clin. Nucl. Med.* **44** (2019) 929–935.
- [3.30] SUH, Y.J., et al., Comparison of 4D CT, ultrasonography, and ^{99m}Tc sestamibi SPECT–CT in localizing single-gland primary hyperparathyroidism, *Otolaryngol. Head Neck Surg.* **152** (2015) 438–443.
- [3.31] CHRISTAKIS, I., et al., The diagnostic accuracy of neck ultrasound, 4D-computed tomography and sestamibi imaging in parathyroid carcinoma, *Eur. J. Radiol.* **95** (2017) 82–88.
- [3.32] KEDARISSETTY, S., FUNDAKOWSKI, C., RAMAKRISHNAN, K., DADPARVAR, S., Clinical value of Tc99m-MIBI SPECT–CT versus 4D-CT or US in management of patients with hyperparathyroidism, *Ear Nose Throat J.* **98** (2019) 149–157.
- [3.33] YEH, R., et al., Diagnostic performance of 4D CT and Sestamibi SPECT–CT in localizing parathyroid adenomas in primary hyperparathyroidism, *Radiology* **291** (2019) 469–476.
- [3.34] VU, T.H., et al., Solitary parathyroid adenoma localization in technetium Tc99m sestamibi SPECT and multiphase multidetector 4D CT, *Am. J. Neuroradiol.* **40** (2019) 142–149.
- [3.35] QUAK, E., et al., F18-choline PET–CT guided surgery in primary hyperparathyroidism when ultrasound and MIBI SPECT–CT are negative or inconclusive: the APACH1 study, *Eur. J. Nucl. Med. Mol. Imaging* **45** (2018) 658–666.
- [3.36] BEHESHTI, M., et al., ¹⁸F-Fluorocholine PET–CT in the assessment of primary hyperparathyroidism compared with ^{99m}Tc-MIBI or ^{99m}Tc-tetrofosmin SPECT–CT: A prospective dual-centre study in 100 patients, *Eur. J. Nucl. Med. Mol. Imaging* **45** (2018) 1762–1771.
- [3.37] KEIDAR, Z., et al., Preoperative ^{99m}Tc-MIBI SPECT–CT interpretation criteria for localization of parathyroid adenomas — correlation with surgical findings, *Mol. Imaging Biol.* **19** (2017) 265–270.
- [3.38] CHENG, Z., ZOU, S., PENG, D., ZHANG, G., ZHU, X., Prognostic value of ^{99m}Tc-sestamibi parathyroid scintigraphy in predicting future surgical eligibility in patients with asymptomatic primary hyperparathyroidism, *Clin. Nucl. Med.* **43** (2018) 151–154.
- [3.39] BARBER, B., et al., Comparison of single photon emission CT (SPECT) with SPECT–CT imaging in preoperative localization of parathyroid adenomas: A cost-effectiveness analysis, *Head Neck* **38** Suppl. 1 (2016) S2062–S2065.
- [3.40] CHROUSTOVA, D., KUBINYI, J., TRNKA, J., ADAMEK, S., The role of ^{99m}Tc-MIBI SPECT/low dose CT with 3D subtraction in patients with secondary hyperparathyroidism due to chronic kidney disease, *Endocr. Regul.* **48** (2014) 55–63.
- [3.41] DORUYTER, A.G., HARTLEY, T., AMEYO, J.W., DAVIDS, M., WARWICK, J., Hybrid imaging using low-dose, localizing computed tomography enhances lesion localization in renal hyperparathyroidism, *Nucl. Med. Commun.* **35** (2014) 884–889.

- [3.42] ZHEN, L., et al., The application of SPECT–CT for preoperative planning in patients with secondary hyperparathyroidism, *Nucl. Med. Commun.* **34** (2013) 439–444.
- [3.43] YANG, J., et al., Value of dual-phase ^{99m}Tc-sestamibi scintigraphy with neck and thoracic SPECT–CT in secondary hyperparathyroidism, *Am. J. Roentgenol.* **202** (2014) 180–184.
- [3.44] LI, P., et al., Lesion based diagnostic performance of dual phase ^{99m}Tc-MIBI SPECT–CT imaging and ultrasonography in patients with secondary hyperparathyroidism, *BMC Med. Imaging* **17** (2017) 60.
- [3.45] LAVELY, W.C., et al., Comparison of SPECT–CT, SPECT, and planar imaging with single- and dual-phase ^{99m}Tc-sestamibi parathyroid scintigraphy, *J. Nucl. Med.* **48** (2007) 1084–1089.
- [3.46] XU, F., et al., The value of scintigraphy, computed tomography, magnetic resonance imaging, and single-photon emission computed tomography/computed tomography for the diagnosis of ectopic thyroid in the head and neck: A STROBE-compliant retrospective study, *Medicine* **97** (2018) e0239.
- [3.47] DONG, F., et al., Standardized uptake value using thyroid quantitative SPECT–CT for the diagnosis and evaluation of Graves’ disease: A prospective multicenter study, *Biomed. Res. Int.* **2019** (2019) 7589853.
- [3.48] LEE, R., SO, Y., SONG, Y.S., LEE, W.W., Evaluation of hot nodules of thyroid gland using Tc-99m pertechnetate: A novel approach using quantitative single-photon emission computed tomography/computed tomography, *Nucl. Med. Mol. Imaging* **52** (2018) 468–472.
- [3.49] KIM, J.-Y., et al., Utility of quantitative parameters from single-photon emission computed tomography/computed tomography in patients with destructive thyroiditis, *Korean J. Radiol.* **19** (2018) 470–480.
- [3.50] LEE, H., et al., Quantitative single-photon emission computed tomography/computed tomography for technetium pertechnetate thyroid uptake measurement, *Medicine* **95** 27 (2016) e4170.
- [3.51] HACHAMOVITCH, R., et al., Determinants of risk and its temporal variation in patients with normal stress myocardial perfusion scans: What is the warranty period of a normal scan? *J. Am. Coll. Cardiol.* **41** (2003) 1329–1340.
- [3.52] ALI, I., RUDDY, T.D., ALMGRAHI, A., ANSTETT, F., WELLS, R.G., Half-time SPECT myocardial perfusion imaging with attenuation correction, *J. Nucl. Med.* **50** (2009) 554–562.
- [3.53] MORDI, I., et al., Efficacy of noninvasive cardiac imaging tests in diagnosis and management of stable coronary artery disease, *Vasc. Health Risk Manage.* **13** (2017) 427–437.
- [3.54] XIN, W., et al., Gated single-photon emission computed tomography myocardial perfusion imaging is superior to computed tomography attenuation correction in discriminating myocardial infarction from attenuation artifacts in men and right coronary artery disease, *Nucl. Med. Commun.* **40** (2019) 491–498.
- [3.55] VAN DIJK, J.D., et al., Value of attenuation correction in stress-only myocardial perfusion imaging using CZT-SPECT, *J. Nucl. Cardiol.* **24** (2017) 395–401.

- [3.56] PRETORIUS, P.H., et al., Retrospective fractional dose reduction in Tc-99m cardiac perfusion SPECT–CT patients: A human and model observer study, *J. Nucl. Cardiol.* **28** (2021) 624–637.
- [3.57] GROSSMANN, M., et al., Ultra-low-dose computed tomography for attenuation correction of cadmium-zinc-telluride single photon emission computed tomography myocardial perfusion imaging, *J. Nucl. Cardiol.* **27** (2020) 228–237.
- [3.58] SCHEPIS, T., et al., Use of coronary calcium score scans from stand-alone multislice computed tomography for attenuation correction of myocardial perfusion SPECT, *Eur. J. Nucl. Med. Mol. Imaging* **34** (2007) 11–19.
- [3.59] EINSTEIN, A.J., et al., Agreement of visual estimation of coronary artery calcium from low-dose CT attenuation correction scans in hybrid PET–CT and SPECT–CT with standard Agatston score, *J. Am. Coll. Cardiol.* **56** (2010) 1914–1921.
- [3.60] RENNENBERG, R.J.M.W., et al., Vascular calcifications as a marker of increased cardiovascular risk: A meta-analysis, *Vasc. Health Risk Manage.* **5** (2009) 185–197.
- [3.61] DETRANO, R., et al., Coronary calcium as a predictor of coronary events in four racial or ethnic groups, *N. Engl. J. Med.* **358** (2008) 1336–1345.
- [3.62] BUDOFF, M.J., et al., Progression of coronary artery calcium predicts all-cause mortality, *JACC Cardiovasc. Imaging* **3** (2010) 1229–1236.
- [3.63] BUDOFF, M.J., et al., Progression of coronary calcium and incident coronary heart disease events: MESA Multi-Ethnic Study of Atherosclerosis, *J. Am. Coll. Cardiol.* **61** (2013) 1231–1239.
- [3.64] BUDOFF, M.J., et al., Diagnostic performance of 64-multidetector row coronary computed tomographic angiography for evaluation of coronary artery stenosis in individuals without known coronary artery disease: Results from the prospective multicenter ACCURACY (Assessment by Coronary Computed Tomographic Angiography of Individuals Undergoing Invasive Coronary Angiography) trial, *J. Am. Coll. Cardiol.* **52** (2008) 1724–1732.
- [3.65] MILLER, J.M., et al., Diagnostic performance of coronary angiography by 64-row CT, *N. Engl. J. Med.* **359** (2008) 2324–2336.
- [3.66] MEIJBOOM, W.B., et al., Diagnostic accuracy of 64-slice computed tomography coronary angiography: A prospective, multicenter, multivendor study, *J. Am. Coll. Cardiol.* **52** (2008) 2135–2144.
- [3.67] DE GRAAF, F.R., et al., Diagnostic accuracy of 320-row multidetector computed tomography coronary angiography in the non-invasive evaluation of significant coronary artery disease, *Eur. Heart J.* **31** (2010) 1908–1915.
- [3.68] DEWEY, M., et al., Noninvasive coronary angiography by 320-row computed tomography with lower radiation exposure and maintained diagnostic accuracy: Comparison of results with cardiac catheterization in a head-to-head pilot investigation, *Circulation* **120** (2009) 867–875.
- [3.69] VAN VELZEN, J.E., et al., Performance and efficacy of 320-row computed tomography coronary angiography in patients presenting with acute chest pain: Results from a clinical registry, *Int. J. Cardiovasc. Imaging* **28** (2012) 865–876.

- [3.70] PAZHENKOTTIL, A.P., et al., Non-invasive assessment of coronary artery disease with CT coronary angiography and SPECT: A novel dose-saving fast-track algorithm, *Eur. J. Nucl. Med. Mol. Imaging* **37** (2010) 522–527.
- [3.71] RISPLER, S., et al., Integrated single-photon emission computed tomography and computed tomography coronary angiography for the assessment of hemodynamically significant coronary artery lesions, *J. Am. Coll. Cardiol.* **49** (2007) 1059–1067.
- [3.72] SCHAAP, J., et al., Incremental diagnostic accuracy of hybrid SPECT–CT coronary angiography in a population with an intermediate to high pre-test likelihood of coronary artery disease, *Eur. Heart J. Cardiovasc. Imaging* **14** (2013) 642–649.
- [3.73] SATO, A., et al., Incremental value of combining 64-slice computed tomography angiography with stress nuclear myocardial perfusion imaging to improve noninvasive detection of coronary artery disease, *J. Nucl. Cardiol.* **17** (2010) 19–26.
- [3.74] SCHAAP, J., et al., Hybrid myocardial perfusion SPECT–CT coronary angiography and invasive coronary angiography in patients with stable angina pectoris lead to similar treatment decisions, *Heart* **99** (2013) 188–194.
- [3.75] ACHENBACH, S., et al., Coronary computed tomography angiography with a consistent dose below 1 mSv using prospectively electrocardiogram-triggered high-pitch spiral acquisition, *Eur. Heart J.* **31** (2010) 340–346.
- [3.76] BUECHEL, R.R., et al., Low-dose computed tomography coronary angiography with prospective electrocardiogram triggering: Feasibility in a large population, *J. Am. Coll. Cardiol.* **57** (2011) 332–336.
- [3.77] MARCUS, C., et al., Adding value to myocardial perfusion SPECT–CT studies that include coronary calcium CT: Detection of incidental pulmonary arterial dilatation, *Medicine* **97** (2018) e11359.
- [3.78] CAOBELLI, F., BRAUN, M., HAAF, P., WILD, D., ZELLWEGER, M., Quantitative ^{99m}Tc-DPD SPECT–CT in patients with suspected ATTR cardiac amyloidosis: Feasibility and correlation with visual scores, *J. Nucl. Cardiol.* **27** (2019) 1456–1463.
- [3.79] RAMSAY, S.C., et al., Tc-HDP quantitative SPECT–CT in transthyretin cardiac amyloid and the development of a reference interval for myocardial uptake in the non-affected population, *Eur. J. Hybrid. Imaging* **2** (2018) 17.
- [3.80] STIRRUP, J., et al., Hybrid solid-state SPECT–CT left atrial innervation imaging for identification of left atrial ganglionated plexi: Technique and validation in patients with atrial fibrillation, *J. Nucl. Cardiol.* **27** (2020) 1939–1950.
- [3.81] METTER, D., TULCHINSKY, M., FREEMAN, L.M., Current status of ventilation-perfusion scintigraphy for suspected pulmonary embolism, *Am. J. Roentgenol.* **208** (2017) 489–494.
- [3.82] MOORE, A.J.E., et al., Imaging of acute pulmonary embolism: An update, *Cardiovasc. Diagn. Ther.* **8** (2018) 225–243.
- [3.83] HEPBURN-BROWN, M., DARVALL, J., HAMMERSCHLAG, G., Acute pulmonary embolism: A concise review of diagnosis and management, *Intern. Med. J.* **49** (2019) 15–27.
- [3.84] KRUGER, P.C., EIKELBOOM, J.W., DOUKETIS, J.D., HANKEY, G.J., Pulmonary embolism: Update on diagnosis and management, *Med. J. Aust.* **211** (2019) 82–87.

- [3.85] MORRELL, N.W., NIJRAN, K.S., JONES, B.E., BIGGS, T., The underestimation of segmental defect size in radionuclide lung scanning, *J. Nucl. Med.* **34** (1993) 370–374.
- [3.86] MEIGNAN, M.A., Lung ventilation/perfusion SPECT: The right technique for hard times, *J. Nucl. Med.* **43** (2002) 648–651.
- [3.87] GOTTSCHALK, A., et al., Ventilation-perfusion scintigraphy in the PIOPED study. Part I. Data collection and tabulation, *J. Nucl. Med.* **34** (1993) 1109–1118.
- [3.88] GOTTSCHALK, A., et al., Ventilation-perfusion scintigraphy in the PIOPED study. Part II. Evaluation of the scintigraphic criteria and interpretations, *J. Nucl. Med.* **34** (1993) 1119–1126.
- [3.89] SOSTMAN, H.D., COLEMAN, R.E., DELONG, D.M., NEWMAN, G.E., PAINE, S., Evaluation of revised criteria for ventilation-perfusion scintigraphy in patients with suspected pulmonary embolism, *Radiology* **193** (1994) 103–107.
- [3.90] STEIN, P.D., et al., SPECT in acute pulmonary embolism, *J. Nucl. Med.* **50** (2009) 1999–2007.
- [3.91] ROACH, P.J., SCHEMBRI, G.P., BAILEY, D.L., V/Q scanning using SPECT and SPECT–CT, *J. Nucl. Med.* **54** (2013) 1588–1596.
- [3.92] REMY-JARDIN, M., et al., Management of suspected acute pulmonary embolism in the era of CT angiography: A statement from the Fleischner Society, *Radiology* **245** (2007) 315–329.
- [3.93] REID, J.H., et al., Is the lung scan alive and well? Facts and controversies in defining the role of lung scintigraphy for the diagnosis of pulmonary embolism in the era of MDCT, *Eur. J. Nucl. Med. Mol. Imaging* **36** (2009) 505–521.
- [3.94] JONES, S.E., WITTRAM, C., The indeterminate CT pulmonary angiogram: Imaging characteristics and patient clinical outcome, *Radiology* **237** (2005) 329–337.
- [3.95] STEIN, P.D., et al., Gadolinium-enhanced magnetic resonance angiography for pulmonary embolism: A multicenter prospective study (PIOPED III), *Ann. Intern. Med.* **152** (2010) 434–443.
- [3.96] JHA, S., The road to overdiagnosis: The case of subsegmental pulmonary embolism, *Acad. Radiol.* **22** (2015) 985–987.
- [3.97] LU, Y., Scintigraphic evidence for overdiagnosis of small PE on CT pulmonary angiography, *Nucl. Med. Mol. Imaging* **51** (2017) 97–98.
- [3.98] RASLAN, I.A., CHONG, J., GALLIX, B., LEE, T.C., McDONALD, E.G., Rates of overtreatment and treatment-related adverse effects among patients with subsegmental pulmonary embolism, *JAMA Intern. Med.* **178** (2018) 1272–1274.
- [3.99] DOBLER, C.C., Overdiagnosis of pulmonary embolism: Definition, causes and implications, *Breathe* **15** (2019) 46–53.
- [3.100] REINARTZ, P., et al., Tomographic imaging in the diagnosis of pulmonary embolism: A comparison between V/Q lung scintigraphy in SPECT technique and multislice spiral CT, *J. Nucl. Med.* **45** (2004) 1501–1508.
- [3.101] HARRIS, B., BAILEY, D., ROACH, P., BAILEY, E., KING, G., Fusion imaging of computed tomographic pulmonary angiography and SPECT ventilation/perfusion scintigraphy: Initial experience and potential benefit, *Eur. J. Nucl. Med. Mol. Imaging* **34** (2007) 135–142.

- [3.102] Harris, B., et al., Objective analysis of tomographic ventilation-perfusion scintigraphy in pulmonary embolism, *Am. J. Respir. Crit. Care Med.* **175** (2007) 1173–1180.
- [3.103] BAJC, M., et al., Lung ventilation/perfusion SPECT in the artificially embolized pig, *J. Nucl. Med.* **43** (2002) 640–647.
- [3.104] LEBLANC, M., LEVEILLÉE, F., TURCOTTE, E., Prospective evaluation of the negative predictive value of V/Q SPECT using ^{99m}Tc-Technegas, *Nucl. Med. Commun.* **28** (2007) 667–672.
- [3.105] BAJC, M., et al., EANM guidelines for ventilation/perfusion scintigraphy: Part 1. Pulmonary imaging with ventilation/perfusion single photon emission tomography, *Eur. J. Nucl. Med. Mol. Imaging* **36** (2009) 1356–1370.
- [3.106] BAJC, M., et al., EANM guidelines for ventilation/perfusion scintigraphy: Part 2. Algorithms and clinical considerations for diagnosis of pulmonary emboli with V/P(SPECT) and MDCT, *Eur. J. Nucl. Med. Mol. Imaging* **36** (2009) 1528–1538.
- [3.107] COLLART, J.-P., et al., Is a lung perfusion scan obtained by using single photon emission computed tomography able to improve the radionuclide diagnosis of pulmonary embolism? *Nucl. Med. Commun.* **23** (2002) 1107–1113.
- [3.108] BAJC, M., OLSSON, C.-G., OLSSON, B., PALMER, J., JONSON, B., Diagnostic evaluation of planar and tomographic ventilation/perfusion lung images in patients with suspected pulmonary emboli, *Clin. Physiol. Funct. Imaging* **24** (2004) 249–256.
- [3.109] ROACH, P.J., et al., SPECT–CT in V/Q scanning, *Semin. Nucl. Med.* **40** (2010) 455–466.
- [3.110] GUTTE, H., et al., Detection of pulmonary embolism with combined ventilation-perfusion SPECT and low-dose CT: Head-to-head comparison with multidetector CT angiography, *J. Nucl. Med.* **50** (2009) 1987–1992.
- [3.111] BAJC, M., et al., EANM guideline for ventilation/perfusion single-photon emission computed tomography (SPECT) for diagnosis of pulmonary embolism and beyond, *Eur. J. Nucl. Med. Mol. Imaging* **46** (2019) 2429–2451.
- [3.112] HESS, S., FRARY, E.C., GERKE, O., MADSEN, P.H., State-of-the-art imaging in pulmonary embolism: Ventilation/perfusion single-photon emission computed tomography versus computed tomography angiography — controversies, results, and recommendations from a systematic review, *Semin. Thromb. Hemostasis* **42** (2016) 833–845.
- [3.113] TONEY, L.K., KIM, R.D., PALLI, S.R., The economic value of hybrid single-photon emission computed tomography with computed tomography imaging in pulmonary embolism diagnosis, *Acad. Emerg. Med.* **24** (2017) 1110–1123.
- [3.114] MAZUREK, A., DZIUK, M., WITKOWSKA-PATENA, E., PISZCZEK, S., GIZEWSKA, A., The utility of hybrid SPECT–CT lung perfusion scintigraphy in pulmonary embolism diagnosis, *Respiration* **90** (2015) 393–401.
- [3.115] KUMAR, N., et al., Software-based hybrid perfusion SPECT–CT provides diagnostic accuracy when other pulmonary embolism imaging is indeterminate, *Nucl. Med. Mol. Imaging* **49** (2015) 303–311.

- [3.116] BHATIA, K.D., et al., SPECT-CT/VQ versus CTPA for diagnosing pulmonary embolus and other lung pathology: Pre-existing lung disease should not be a contraindication, *J. Med. Imaging Radiat. Oncol.* **60** (2016) 492–497.
- [3.117] SIMANEK, M., KORANDA, P., The benefit of personalized hybrid SPECT–CT pulmonary imaging, *Am. J. Nucl. Med. Mol. Imaging* **6** (2016) 215–222.
- [3.118] LIU, J., LARCOS, G., Radionuclide lung scans for suspected acute pulmonary embolism: Single photon emission computed tomography (SPECT) or hybrid SPECT–CT? *J. Med. Imaging Radiat. Oncol.* **63** (2019) 731–736.
- [3.119] RANKA, S., et al., Chronic thromboembolic pulmonary hypertension — management strategies and outcomes, *J. Cardiothorac. Vasc. Anesth.* **34** (2020) 2513–2523.
- [3.120] SAHAY, S., Evaluation and classification of pulmonary arterial hypertension, *J. Thorac. Dis.* **11** Suppl. 14 (2019) S1789–S1799.
- [3.121] DOURNES, G., et al., Dual-energy CT perfusion and angiography in chronic thromboembolic pulmonary hypertension: Diagnostic accuracy and concordance with radionuclide scintigraphy, *Eur. Radiol.* **24** (2014) 42–51.
- [3.122] MORADI, F., MORRIS, T.A., HOH, C.K., Perfusion scintigraphy in diagnosis and management of thromboembolic pulmonary hypertension, *Radiographics* **39** (2019) 169–185.
- [3.123] ENDE-VERHAAR, Y.M., et al., Usefulness of standard computed tomography pulmonary angiography performed for acute pulmonary embolism for identification of chronic thromboembolic pulmonary hypertension: Results of the InShape III study, *J. Heart Lung Transpl.* **38** (2019) 731–738.
- [3.124] TONKOPI, E., MANOS, D., ROSS, A., Does the use of contemporary CT scanners alter the radiation dose debate in the imaging work up for pulmonary embolism? *Radiat. Prot. Dosim.* **187** (2019) 353–360.
- [3.125] TAMURA, M., et al., Diagnostic accuracy of lung subtraction iodine mapping CT for the evaluation of pulmonary perfusion in patients with chronic thromboembolic pulmonary hypertension: Correlation with perfusion SPECT–CT, *Int. J. Cardiol.* **243** (2017) 538–543.
- [3.126] CHAN, K., IOANNIDIS, S., COGHLAN, J.G., HALL, M., SCHREIBER, B.E., Pulmonary arterial hypertension with abnormal V/Q single-photon emission computed tomography, *JACC Cardiovasc. Imaging* **11** (2018) 1487–1493.
- [3.127] DERLIN, T., et al., Quantitation of perfused lung volume using hybrid SPECT–CT allows refining the assessment of lung perfusion and estimating disease extent in chronic thromboembolic pulmonary hypertension, *Clin. Nucl. Med.* **43** (2018) e170–e177.
- [3.128] RENAPURKAR, R.D., et al., Comparative assessment of qualitative and quantitative perfusion with dual-energy CT and planar and SPECT-CT V/Q scanning in patients with chronic thromboembolic pulmonary hypertension, *Cardiovasc. Diagn. Ther.* **8** (2018) 414–422.
- [3.129] HERNANDO, M.L., et al., Radiation-induced pulmonary toxicity: A dose-volume histogram analysis in 201 patients with lung cancer, *Int. J. Radiat. Oncol. Biol. Phys.* **51** (2001) 650–659.

- [3.130] KONG, F.-M., et al., Final toxicity results of a radiation-dose escalation study in patients with non-small-cell lung cancer (NSCLC): Predictors for radiation pneumonitis and fibrosis, *Int. J. Radiat. Oncol. Biol. Phys.* **65** (2006) 1075–1086.
- [3.131] MAZERON, R., et al., Predictive factors of late radiation fibrosis: A prospective study in non-small cell lung cancer, *Int. J. Radiat. Oncol. Biol. Phys.* **7** (2010) 38–43.
- [3.132] ROEDER, F., et al., Correlation of patient-related factors and dose-volume histogram parameters with the onset of radiation pneumonitis in patients with small cell lung cancer, *Strahlenther. Onkol.* **186** (2010) 149–156.
- [3.133] WOEL, R.T., et al., The time course of radiation therapy-induced reductions in regional perfusion: A prospective study with >5 years of follow-up, *Int. J. Radiat. Oncol. Biol. Phys.* **52** (2002) 58–67.
- [3.134] ZHANG, J., et al., Radiation-induced reductions in regional lung perfusion: 0.1–12 year data from a prospective clinical study, *Int. J. Radiat. Oncol. Biol. Phys.* **76** (2010) 425–432.
- [3.135] MUNAWAR, I., et al., Intensity modulated radiotherapy of non-small-cell lung cancer incorporating SPECT ventilation imaging, *Med. Phys.* **37** (2010) 1863–1872.
- [3.136] BUCKNELL, N.W., et al., Functional lung imaging in radiation therapy for lung cancer: A systematic review and meta-analysis, *Radiother. Oncol.* **129** (2018) 196–208.
- [3.137] LEE, H.J. Jr., et al., Correlation of functional lung heterogeneity and dosimetry to radiation pneumonitis using perfusion SPECT–CT and FDG PET–CT imaging, *Int. J. Radiat. Oncol. Biol. Phys.* **102** (2018) 1255–1264.
- [3.138] THOMAS, H.M.T., et al., Comparison of regional lung perfusion response on longitudinal MAA SPECT–CT in lung cancer patients treated with and without functional tissue-avoidance radiation therapy, *Br. J. Radiol.* **92** 1103 (2019) 20190174.
- [3.139] LISS, A.L., et al., Decreased lung perfusion after breast/chest wall irradiation: Quantitative results from a prospective clinical trial, *Int. J. Radiat. Oncol. Biol. Phys.* **97** (2017) 296–302.
- [3.140] PROVOST, K., et al., Reproducibility of lobar perfusion and ventilation quantification using SPECT–CT segmentation software in lung cancer patients, *J. Nucl. Med. Technol.* **45** (2017) 185–192.
- [3.141] SCHAEFER, W.M., KNOLLMANN, D., AVONDO, J., MEYER, A., Volume/perfusion ratio from lung SPECT–CT, *Nuklearmedizin* **57** (2018) 31–34.
- [3.142] GENSEKE, P., et al., Pre-operative quantification of pulmonary function using hybrid-SPECT/low-dose-CT: A pilot study, *Lung Cancer* **118** (2018) 155–160.
- [3.143] SIMON, D., IRUSEN, E.M., WARWICK, J.M., DORUYTER, A., KOEGELENBERG, C.F.N., Simple anatomical calculations possibly as accurate as three-dimensional lobar quantification with SPECT-CT in predicting lung function after pulmonary resection, *Respiration* **98** (2019) 82–85.
- [3.144] KRISTIANSEN, J.F., PERCH, M., IVERSEN, M., KRAKAUER, M., MORTENSEN, J., Lobar quantification by ventilation/perfusion SPECT–CT in patients with severe emphysema undergoing lung volume reduction with endobronchial valves, *Respiration* **98** (2019) 230–238.

- [3.145] ARNON-SHELEG, E., HABERFELD, O., KREMER, R., KEIDAR, Z., WEILER-SAGIE, M., Head-to-head prospective comparison of quantitative lung scintigraphy and segment counting in predicting pulmonary function in lung cancer patients undergoing video-assisted thoracoscopic lobectomy, *J. Nucl. Med.* **61** (2020) 981–989.
- [3.146] SUH, H.Y., et al., Comparative analysis of lung perfusion scan and SPECT–CT for the evaluation of functional lung capacity, *Nucl. Med. Mol. Imaging* **53** (2019) 406–413.
- [3.147] OHNO, Y., et al., Xenon-enhanced CT using subtraction CT: Basic and preliminary clinical studies for comparison of its efficacy with that of dual-energy CT and ventilation SPECT–CT to assess regional ventilation and pulmonary functional loss in smokers, *Eur. J. Radiol.* **86** (2017) 41–51.
- [3.148] DOGANAY, O., et al., Time-series hyperpolarized xenon-129 MRI of lobar lung ventilation of COPD in comparison to V/Q-SPECT–CT and CT, *Eur. Radiol.* **29** (2019) 4058–4067.
- [3.149] LING, T., et al., Ventilation/perfusion SPECT–CT in patients with severe and rigid scoliosis: An evaluation by relationship to spinal deformity and lung function, *Clin. Neurol. Neurosurg.* **176** (2019) 97–102.
- [3.150] NAKASHIMA, M., SHINYA, T., OTO, T., OKAWA, T., TAKEDA, Y., Diagnostic value of ventilation/perfusion single-photon emission computed tomography/computed tomography for bronchiolitis obliterans syndrome in patients after lung transplantation, *Nucl. Med. Commun.* **40** (2019) 703–710.
- [3.151] ISRAEL, O., et al., Two decades of SPECT–CT — the coming of age of a technology: An updated review of literature evidence, *Eur. J. Nucl. Med. Mol. Imaging* **46** (2019) 1990–2012.
- [3.152] GNANASEGARAN, G., et al., Bone SPECT–CT in postoperative spine, *Semin. Nucl. Med.* **48** (2018) 410–424.
- [3.153] VAN DER BRUGGEN, W., et al., SPECT–CT in the postoperative painful knee, *Semin. Nucl. Med.* **48** (2018) 439–453.
- [3.154] THÉLU-VANYSACKER, M., et al., SPECT–CT in postoperative shoulder pain, *Semin. Nucl. Med.* **48** (2018) 469–482.
- [3.155] BHURE, U., ROOS, J.E., PEREZ-LAGO, M.D.S., STROBEL, K., Single photon emission computed tomography/computed tomography arthrography of wrist, ankle, and knee joints, *Nucl. Med. Commun.* **41** (2020) 182–188.
- [3.156] KIM, J., et al., Maximum standardised uptake value of quantitative bone SPECT–CT in patients with medial compartment osteoarthritis of the knee, *Clin. Radiol.* **72** (2017) 580–589.
- [3.157] RUSSO, V.M., et al., Hybrid bone SPECT–CT imaging in evaluation of chronic low back pain: Correlation with facet joint arthropathy, *World Neurosurg.* **107** (2017) 732–738.
- [3.158] RUSSO, V.M., et al., Hybrid bone single photon emission computed tomography imaging in evaluation of chronic low back pain: Correlation with modic changes and degenerative disc disease, *World Neurosurg.* **104** (2017) 816–823.

- [3.159] JAIN, A., et al., Evaluation of efficacy of bone scan with SPECT–CT in the management of low back pain: A study supported by differential diagnostic local anaesthetic blocks, *Clin. J. Pain* **31** (2015) 1054–1059.
- [3.160] LEE, I., et al., The value of SPECT–CT in localizing pain site and prediction of treatment response in patients with chronic low back pain, *J. Korean Med. Sci.* **29** (2014) 1711–1716.
- [3.161] RUTHERFORD, E.E., TARPLETT, L.J., DAVIES, E.M., HARLEY, J.M., KING, L.J., Lumbar spine fusion and stabilization: Hardware, techniques, and imaging appearances, *Radiographics* **27** (2007) 1737–1749.
- [3.162] AL-RIYAMI, K., GNANASEGARAN, G., VAN DEN WYNGAERT, T., BOMANJI, J., Bone SPECT–CT in the postoperative spine: A focus on spinal fusion, *Eur. J. Nucl. Med. Mol. Imaging* **44** (2017) 2094–2104.
- [3.163] RAGER, O., et al., SPECT–CT in differentiation of pseudarthrosis from other causes of back pain in lumbar spinal fusion: Report on 10 consecutive cases, *Clin. Nucl. Med.* **37** (2012) 339–343.
- [3.164] SUMER, J., et al., SPECT–CT in patients with lower back pain after lumbar fusion surgery, *Nucl. Med. Commun.* **34** (2013) 964–970.
- [3.165] HUDYANA, H., et al., Accuracy of bone SPECT–CT for identifying hardware loosening in patients who underwent lumbar fusion with pedicle screws, *Eur. J. Nucl. Med. Mol. Imaging* **43** (2016) 349–354.
- [3.166] CUSI, M., SAUNDERS, J., VAN DER WALL, H., FOGELMAN, I., Metabolic disturbances identified by SPECT-CT in patients with a clinical diagnosis of sacroiliac joint incompetence, *Eur. Spine J.* **22** (2013) 1674–1682.
- [3.167] ROSS, TD., EVANS, S., AHERN, D.P., McDONNELL, J., BUTLER, J.S., Discography or SPECT–CT: What is the best diagnostic tool for the surgical assessment of degenerative disk disease? *Clin. Spine Surg.* **34** (2021) 355–358.
- [3.168] GATES, G.F., SPECT bone scanning of the spine, *Semin. Nucl. Med.* **28** (1998) 78–94.
- [3.169] ISEDA, T., et al., Radiographic and scintigraphic courses of union in cervical interbody fusion: Hydroxyapatite grafts versus iliac bone autografts, *J. Nucl. Med.* **41** (2000) 1642–1645.
- [3.170] HUDYANA, H., et al., Accuracy of bone SPECT–CT for identifying hardware loosening in patients who underwent lumbar fusion with pedicle screws, *Eur. J. Nucl. Med. Mol. Imaging* **43** (2016) 349–354.
- [3.171] HUELLNER, M.W., STROBEL, K., Clinical applications of SPECT–CT in imaging the extremities, *Eur. J. Nucl. Med. Mol. Imaging* **41** Suppl. 1 (2014) S50–S58.
- [3.172] ALLAINMAT, L., et al., Use of hybrid SPECT–CT for diagnosis of radiographic occult fractures of the wrist, *Clin. Nucl. Med.* **38** (2013) 246–251.
- [3.173] KRÜGER, T., et al., SPECT–CT arthrography of the wrist in ulnocarpal impaction syndrome, *Eur. J. Nucl. Med. Mol. Imaging* **38** (2011) 792.
- [3.174] SCHLEICH, F.S., et al., Diagnostic and therapeutic impact of SPECT–CT in patients with unspecific pain of the hand and wrist, *Eur. J. Nucl. Med. Mol. Imaging Res.* **28** (2012) 53.

- [3.175] HUELLNER, M.W., et al., SPECT–CT versus MRI in patients with nonspecific pain of the hand and wrist — a pilot study, *Eur. J. Nucl. Med. Mol. Imaging* **39** (2012) 750–759.
- [3.176] SCHWEIZER, T., et al., Patterns of bone tracer uptake on SPECT-CT in symptomatic and asymptomatic patients with primary total hip arthroplasty, *Eur. J. Nucl. Med. Mol. Imaging* **45** (2018) 283–291.
- [3.177] DIEDERICHS, G., et al., Evaluation of bone viability in patients after girdlestone arthroplasty: Comparison of bone SPECT–CT and MRI, *Skelet. Radiol.* **46** (2017) 1249–1258.
- [3.178] BARTHASSAT, E., AFIFI, F., KONALA, P., RASCH, H., HIRSCHMANN, M.T., Evaluation of patients with painful total hip arthroplasty using combined single photon emission tomography and conventional computerized tomography (SPECT–CT) — a comparison of semi-quantitative versus 3D volumetric quantitative measurements, *BMC Med. Imaging* **17** (2017) 31.
- [3.179] SLEVIN, O., SCHMID, F.A., SCHIAPPARELLI, F., RASCH, H., HIRSCHMANN, M.T., Increased in vivo patellofemoral loading after total knee arthroplasty in resurfaced patellae, *Knee Surg. Sports Traumatol. Arthroscopy* **26** (2018) 1805–1810.
- [3.180] AWENGEN, R., RASCH, H., AMSLER, F., HIRSCHMANN, M.T., Symptomatic versus asymptomatic knees after bilateral total knee arthroplasty: What is the difference in SPECT–CT? *Eur. J. Nucl. Med. Mol. Imaging* **43** (2016) 762–772.
- [3.181] MATHIS, D.T., et al., Increased bone tracer uptake in symptomatic patients with ACL graft insufficiency: A correlation of MRI and SPECT–CT findings, *Knee Surg. Sports Traumatol. Arthroscopy* **26** (2018) 563–573.
- [3.182] HIRSCHMANN, M.T., et al., SPECT–CT tracer uptake is influenced by tunnel orientation and position of the femoral and tibial ACL graft insertion site, *Int. Orthop.* **37** (2013) 301–309.
- [3.183] BHURE, U., et al., SPECT–CT arthrography, *Br. J. Radiol.* **91** (2018) 20170635.
- [3.184] MURER, A.M., HIRSCHMANN, M.T., AMSLER, F., RASCH, H., HUEGLI, R.W., Bone SPECT–CT has excellent sensitivity and specificity for diagnosis of loosening and patellofemoral problems after total knee arthroplasty, *Knee Surg. Sports Traumatol. Arthroscopy* **28** (2019) 1029–1035.
- [3.185] VERSCHUEREN, J., et al., Bloodpool SPECT as part of bone SPECT–CT in painful total knee arthroplasty (TKA): Validation and potential biomarker of prosthesis biomechanics, *Eur. J. Nucl. Med. Mol. Imaging* **46** (2019) 1009–1018.
- [3.186] ARICAN, P., et al., The role of bone SPECT–CT in the evaluation of painful joint prostheses, *Nucl. Med. Commun.* **36** (2015) 931–940.
- [3.187] AL-NABHANI, K., et al., Painful knee prosthesis: can we help with bone SPECT–CT? *Nucl. Med. Commun.* **35** (2014) 182–188.
- [3.188] CHEW, C.G., LEWIS, P., MIDDLETON, F., VAN DEN WIJNGAARD, R., DESHAIES, A., Radionuclide arthrogram with SPECT–CT for the evaluation of mechanical loosening of hip and knee prostheses, *Ann. Nucl. Med.* **24** (2010) 735–743.

- [3.189] HIRSCHMANN, M.T., et al., Assessment of loading history of compartments in the knee using bone SPECT-CT: A study combining alignment and ^{99m}Tc-HDP tracer uptake/distribution patterns, *J. Orthop. Res.* **31** (2013) 268–274.
- [3.190] DIEDERICHS, G., et al., Evaluation of bone viability in patients after girdlestone arthroplasty: Comparison of bone SPECT-CT and MRI, *Skelet. Radiol.* **46** (2017) 1249–1258.
- [3.191] VAN DEN WYNGAERT, T., PALLI, S.R., IMHOFF, R.J., HIRSCHMANN, M.T., Cost-effectiveness of bone SPECT-CT in painful total knee arthroplasty, *J. Nucl. Med.* **59** (2018) 1742–1750.
- [3.192] REMÉRAND, F., et al., Chronic pain 1 year after foot surgery: Epidemiology and associated factors, *Orthop. Traumatol. Surg. Res.* **100** (2014) 767–773.
- [3.193] NATHAN, M., MOHAN, H., VIJAYANATHAN, S., FOGELMAN, I., GNANASEGARAN, G., The role of ^{99m}Tc-diphosphonate bone SPECT-CT in the ankle and foot, *Nucl. Med. Commun.* **33** (2012) 799–807.
- [3.194] BIERSACK, H.-J., WINGENFELD, C., HINTERTHANER, B., FRANK, D., SABET, A., SPECT-CT des Fußes, *Nuklearmedizin* **51** (2012) 26–31.
- [3.195] HA, S., et al., Comparison of SPECT-CT and MRI in diagnosing symptomatic lesions in ankle and foot pain patients: Diagnostic performance and relation to lesion type, *PLoS One* **10** (2015) e0117583.
- [3.196] CHICKLORE, S., GNANASEGARAN, G., VIJAYANATHAN, S., FOGELMAN, I., Potential role of multislice SPECT-CT in impingement syndrome and soft-tissue pathology of the ankle and foot, *Nucl. Med. Commun.* **34** (2013) 130–139.
- [3.197] SINGH, V.K., JAVED, S., PARTHIPUN, A., SOTT, A.H., The diagnostic value of single photon-emission computed tomography bone scans combined with CT (SPECT-CT) in diseases of the foot and ankle, *Foot Ankle Surg.* **19** (2013) 80–83.
- [3.198] KNUPP, M., et al., SPECT-CT compared with conventional imaging modalities for the assessment of the varus and valgus malaligned hindfoot, *J. Orthop. Res.* **27** (2009) 1461–1466.
- [3.199] BERTH, A., et al., SPECT-CT demonstrates the osseointegrative response of a stemless shoulder prosthesis, *J. Shoulder Elbow Surg.* **25** (2016) e96–103.
- [3.200] HIRSCHMANN, M.T., et al., Combined single photon emission computerized tomography and conventional computerized tomography: Clinical value for the shoulder surgeons? *Int. J. Shoulder Surg.* **5** (2011) 72–76.
- [3.201] EVEN-SAPIR, E., Imaging of malignant bone involvement by morphologic, scintigraphic, and hybrid modalities, *J. Nucl. Med.* **46** (2005) 1356–1367.
- [3.202] DAVILA, D., ANTONIOU, A., CHAUDHRY, M.A., Evaluation of osseous metastasis in bone scintigraphy, *Semin. Nucl. Med.* **45** (2015) 3–15.
- [3.203] RATHKE, H., et al., Intra-individual comparison of Tc-99m-MDP bone scan and the PSMA-ligand Tc-99m-MIP-1427 in patients with osseous metastasized prostate cancer, *J. Nucl. Med.* **59** (2018) 1373–1379.
- [3.204] AZAD, G.K., et al., Molecular and functional imaging of bone metastases in breast and prostate cancers: An overview, *Clin. Nucl. Med.* **41** (2016) e44–e50.
- [3.205] COOK, G.J.R., AZAD, G.K., GOH, V., Imaging bone metastases in breast cancer: Staging and response assessment, *J. Nucl. Med. Suppl.* **57** (2016) 27S–33S.

- [3.206] LIU, T., et al., Detection of vertebral metastases: A meta-analysis comparing MRI, CT, PET, BS and BS with SPECT, *J. Cancer Res. Clin. Oncol.* **143** (2017) 457–465.
- [3.207] RITT, P., VIJA, H., HORNEGGER, J., KUWERT, T., Absolute quantification in SPECT, *Eur. J. Nucl. Med. Mol. Imaging* **38** Suppl. 1 (2011) S69–S77.
- [3.208] JAMBOR, I., et al., Prospective evaluation of planar bone scintigraphy, SPECT, SPECT–CT, ¹⁸F-NaF PET–CT and whole body 1.5T MRI, including DWI, for the detection of bone metastases in high risk breast and prostate cancer patients: SKELETA clinical trial, *Acta Oncol.* **55** (2016) 59–67.
- [3.209] KUWERT, T., Skeletal SPECT–CT: A review, *Clin. Transl. Imaging* **2** (2014) 505–517.
- [3.210] HORGER, M., et al., Evaluation of combined transmission and emission tomography for classification of skeletal lesions, *Am. J. Roentgenol.* **183** (2004) 655–661.
- [3.211] RÖMER, W., NÖMAYR, A., UDER, M., BAUTZ, W., KUWERT, T., SPECT-guided CT for evaluating foci of increased bone metabolism classified as indeterminate on SPECT in cancer patients, *J. Nucl. Med.* **47** (2006) 1102–1106.
- [3.212] HELYAR, V., et al., The added value of multislice SPECT–CT in patients with equivocal bony metastasis from carcinoma of the prostate, *Eur. J. Nucl. Med. Mol. Imaging* **37** (2010) 706–713.
- [3.213] ZHAO, Z., LI, L., LI, F., ZHAO, L., Single photon emission computed tomography/spiral computed tomography fusion imaging for the diagnosis of bone metastasis in patients with known cancer, *Skelet. Radiol.* **39** (2010) 147–153.
- [3.214] NDLOVU, X., GEORGE, R., ELLMANN, A., WARWICK, J., Should SPECT-CT replace SPECT for the evaluation of equivocal bone scan lesions in patients with underlying malignancies? *Nucl. Med. Commun.* **31** (2010) 659–665.
- [3.215] ZHANG, Y., et al., Differential diagnostic value of single-photon emission computed tomography/spiral computed tomography with Tc-99m-methylene diphosphonate in patients with spinal lesions, *Nucl. Med. Commun.* **32** (2011) 1194–1200.
- [3.216] SHARMA, P., et al., Indeterminate lesions on planar bone scintigraphy in lung cancer patients: SPECT, CT or SPECT-CT? *Skelet. Radiol.* **41** (2012) 843–850.
- [3.217] SHARMA, P., et al., Bone scintigraphy in breast cancer: Added value of hybrid SPECT-CT and its impact on patient management, *Nucl. Med. Commun.* **33** (2012) 139–147.
- [3.218] SHARMA, P., et al., Hybrid SPECT-CT for characterizing isolated vertebral lesions observed by bone scintigraphy: Comparison with planar scintigraphy, SPECT, and CT, *Diagn. Interv. Radiol.* **19** (2013) 33–40.
- [3.219] ZHANG, Y., et al., The added value of SPECT/spiral CT in patients with equivocal bony metastasis from hepatocellular carcinoma, *Nuklearmedizin* **54** 6 (2015) 255–261.
- [3.220] ZHANG, Y., et al., Added value of SPECT/spiral CT versus SPECT or CT alone in diagnosing solitary skeletal lesions, *Nuklearmedizin* **56** (2017) 139–145.
- [3.221] GUEZENNEC, C., et al., Incremental diagnostic utility of systematic double-bed SPECT–CT for bone scintigraphy in initial staging of cancer patients, *Cancer Imaging* **17** (2017) 16.

- [3.222] LÖFGREN, J., et al., A prospective study comparing ^{99m}Tc -hydroxyethylene-diphosphonate planar bone scintigraphy and whole-body SPECT-CT with ^{18}F -fluoride PET-CT and ^{18}F -fluoride PET/MRI for diagnosing bone metastases, *J. Nucl. Med.* **58** (2017) 1778–1785.
- [3.223] MAHALETCHUMY, T., ABAZIZ, A., Incremental value of single-photon emission computed tomography-computed tomography for characterization of skeletal lesions in breast cancer patients, *World J. Nucl. Med.* **16** (2017) 303–310.
- [3.224] PENG, H., et al., Characterization of solitary lesions in the extremities on whole-body bone scan in patients with known cancer: Contribution of single-photon emission computed tomography/computed tomography, *Front. Oncol.* **9** (2019) 607.
- [3.225] ZACHO, H.D., et al., Three-minute SPECT-CT is sufficient for the assessment of bone metastasis as add-on to planar bone scintigraphy: Prospective head-to-head comparison to 11-min SPECT-CT, *Eur. J. Nucl. Med. Mol. Imaging Res.* **7** (2017) 1.
- [3.226] FLEURY, V., et al., Advantages of systematic trunk SPECT-CT to planar bone scan (PBS) in more than 300 patients with breast or prostate cancer, *Oncotarget* **9** (2018) 31744–31752.
- [3.227] UTSUNOMIYA, D., et al., Added value of SPECT-CT fusion in assessing suspected bone metastasis: Comparison with scintigraphy alone and nonfused scintigraphy and CT, *Radiology* **238** (2006) 264–271.
- [3.228] PALMEDO, H., et al., Whole-body SPECT-CT for bone scintigraphy: Diagnostic value and effect on patient management in oncological patients, *Eur. J. Nucl. Med. Mol. Imaging* **41** (2014) 59–67.
- [3.229] HARALDSEN, A., et al., Single photon emission computed tomography (SPECT) and SPECT/low-dose computerized tomography did not increase sensitivity or specificity compared to planar bone scintigraphy for detection of bone metastases in advanced breast cancer, *Clin. Physiol. Funct. Imaging* **36** (2016) 40–46.
- [3.230] FONAGER, R.F., et al., Diagnostic test accuracy study of ^{18}F -sodium fluoride PET-CT, ^{99m}Tc -labelled diphosphonate SPECT-CT, and planar bone scintigraphy for diagnosis of bone metastases in newly diagnosed, high-risk prostate cancer, *Am. J. Nucl. Med. Mol. Imaging* **7** (2017) 218–227.
- [3.231] SHARMA, P., et al., Comparison of single photon emission computed tomography-computed tomography, computed tomography, single photon emission computed tomography and planar scintigraphy for characterization of isolated skull lesions seen on bone scintigraphy in cancer patients, *Indian J. Nucl. Med.* **29** (2014) 22–29.
- [3.232] ZHANG, L., et al., Accurate characterization of ^{99m}Tc -MDP uptake in extraosseous neoplasm mimicking bone metastasis on whole-body bone scan: Contribution of SPECT-CT, *BMC Med. Imaging* **19** (2019) 44.
- [3.233] MAVRIOPOULOU, E., et al., Whole body bone SPET-CT can successfully replace the conventional bone scan in breast cancer patients. A prospective study of 257 patients, *Hell. J. Nucl. Med.* **21** (2018) 125–133.
- [3.234] ABIKHZER, G., et al., Whole-body bone SPECT in breast cancer patients: The future bone scan protocol? *Nucl. Med. Commun.* **37** (2016) 247–253.

- [3.235] WEISSINGER, M., KUPFERSCHLÄGER, J., LA FOUGÈRE, C., DITTMANN, H., FIZ, F., Transitioning to whole-body SPECT–CT in prostate cancer staging: A new concept for a better imaging workflow, *Nuklearmedizin* **58** (2019) 451–459.
- [3.236] DE SCHEPPER, S., RITT, P., VAN DEN WYNGAERT, T., KUWERT, T., Quantitative radionuclide imaging of bone metastases, *Q. J. Nucl. Med. Mol. Imaging* **63** (2019) 129–135.
- [3.237] RAGER, O., et al., Whole-body SPECT–CT versus planar bone scan with targeted SPECT–CT for metastatic workup, *Biomed. Res. Int.* **2017** (2017) 7039406.
- [3.238] ZEINTL, J., VIJA, A.H., YAHIL, A., HORNEGGER, J., KUWERT, T., Quantitative accuracy of clinical ^{99m}Tc SPECT–CT using ordered-subset expectation maximization with 3-dimensional resolution recovery, attenuation, and scatter correction, *J. Nucl. Med.* **51** (2010) 921–928.
- [3.239] CACHOVAN, M., VIJA, A.H., HORNEGGER, J., KUWERT, T., Quantification of ^{99m}Tc -DPD concentration in the lumbar spine with SPECT–CT, *Eur. J. Nucl. Med. Mol. Imaging Res.* **3** (2013) 45.
- [3.240] ARVOLA, S., et al., Comparison of standardized uptake values between ^{99m}Tc -HDP SPECT–CT and ^{18}F -NaF PET–CT in bone metastases of breast and prostate cancer, *Eur. J. Nucl. Med. Mol. Imaging Res.* **9** (2019) 6.
- [3.241] BECK, M., SANDERS, J.C., RITT, P., REINFELDER, J., KUWERT, T., Longitudinal analysis of bone metabolism using SPECT/CT and (99m) Tc-diphosphono-propanedicarboxylic acid: Comparison of visual and quantitative analysis. *Eur. J. Nucl. Med. Mol. Imaging Res.* **6** (2016) 60.
- [3.242] KUJI, I., et al., Skeletal standardized uptake values obtained by quantitative SPECT–CT as an osteoblastic biomarker for the discrimination of active bone metastasis in prostate cancer, *Eur. J. Hybrid Imaging* **1** (2017) 2.
- [3.243] TABOTTA, F., et al., Quantitative bone SPECT–CT: High specificity for identification of prostate cancer bone metastases, *BMC Musculoskelet. Disord.* **20** (2019) 619.
- [3.244] MOHD ROHANI, M.F., et al., Maximum standardized uptake value from quantitative bone single-photon emission computed tomography/computed tomography in differentiating metastatic and degenerative joint disease of the spine in prostate cancer patients, *Ann. Nucl. Med.* **34** (2020) 39–48.
- [3.245] UMEDA, T., et al., Evaluation of bone metastatic burden by bone SPECT–CT in metastatic prostate cancer patients: Defining threshold value for total bone uptake and assessment in radium-223 treated patients, *Ann. Nucl. Med.* **32** (2018) 105–113.
- [3.246] FIZ, F., et al., Automated definition of skeletal disease burden in metastatic prostate carcinoma: A 3D analysis of SPECT–CT images, *Cancers* **11** (2019) 869.
- [3.247] WEISMAN, A.J., et al., Quantification of bone flare on ^{18}F -NaF PET–CT in metastatic castration-resistant prostate cancer, *Prostate Cancer Prostatic Dis.* **22** (2019) 324–330.
- [3.248] HARMON, S.A., et al., Quantitative assessment of early [^{18}F]sodium fluoride positron emission tomography/computed tomography response to treatment in men with metastatic prostate cancer to bone, *J. Clin. Oncol.* **35** (2017) 2829–2837.

- [3.249] ERBA, P.A., ISRAEL, O., SPECT-CT in infection and inflammation, *Clin. Transl. Imaging* **2** (2014) 519–535.
- [3.250] LAZZERI, E., et al., Clinical impact of SPECT-CT with In-111 biotin on the management of patients with suspected spine infection, *Clin. Nucl. Med.* **35** (2010) 12–17.
- [3.251] HORGER, M., et al., The value of SPET-CT in chronic osteomyelitis, *Eur. J. Nucl. Med. Mol. Imaging* **30** (2003) 1665–1673.
- [3.252] GRAUTE, V., et al., Detection of low-grade prosthetic joint infections using ^{99m}Tc-antigranulocyte SPECT-CT: Initial clinical results, *Eur. J. Nucl. Med. Mol. Imaging* **37** (2010) 1751–1759.
- [3.253] SATHEKGE, M., et al., Molecular imaging in musculoskeletal infections with ^{99m}Tc-UBI 29-41 SPECT-CT, *Ann. Nucl. Med.* **32** (2018) 54–59.
- [3.254] BAR-SHALOM, R., et al., SPECT-CT using ⁶⁷Ga and ¹¹¹In-labeled leukocyte scintigraphy for diagnosis of infection, *J. Nucl. Med.* **47** (2006) 587–594.
- [3.255] FUSTER, D., et al., A prospective study comparing whole-body FDG PET-CT to combined planar bone scan with ⁶⁷Ga SPECT-CT in the diagnosis of spondylodiskitis, *Clin. Nucl. Med.* **37** (2012) 827–832.
- [3.256] TAMM, A.S., ABELE, J.T., Bone and gallium single-photon emission computed tomography-computed tomography is equivalent to magnetic resonance imaging in the diagnosis of infectious spondylodiscitis: A retrospective study, *Can. Assoc. Radiol. J.* **68** (2017) 41–46.
- [3.257] ASLANGUL, E., et al., Diagnosing diabetic foot osteomyelitis in patients without signs of soft tissue infection by coupling hybrid ⁶⁷Ga SPECT-CT with bedside percutaneous bone puncture, *Diabetes Care* **36** (2013) 2203–2210.
- [3.258] JAMAR, F., et al., EANM/SNMMI guideline for ¹⁸F-FDG use in inflammation and infection, *J. Nucl. Med.* **54** (2013) 647–658.
- [3.259] FILIPPI, L., SCHILLACI, O., Usefulness of hybrid SPECT-CT in ^{99m}Tc-HMPAO-labeled leukocyte scintigraphy for bone and joint infections, *J. Nucl. Med.* **47** (2006) 1908–1913.
- [3.260] HORGER, M., et al., Added value of SPECT-CT in patients suspected of having bone infection: Preliminary results, *Arch. Orthop. Trauma Surg.* **127** (2007) 211–221.
- [3.261] DJEKIDEL, M., BROWN, R.K.J., PIERT, M., Benefits of hybrid SPECT-CT for ¹¹¹In-oxine- and Tc-99m-hexamethylpropylene amine oxime-labeled leukocyte imaging, *Clin. Nucl. Med.* **36** (2011) e50–e56.
- [3.262] FILIPPI, L., UCCIOLI, L., GIURATO, L., SCHILLACI, O., Diabetic foot infection: Usefulness of SPECT-CT for ^{99m}Tc-HMPAO-labeled leukocyte imaging, *J. Nucl. Med.* **50** (2009) 1042–1046.
- [3.263] HEIBA, S.I., et al., The optimized evaluation of diabetic foot infection by dual isotope SPECT-CT imaging protocol, *J. Foot Ankle Surg.* **49** (2010) 529–536.
- [3.264] HEIBA, S., et al., Dual-isotope SPECT-CT impact on hospitalized patients with suspected diabetic foot infection: Saving limbs, lives, and resources, *Nucl. Med. Commun.* **34** (2013) 877–884.

- [3.265] VOUILLARMET, J., MORELEC, I., THIVOLET, C., Assessing diabetic foot osteomyelitis remission with white blood cell SPECT–CT imaging, *Diabetes Med.* **31** (2014) 1093–1099.
- [3.266] LA FONTAINE, J., et al., Comparison between Tc-99m WBC SPECT–CT and MRI for the diagnosis of biopsy-proven diabetic foot osteomyelitis, *Wounds* **28** (2016) 271–278.
- [3.267] ERDMAN, W.A., et al., Indexing severity of diabetic foot infection with ^{99m}Tc-WBC SPECT–CT hybrid imaging, *Diabetes Care* **35** (2012) 1826–1831.
- [3.268] LAZAGA, F., et al., Hybrid imaging with ^{99m}Tc-WBC SPECT–CT to monitor the effect of therapy in diabetic foot osteomyelitis, *Int. Wound J.* **13** (2016) 1158–1160.
- [3.269] VOUILLARMET, J., MORET, M., MORELEC, I., MICHON, P., DUBREUIL, J., Application of white blood cell SPECT–CT to predict remission after a 6 or 12 week course of antibiotic treatment for diabetic foot osteomyelitis, *Diabetologia* **60** (2017) 2486–2494.
- [3.270] KIM, H.O., et al., Usefulness of adding SPECT–CT to ^{99m}Tc-hexamethylpropylene amine oxime (HMPAO)-labeled leukocyte imaging for diagnosing prosthetic joint infections, *J. Comput. Assist. Tomogr.* **34** (2014) 313–319.
- [3.271] SENGOZ, T., YAYLALI, O., YUKSEL, D., DEMIRKAN, F., ULUYOL, O., The clinical contribution of SPECT–CT with ^{99m}Tc-HMPAO-labeled leukocyte scintigraphy in hip and knee prosthetic infections, *Rev. Esp. Med. Nucl. Imagen Mol.* **38** (2019) 212–217.
- [3.272] BOLOURI, C., et al., Performance of orthopantomography, planar scintigraphy, CT alone and SPECT–CT in patients with suspected osteomyelitis of the jaw, *Eur. J. Nucl. Med. Mol. Imaging* **40** (2013) 411–414.
- [3.273] CHAKRABORTY, D., et al., Skull base osteomyelitis in otitis externa: The utility of triphasic and single photon emission computed tomography/computed tomography bone scintigraphy, *Indian J. Nucl. Med.* **28** (2013) 65–69.
- [3.274] SHARMA, P., et al., Utility of ^{99m}Tc-MDP hybrid SPECT–CT for diagnosis of skull base osteomyelitis: Comparison with planar bone scintigraphy, SPECT, and CT, *Jpn. J. Radiol.* **31** (2013) 81–88.
- [3.275] HEIBA, S.I., STEMLER, L., SULLIVAN, T., KOLKER, D., KOSTAKOGLU, L., The ideal dual-isotope imaging combination in evaluating patients with suspected infection of pelvic pressure ulcers, *Nucl. Med. Commun.* **38** (2017) 129–134.
- [3.276] KHAJA, M.S., et al., Prosthetic vascular graft infection imaging, *Clin. Imaging* **37** (2013) 239–244.
- [3.277] LOU, L., et al., ^{99m}Tc-WBC scintigraphy with SPECT–CT in the evaluation of arterial graft infection, *Nucl. Med. Commun.* **31** (2010) 411–416.
- [3.278] ERBA, P.A., et al., Radiolabelled leucocyte scintigraphy versus conventional radiological imaging for the management of late, low-grade vascular prosthesis infections, *Eur. J. Nucl. Med. Mol. Imaging* **41** (2014) 357–368.

- [3.279] MEDRICKA, M., JANECKOVA, J., KORANDA, P., BURIANKOVA, E., BACHLEDA, P., ^{18}F -FDG PET-CT and $^{99\text{m}}\text{Tc}$ -HMPAO-WBC SPECT-CT effectively contribute to early diagnosis of infection of arteriovenous graft for hemodialysis, *Biomed. Pap. Med. Fac. Univ. Palacky Olomouc Czech Repub.* **163** (2019) 341–348.
- [3.280] ERBA, P.A., et al., Added value of $^{99\text{m}}\text{Tc}$ -HMPAO-labeled leukocyte SPECT-CT in the characterization and management of patients with infectious endocarditis, *J. Nucl. Med.* **53** (2012) 1235–1243.
- [3.281] LAURIDSEN, T.K., et al., Clinical utility of ^{18}F -FDG positron emission tomography/computed tomography scan vs. $^{99\text{m}}\text{Tc}$ -HMPAO white blood cell single-photon emission computed tomography in extra-cardiac work-up of infective endocarditis, *Int. J. Cardiovasc. Imaging* **33** (2017) 751–760.
- [3.282] ERBA, P.A., et al., Radiolabeled WBC scintigraphy in the diagnostic workup of patients with suspected device-related infections, *JACC Cardiovasc. Imaging* **6** (2013) 1075–1086.
- [3.283] LITZLER, P.Y., et al., Leukocyte SPECT-CT for detecting infection of left-ventricular-assist devices: Preliminary results, *J. Nucl. Med.* **51** (2010) 1044–1048.
- [3.284] CALAIS, J., et al., Diagnostic impact of ^{18}F -fluorodeoxyglucose positron emission tomography/computed tomography and white blood cell SPECT/computed tomography in patients with suspected cardiac implantable electronic device chronic infection, *Circ. Cardiovasc. Imaging* **12** (2019) e007188.
- [3.285] KIMURA, Y., et al., Role of gallium-SPECT-CT in the management of patients with ventricular assist device-specific percutaneous driveline infection, *J. Card. Fail.* **25** (2019) 795–802.
- [3.286] DE VAUGELADE, C., et al., Infections in patients using ventricular-assist devices: Comparison of the diagnostic performance of ^{18}F -FDG PET-CT scan and leucocyte-labeled scintigraphy, *J. Nucl. Cardiol.* **26** (2019) 42–55.
- [3.287] BOUTER, C., MELLER, B., SAHLMANN, C.O., MELLER, J., $^{99\text{m}}\text{Tc}$ -Besilesomab-SPECT-CT in infectious endocarditis: Upgrade of a forgotten method? *Front. Med.* **6** (2019) 40.
- [3.288] HUNG, B.-T., et al., The efficacy of ^{18}F -FDG PET-CT and ^{67}Ga SPECT-CT in diagnosing fever of unknown origin, *Int. J. Infect. Dis.* **62** (2017) 10–17.
- [3.289] NOWOSINSKA, E., NAVALKISSOOR, S., QUIGLEY, A.M., BUSCOMBE, J.R., Is there a role for Gallium-67 citrate SPECT-CT, in patients with renal impairment or who are renal transplant recipients, in identifying and localizing suspected infection? *World J. Nucl. Med.* **14** (2015) 184–188.
- [3.290] HAUGEN, B.R., et al., 2015 American Thyroid Association management guidelines for adult patients with thyroid nodules and differentiated thyroid cancer, *Thyroid* **26** (2016) 1–133.
- [3.291] VERBURG, F.A., et al., Why the European Association of Nuclear Medicine has declined to endorse the 2015 American Thyroid Association management guidelines for adult patients with thyroid nodules and differentiated thyroid cancer, *Eur. J. Nucl. Med. Mol. Imaging* **43** (2016) 1001–1005.

- [3.292] FRANGOS, S., et al., Acknowledging gray areas: 2015 vs. 2009 American Thyroid Association differentiated thyroid cancer guidelines on ablating putatively low-intermediate-risk patients, *Eur. J. Nucl. Med. Mol. Imaging* **44** (2017) 185–189.
- [3.293] VAN NOSTRAND, D., Selected controversies of radioiodine imaging and therapy in differentiated thyroid cancer, *Endocrinol. Metab. Clin. N. Am.* **46** (2017) 783–793.
- [3.294] YLLI, D., VAN NOSTRAND, D., WARTOFSKY, L., Conventional radioiodine therapy for differentiated thyroid cancer, *Endocrinol. Metab. Clin. N. Am.* **48** (2019) 181–197.
- [3.295] CHOUDHURY, P.S., GUPTA, M., Differentiated thyroid cancer theranostics: Radioiodine and beyond, *Br. J. Radiol.* **91** (2018) 20180136.
- [3.296] LEE, S.W., SPECT–CT in the treatment of differentiated thyroid cancer, *Nucl. Med. Mol. Imaging* **51** (2017) 297–303.
- [3.297] ISRAEL, O., et al., Two decades of SPECT–CT — the coming of age of a technology: An updated review of literature evidence, *Eur. J. Nucl. Med. Mol. Imaging* **46** (2019) 1990–2012.
- [3.298] SHAPIRO, B., et al., Artifacts, anatomical and physiological variants, and unrelated diseases that might cause false-positive whole-body ¹³¹I scans in patients with thyroid cancer, *Semin. Nucl. Med.* **30** (2000) 115–132.
- [3.299] AHMED, N., et al., Hybrid SPECT–CT imaging in the management of differentiated thyroid carcinoma, *Asian Pac. J. Cancer Prev.* **19** (2018) 303–308.
- [3.300] WONG, K.K., SISSON, J.C., KORAL, K.F., FREY, K.A., AVRAM, A.M., Staging of differentiated thyroid carcinoma using diagnostic ¹³¹I SPECT–CT, *Am. J. Roentgenol.* **195** (2010) 730–736.
- [3.301] AVRAM, A.M., FIG, L.M., FREY, K.A., GROSS, M.D., WONG, K.K., Preablation ¹³¹I scans with SPECT–CT in postoperative thyroid cancer patients: What is the impact on staging? *J. Clin. Endocrinol. Metab.* **98** (2013) 1163–1171.
- [3.302] AGRAWAL, K., BHATTACHARYA, A., MITTAL, B.R., Role of single photon emission computed tomography/computed tomography in diagnostic iodine-131 scintigraphy before initial radioiodine ablation in differentiated thyroid cancer, *Indian J. Nucl. Med.* **30** (2015) 221–226.
- [3.303] AVRAM, A.M., ESFANDIARI, N.H., WONG, K.K., Preablation ¹³¹I scans with SPECT–CT contribute to thyroid cancer risk stratification and ¹³¹I therapy planning, *J. Clin. Endocrinol. Metab.* **100** (2015) 1895–1902.
- [3.304] MILLER, J.E., et al., Location and causation of residual lymph node metastasis after surgical treatment of regionally advanced differentiated thyroid cancer, *Thyroid* **28** (2018) 593–600.
- [3.305] PALANISWAMY, S.S., SUBRAMANYAM, P., Unusual sites of metastatic and benign I ¹³¹ uptake in patients with differentiated thyroid carcinoma, *Indian J. Endocrinol. Metab.* **22** (2018) 740–750.
- [3.306] LOU, K., GU, Y., HU, Y., WANG, S., SHI, H., Technetium-99m-pertechnetate whole-body SPET–CT scan in thyroidectomized differentiated thyroid cancer patients is a useful imaging modality in detecting remnant thyroid tissue, nodal and distant metastases before ¹³¹I therapy. A study of 416 patients, *Hell. J. Nucl. Med.* **21** (2018) 121–124.

- [3.307] MÍNGUEZ, P., et al., Whole-remnant and maximum-voxel SPECT–CT dosimetry in ¹³¹I-NaI treatments of differentiated thyroid cancer, *Med. Phys.* **43** (2016) 5279–5287.
- [3.308] HONG, C.M., et al., I-131 biokinetics of remnant normal thyroid tissue and residual thyroid cancer in patients with differentiated thyroid cancer: Comparison between recombinant human TSH administration and thyroid hormone withdrawal, *Ann. Nucl. Med.* **31** (2017) 582–589.
- [3.309] MÍNGUEZ, P., et al., Analysis of activity uptake, effective half-life and time-integrated activity for low- and high-risk papillary thyroid cancer patients treated with 1.11 GBq and 3.7 GBq of ¹³¹I-NaI respectively, *Phys. Med.* **65** (2019) 143–149.
- [3.310] BARBER, T.W., et al., The prevalence of thyroglossal tract thyroid tissue on SPECT–CT following ¹³¹I ablation therapy after total thyroidectomy for thyroid cancer, *Clin. Endocrinol.* **81** (2014) 266–270.
- [3.311] LEE, M., et al., Frequent visualization of thyroglossal duct remnant on post-ablation ¹³¹I-SPECT–CT and its clinical implications, *Clin. Radiol.* **70** (2015) 638–643.
- [3.312] KAIREMO, K., KANGASMÄKI, A., BOM, H.-S., Comparison of I-131 biokinetics after recombinant human TSH stimulation and thyroid hormone withdrawal measured by external detector in patients with differentiated thyroid cancer, *Chonnam Med. J.* **55** (2019) 20–24.
- [3.313] RUF, J., et al., Impact of SPECT and integrated low-dose CT after radioiodine therapy on the management of patients with thyroid carcinoma, *Nucl. Med. Commun.* **25** (2004) 1177–1182.
- [3.314] SCHMIDT, D., SZIKSZAI, A., LINKE, R., BAUTZ, W., KUWERT, T., Impact of ¹³¹I SPECT/spiral CT on nodal staging of differentiated thyroid carcinoma at the first radioablation, *J. Nucl. Med.* **50** (2009) 18–23.
- [3.315] AIDE, N., et al., Clinical relevance of single-photon emission computed tomography/computed tomography of the neck and thorax in postablation ¹³¹I scintigraphy for thyroid cancer, *J. Clin. Endocrinol. Metab.* **94** (2009) 2075–2084.
- [3.316] SCHMIDT, D., LINKE, R., UDER, M., KUWERT, T., Five months’ follow-up of patients with and without iodine-positive lymph node metastases of thyroid carcinoma as disclosed by ¹³¹I-SPECT–CT at the first radioablation, *Eur. J. Nucl. Med. Mol. Imaging* **37** (2010) 699–705.
- [3.317] MUSTAFA, M., et al., Regional lymph node involvement in T1 papillary thyroid carcinoma: A bicentric prospective SPECT–CT study, *Eur. J. Nucl. Med. Mol. Imaging* **37** (2010) 1462–1466.
- [3.318] WAKABAYASHI, H., et al., Double-phase ¹³¹I whole body scan and ¹³¹I SPECT-CT images in patients with differentiated thyroid cancer: Their effectiveness for accurate identification, *Ann. Nucl. Med.* **25** (2011) 609–615.
- [3.319] CIAPPUCCINI, R., et al., Postablation ¹³¹I scintigraphy with neck and thorax SPECT-CT and stimulated serum thyroglobulin level predict the outcome of patients with differentiated thyroid cancer, *Eur. J. Endocrinol.* **164** (2011) 961–969.
- [3.320] MARUOKA, Y., et al., Incremental diagnostic value of SPECT–CT with ¹³¹I scintigraphy after radioiodine therapy in patients with well-differentiated thyroid carcinoma, *Radiology* **265** (2012) 902–909.

- [3.321] JEONG, S.Y., et al., Clinical applications of SPECT–CT after first I-131 ablation in patients with differentiated thyroid cancer, *Clin. Endocrinol.* **81** (2014) 445–451.
- [3.322] ZEUREN, R., et al., RAI thyroid bed uptake after total thyroidectomy: A novel SPECT-CT anatomic classification system, *Laryngoscope* **125** (2015) 2417–2424.
- [3.323] SRIPRAPAPORN, J., et al., Utility of adding SPECT–CT imaging to post-therapeutic radioiodine whole-body scan in patients with differentiated thyroid cancer, *J. Med. Assoc. Thai.* **98** (2015) 596–605.
- [3.324] GONZALEZ CARVALHO, J.M., et al., Evaluation of ¹³¹I scintigraphy and stimulated thyroglobulin levels in the follow up of patients with DTC: A retrospective analysis of 1420 patients, *Eur. J. Nucl. Med. Mol. Imaging* **44** (2017) 744–756.
- [3.325] SZUJO, S., et al., The impact of post-radioiodine therapy SPECT–CT on early risk stratification in differentiated thyroid cancer; a bi-institutional study, *Oncotarget* **8** (2017) 79825–79834.
- [3.326] ZILIOLI, V., et al., Differentiated thyroid carcinoma: Incremental diagnostic value of ¹³¹I SPECT–CT over planar whole body scan after radioiodine therapy, *Endocrine* **56** (2017) 551–559.
- [3.327] CAMPENNI, A., et al., Undetectable or low (<1 ng/ml) postsurgical thyroglobulin values do not rule out metastases in early stage differentiated thyroid cancer patients, *Oncotarget* **9** (2018) 17491–17500.
- [3.328] LEE, C.-H., et al., Risk factors for radioactive iodine-avid metastatic lymph nodes on post I-131 ablation SPECT–CT in low- or intermediate-risk groups of papillary thyroid cancer, *PLoS One* **13** (2018) e0202644.
- [3.329] MALAMITSI, J.V., et al., I-131 postablation SPECT–CT predicts relapse of papillary thyroid carcinoma more accurately than whole body scan, *In Vivo* **33** (2019) 2255–2263.
- [3.330] BARWICK, T., et al., Single photon emission computed tomography (SPECT)/computed tomography using iodine-123 in patients with differentiated thyroid cancer: Additional value over whole body planar imaging and SPECT, *Eur. J. Endocrinol.* **162** (2010) 1131–1139.
- [3.331] CHEN, L., et al., Incremental value of ¹³¹I SPECT–CT in the management of patients with differentiated thyroid carcinoma, *J. Nucl. Med.* **49** (2008) 1952–1957.
- [3.332] SHEN, C.-T., WEI, W.-J., QIU, Z.-L., SONG, H.-J., LUO, Q.-Y., Value of post-therapeutic ¹³¹I scintigraphy in stimulated serum thyroglobulin-negative patients with metastatic differentiated thyroid carcinoma, *Endocrine* **51** (2016) 283–290.
- [3.333] RUHLMANN, M., et al., High level of agreement between pretherapeutic ¹²⁴I PET and intratherapeutic ¹³¹I imaging in detecting iodine-positive thyroid cancer metastases, *J. Nucl. Med.* **57** (2016) 1339–1342.
- [3.334] OH, J.-R., et al., Comparison of ¹³¹I whole-body imaging, ¹³¹I SPECT–CT, and ¹⁸F-FDG PET–CT in the detection of metastatic thyroid cancer, *Eur. J. Nucl. Med. Mol. Imaging* **38** (2011) 1459–1468.
- [3.335] THARP, K., et al., Impact of ¹³¹I-SPECT–CT images obtained with an integrated system in the follow-up of patients with thyroid carcinoma, *Eur. J. Nucl. Med. Mol. Imaging* **31** (2004) 1435–1442.

- [3.336] WONG, K.K., ZARZHEVSKY, N., CAHILL, J.M., FREY, K.A., AVRAM, A.M., Incremental value of diagnostic ^{131}I SPECT–CT fusion imaging in the evaluation of differentiated thyroid carcinoma, *Am. J. Roentgenol.* **191** (2008) 1785–1794.
- [3.337] WANG, H., et al., The role of single-photon emission computed tomography/computed tomography for precise localization of metastases in patients with differentiated thyroid cancer, *Clin. Imaging* **33** (2009) 49–54.
- [3.338] SPANU, A., et al., ^{131}I SPECT–CT in the follow-up of differentiated thyroid carcinoma: Incremental value versus planar imaging, *J. Nucl. Med.* **50** (2009) 184–190.
- [3.339] KOHLFUERST, S., et al., Posttherapeutic ^{131}I SPECT-CT offers high diagnostic accuracy when the findings on conventional planar imaging are inconclusive and allows a tailored patient treatment regimen, *Eur. J. Nucl. Med. Mol. Imaging* **36** (2009) 886–893.
- [3.340] GREWAL, R.K., et al., The effect of posttherapy ^{131}I SPECT–CT on risk classification and management of patients with differentiated thyroid cancer, *J. Nucl. Med.* **51** (2010) 1361–1367.
- [3.341] HASSAN, F.U., MOHAN, H.K., Clinical utility of SPECT–CT imaging post radioiodine therapy: Does it enhance patient management in thyroid cancer? *Eur. Thyroid J.* **4** (2015) 239–245.
- [3.342] CZEPCZYŃSKI, R., GRZYCYŃSKA, M., RUCHAŁA, M., $^{99\text{m}}\text{Tc}$ -EDDA/HYNIC-TOC in the diagnosis of differentiated thyroid carcinoma refractory to radioiodine treatment, *Nucl. Med. Rev. Cent. East. Eur.* **19** (2016) 67–73.
- [3.343] GAO, R., et al., Clinical value of $^{99\text{m}}\text{Tc}$ -3PRGD2 SPECT–CT in differentiated thyroid carcinoma with negative ^{131}I whole-body scan and elevated thyroglobulin level, *Sci. Rep.* **8** (2018) 473.
- [3.344] SPANU, A., et al., Role of diagnostic ^{131}I SPECT–CT in long-term follow-up of patients with papillary thyroid microcarcinoma, *J. Nucl. Med.* **59** (2018) 1510–1515.
- [3.345] GOLDSMITH, S.J., Update on nuclear medicine imaging of neuroendocrine tumors, *Future Oncol.* **5** (2009) 75–84.
- [3.346] CARRASQUILLO, J.A., CHEN, C.C., Molecular imaging of neuroendocrine tumors, *Semin. Oncol.* **37** (2010) 662–679.
- [3.347] BOMBARDIERI, E., et al., Imaging of neuroendocrine tumours with gamma-emitting radiopharmaceuticals, *Q. J. Nucl. Med. Mol. Imaging* **54** (2010) 3–15.
- [3.348] BOMBARDIERI, E., et al., $^{131}\text{I}/^{123}\text{I}$ -metaiodobenzylguanidine (mIBG) scintigraphy: Procedure guidelines for tumour imaging, *Eur. J. Nucl. Med. Mol. Imaging* **37** (2010) 2436–2446.
- [3.349] JACOBSON, A.F., DENG, H., LOMBARD, J., LESSIG, H.J., BLACK, R.R., ^{123}I -meta-iodobenzylguanidine scintigraphy for the detection of neuroblastoma and pheochromocytoma: Results of a meta-analysis, *J. Clin. Endocrinol. Metab.* **95** (2010) 2596–2606.
- [3.350] MOREAU, A., et al., Quantitative analysis of normal and pathologic adrenal glands with ^{18}F -FDOPA PET–CT: Focus on pheochromocytomas, *Nucl. Med. Commun.* **38** (2017) 771–779.

- [3.351] GIAMMARILE, F., et al., ^{18}F -FLT and ^{18}F -FDG positron emission tomography for the imaging of advanced well-differentiated gastro-entero-pancreatic endocrine tumours, *Nucl. Med. Commun.* **32** (2011) 91–97.
- [3.352] BAR-SEVER, Z., et al., Guidelines on nuclear medicine imaging in neuroblastoma, *Eur. J. Nucl. Med. Mol. Imaging* **45** (2018) 2009–2024.
- [3.353] CHRISOULIDOU, A., KALTSAS, G., ILIAS, I., GROSSMAN, A.B., The diagnosis and management of malignant pheochromocytoma and paraganglioma, *Endocr. Relat. Cancer* **14** (2007) 569–585.
- [3.354] HAVEKES, B., et al., Detection and treatment of pheochromocytomas and paragangliomas: Current standing of MIBG scintigraphy and future role of PET imaging, *Q. J. Nucl. Med. Mol. Imaging* **52** (2008) 419–429.
- [3.355] KRAUSZ, Y., et al., SPECT–CT hybrid imaging with ^{111}In -pentetretotide in assessment of neuroendocrine tumours, *Clin. Endocrinol.* **59** (2003) 565–573.
- [3.356] HILLEL, P.G., et al., The clinical impact of a combined gamma camera/CT imaging system on somatostatin receptor imaging of neuroendocrine tumours, *Clin. Radiol.* **61** (2006) 579–587.
- [3.357] CASTALDI, P., et al., Impact of ^{111}In -DTPA-octreotide SPECT–CT fusion images in the management of neuroendocrine tumours, *Radiol. Med.* **113** (2008) 1056–1067.
- [3.358] APOSTOLOVA, I., et al., SPECT–CT stabilizes the interpretation of somatostatin receptor scintigraphy findings: A retrospective analysis of inter-rater agreement, *Ann. Nucl. Med.* **24** (2010) 477–483.
- [3.359] WONG, K.K., CAHILL, J.M., FREY, K.A., AVRAM, A.M. Incremental value of ^{111}In -pentetretotide SPECT–CT fusion imaging of neuroendocrine tumors, *Acad. Radiol.* **17** (2010) 291–297.
- [3.360] BURAL, G.G., MUTHUKRISHNAN, A., OBORSKI, M.J., MOUNTZ, J.M., Improved benefit of SPECT–CT compared to SPECT alone for the accurate localization of endocrine and neuroendocrine tumors, *Mol. Imaging Radionucl. Ther.* **21** (2012) 91–96.
- [3.361] SAINZ-ESTEBAN, A., et al., Contribution of ^{111}In -pentetretotide SPECT–CT imaging to conventional somatostatin receptor scintigraphy in the detection of neuroendocrine tumours, *Nucl. Med. Commun.* **36** (2015) 251–259.
- [3.362] RUF, J., et al., Significance of a single-time-point somatostatin receptor SPECT/multiphase CT protocol in the diagnostic work-up of gastroenteropancreatic neuroendocrine neoplasms, *J. Nucl. Med.* **57** (2016) 180–185.
- [3.363] AIT BOUDAUD, A., et al., Uptake in the pancreatic uncinate process on the ^{111}In -octreotide scintigraphy: How to distinguish physiological from pathological uptake? *Nucl. Med. Commun.* **38** (2017) 737–743.
- [3.364] TROGRILIC, M., TEŽAK, S., Incremental value of $^{99\text{m}}\text{Tc}$ -HYNIC-TOC SPECT–CT over whole-body planar scintigraphy and SPECT in patients with neuroendocrine tumours, *Nuklearmedizin* **56** (2017) 97–107.
- [3.365] AL-CHALABI, H., COOK, A., ELLIS, C., PATEL, C.N., SCARSBROOK, A.F., Feasibility of a streamlined imaging protocol in technetium- $^{99\text{m}}\text{Tc}$ -Tektrotyd somatostatin receptor SPECT–CT, *Clin. Radiol.* **73** (2018) 527–534.

- [3.366] KOLASIŃSKA-ĆWIKŁA, A.D., et al., The value of somatostatin receptor scintigraphy (SRS) in patients with NETG1/G2 pancreatic neuroendocrine neoplasms (p-NENs), *Nucl. Med. Rev. Cent. East. Eur.* **22** (2019) 1–7.
- [3.367] FUKUOKA, M., TAKI, J., MOCHIZUKI, T., KINUYA, S., Comparison of diagnostic value of I-123 MIBG and high-dose I-131 MIBG scintigraphy including incremental value of SPECT–CT over planar image in patients with malignant pheochromocytoma/paraganglioma and neuroblastoma, *Clin. Nucl. Med.* **36** (2011) 1–7.
- [3.368] PERRI, M., et al., Octreo-SPECT–CT imaging for accurate detection and localization of suspected neuroendocrine tumors, *Q. J. Nucl. Med. Mol. Imaging* **52** (2008) 323–333.
- [3.369] NAKAMOTO, R., NAKAMOTO, Y., ISHIMORI, T., TOGASHI, K., Clinical significance of quantitative ¹²³I-MIBG SPECT–CT analysis of pheochromocytoma and paraganglioma, *Clin. Nucl. Med.* **41** (2016) e465–e472.
- [3.370] CHIARAVALLLOTI, A., et al., ¹¹¹In-Pentetreotide SPECT–CT in pulmonary carcinoid, *Anticancer Res.* **35** (2015) 4265–4270.
- [3.371] SPANU, A., et al., Non-functioning gastroenteropancreatic (GEP) tumors: A ¹¹¹In-Pentetreotide SPECT–CT diagnostic study, *Am. J. Nucl. Med. Mol. Imaging* **7** (2017) 181–194.
- [3.372] CHEN, H., LI, Y., GAO, X., SHEN, X., Clinical value of ^{99m}Tc-HYNIC-TOC SPECT–CT for the diagnosis primary small cell neuroendocrine carcinomas of the nasal cavity and paranasal sinuses, *Clin. Imaging* **52** (2018) 365–369.
- [3.373] XU, J., et al., Clinical application of ^{99m}Tc-HYNIC-TOC SPECT–CT in diagnosing and monitoring of pancreatic neuroendocrine neoplasms, *Ann. Nucl. Med.* **32** (2018) 446–452.
- [3.374] DERAKHSHAN, J.J., FARWELL, M.D., Prevalence and quantitative analysis of indium-111 pentetreotide (Octreoscan) uptake in the pancreatic head on SPECT–CT imaging: Establishing a region of interest-based pathological uptake threshold, *Nucl. Med. Commun.* **40** (2019) 727–733.
- [3.375] DERLIN, T., et al., Intraindividual comparison of ¹²³I-mIBG SPECT/MRI, ¹²³I-mIBG SPECT–CT, and MRI for the detection of adrenal pheochromocytoma in patients with elevated urine or plasma catecholamines, *Clin. Nucl. Med.* **38** (2013) e1–e6.
- [3.376] MEYER-ROCHOW, G.Y., et al., The utility of metaiodobenzylguanidine single photon emission computed tomography/computed tomography (MIBG SPECT–CT) for the diagnosis of pheochromocytoma, *Ann. Surg. Oncol.* **17** (2010) 392–400.
- [3.377] ROZOVSKY, K., et al., Added value of SPECT–CT for correlation of MIBG scintigraphy and diagnostic CT in neuroblastoma and pheochromocytoma, *Am. J. Roentgenol.* **190** (2008) 1085–1090.
- [3.378] SENICA, K., et al., Superior diagnostic performance of the GLP-1 receptor agonist [Lys ⁴⁰(AhxHYNIC-[^{99m}Tc]/EDDA)NH₂]-Exendin-4 over conventional imaging modalities for localization of insulinoma, *Mol. Imaging Biol.* **22** (2020) 165–172.
- [3.379] ETCHEBEHERE, E.C., et al., ⁶⁸Ga-DOTATATE PET–CT, ^{99m}Tc-HYNIC-octreotide SPECT–CT, and whole-body MR imaging in detection of neuroendocrine tumors: A prospective trial, *J. Nucl. Med.* **55** (2014) 1598–1604.

- [3.380] SCHREITER, N.F., et al., Searching for primaries in patients with neuroendocrine tumors (NET) of unknown primary and clinically suspected NET: Evaluation of Ga-68 DOTATOC PET-CT and In-111 DTPA octreotide SPECT-CT, *Radiol. Oncol.* **48** (2014) 339–347.
- [3.381] LEE, I., et al., Comparison of diagnostic sensitivity and quantitative indices between ⁶⁸Ga-DOTATOC PET-CT and ¹¹¹In-Pentetreotide SPECT-CT in neuroendocrine tumors: A preliminary report, *Nucl. Med. Mol. Imaging* **49** (2015) 284–290.
- [3.382] KUNIKOWSKA, J., LEWINGTON, V., KROLICKI, L., Optimizing somatostatin receptor imaging in patients with neuroendocrine tumors: The impact of ^{99m}Tc-HYNICTOC SPECT/SPECT-CT versus ⁶⁸Ga-DOTATATE PET-CT upon clinical management, *Clin. Nucl. Med.* **42** (2017) 905–911.
- [3.383] YAMAGA, L.Y.I., et al., ⁶⁸Ga-DOTATATE PET-CT in recurrent medullary thyroid carcinoma: A lesion-by-lesion comparison with ¹¹¹In-octreotide SPECT-CT and conventional imaging, *Eur. J. Nucl. Med. Mol. Imaging* **44** (2017) 1695–1701.
- [3.384] FALLAHI, B., et al., Diagnostic efficiency of ⁶⁸Ga-DOTATATE PET-CT as compared to ^{99m}Tc-octreotide SPECT-CT and conventional morphologic modalities in neuroendocrine tumors, *Asia Ocean. J. Nucl. Med. Biol.* **7** (2019) 129–140.
- [3.385] HOPE, T.A., CALAIS, J., ZHANG, L., DIECKMANN, W., MILLO, C., ¹¹¹In-pentetreotide scintigraphy versus ⁶⁸Ga-DOTATATE PET: Impact on Krenning scores and effect of tumor burden, *J. Nucl. Med.* **60** (2019) 1266–1269.
- [3.386] KROISS, A., et al., ⁶⁸Ga-DOTATOC PET-CT provides accurate tumour extent in patients with extraadrenal paraganglioma compared to ¹²³I-MIBG SPECT-CT, *Eur. J. Nucl. Med. Mol. Imaging* **42** (2015) 33–41.
- [3.387] CHANG, C.A., et al., ⁶⁸Ga-DOTATATE and ¹⁸F-FDG PET-CT in paraganglioma and pheochromocytoma: Utility, patterns and heterogeneity, *Cancer Imaging* **16** (2016) 22.
- [3.388] KROISS, A.S., et al., Compared to ¹²³I-MIBG SPECT-CT, ¹⁸F-DOPA PET-CT provides accurate tumor extent in patients with extra-adrenal paraganglioma, *Ann. Nucl. Med.* **31** (2017) 357–365.
- [3.389] KROISS, A.S., et al., ⁶⁸Ga-DOTATOC PET-CT in the localization of head and neck paraganglioma compared with ¹⁸F-DOPA PET-CT and ¹²³I-MIBG SPECT-CT, *Nucl. Med. Biol.* **71** (2019) 47–53.
- [3.390] GALLOWITSCH, H.-J., et al., Sentinel node SPECT-CT in breast cancer. Can we expect any additional and clinically relevant information? *Nuklearmedizin* **46** (2007) 252–256.
- [3.391] LERMAN, H., et al., Improved sentinel node identification by SPECT-CT in overweight patients with breast cancer, *J. Nucl. Med.* **48** (2007) 201–206.
- [3.392] CHEVILLE, A.L., et al., A pilot study to assess the utility of SPECT-CT-based lymph node imaging to localize lymph nodes that drain the arm in patients undergoing treatment for breast cancer, *Breast Cancer Res. Treat.* **116** (2009) 531–538.
- [3.393] VAN DER PLOEG, I.M., VALDÉS OLMOS, R.A., KROON, B.B., RUTGERS, E.J., NIEWEG, O.E., The hidden sentinel node and SPECT-CT in breast cancer patients, *Eur. J. Nucl. Med. Mol. Imaging* **36** (2009) 6–11.

- [3.394] COFFEY, J.P., HILL, J.C., Breast sentinel node imaging with low-dose SPECT–CT, *Nucl. Med. Commun.* **31** (2010) 107–111.
- [3.395] BROUWER, O.R., et al., Lymphoscintigraphy and SPECT–CT in multicentric and multifocal breast cancer: Does each tumour have a separate drainage pattern? Results of a Dutch multicentre study (MULTISENT), *Eur. J. Nucl. Med. Mol. Imaging* **39** (2012) 1137–1143.
- [3.396] UREN, R.F., et al., SPECT–CT scans allow precise anatomical location of sentinel lymph nodes in breast cancer and redefine lymphatic drainage from the breast to the axilla, *Breast* **21** (2012) 480–486.
- [3.397] YONEYAMA, H., et al., Improved detection of sentinel lymph nodes in SPECT–CT images acquired using a low- to medium-energy general-purpose collimator, *Clin. Nucl. Med.* **39** (2014) e1–e6.
- [3.398] KRAFT, O., HAVEL, M., Sentinel lymph nodes and planar scintigraphy and SPECT–CT in various types of tumours: Estimation of some factors influencing detection success, *Nucl. Med. Rev. Cent. East. Eur.* **16** (2013) 17–25.
- [3.399] SHIMA, H., et al., Risk of node metastasis of sentinel lymph nodes detected in level II/III of the axilla by single-photon emission computed tomography/computed tomography, *Exp. Ther. Med.* **8** (2014) 1447–1452.
- [3.400] JIMENEZ-HEFFERNAN, A., et al., Results of a prospective multicenter International Atomic Energy Agency sentinel node trial on the value of SPECT–CT over planar imaging in various malignancies, *J. Nucl. Med.* **56** (2015) 1338–1344.
- [3.401] POUW, B., et al., The hidden sentinel node in breast cancer: Reevaluating the role of SPECT–CT and tracer reinjection, *Eur. J. Surg. Oncol.* **42** (2016) 497–503.
- [3.402] TOMIGUCHI, M., et al., Prediction of sentinel lymph node status using single-photon emission computed tomography (SPECT)/computed tomography (CT) imaging of breast cancer, *Surg. Today* **46** (2016) 214–223.
- [3.403] ZETTERLUND, L., et al., Impact of previous surgery on sentinel lymph node mapping: Hybrid SPECT–CT before and after a unilateral diagnostic breast excision, *Breast* **30** (2016) 32–38.
- [3.404] BORRELLI, P., et al., Contribution of SPECT–CT for sentinel node localization in patients with ipsilateral breast cancer relapse, *Eur. J. Nucl. Med. Mol. Imaging* **44** (2017) 630–637.
- [3.405] GIŻEWSKA, A., et al., Utility of single-photon emission tomography/computed tomography for sentinel lymph node localization in breast cancer patients, *Nucl. Med. Commun.* **38** (2017) 493–439.
- [3.406] EVEN-SAPIR, E., et al., Lymphoscintigraphy for sentinel node mapping using a hybrid SPECT–CT system, *J. Nucl. Med.* **44** (2003) 1413–1420.
- [3.407] ISHIHARA, T., et al., Management of sentinel lymph nodes in malignant skin tumors using dynamic lymphoscintigraphy and the single-photon-emission computed tomography/computed tomography combined system, *Int. J. Clin. Oncol.* **11** (2006) 214–220.
- [3.408] VAN DER PLOEG, I.M., KROON, B.B., VALDÉS OLMOS, R.A., NIEWEG, O.E., Evaluation of lymphatic drainage patterns to the groin and implications for the extent of groin dissection in melanoma patients, *Ann. Surg. Oncol.* **16** (2009) 2994–2999.

- [3.409] VAN DER PLOEG, I.M., et al., The yield of SPECT–CT for anatomical lymphatic mapping in patients with melanoma, *Ann. Surg. Oncol.* **16** (2009) 1537–1542.
- [3.410] NIELSEN, K.R., et al., The diagnostic value of adding dynamic scintigraphy to standard delayed planar imaging for sentinel node identification in melanoma patients, *Eur. J. Nucl. Med. Mol. Imaging* **38** (2011) 1999–2004.
- [3.411] STOFFELS, I., et al., Association between sentinel lymph node excision with or without preoperative SPECT–CT and metastatic node detection and disease-free survival in melanoma, *JAMA* **308** (2012) 1007–1014.
- [3.412] KRAFT, O., HAVEL, M., Localisation of sentinel lymph nodes in patients with melanomas by planar lymphoscintigraphic and hybrid SPECT–CT imaging, *Nucl. Med. Rev. Cent. East. Eur.* **15** (2012) 101–107.
- [3.413] VEENSTRA, H.J., et al., Lymphatic drainage patterns from melanomas on the shoulder or upper trunk to cervical lymph nodes and implications for the extent of neck dissection, *Ann. Surg. Oncol.* **19** (2012) 3906–3912.
- [3.414] VEENSTRA, H.J., VERMEEREN, L., VALDÉS OLMOS, R.A., NIEWEG, O.E., The additional value of lymphatic mapping with routine SPECT–CT in unselected patients with clinically localized melanoma, *Ann. Surg. Oncol.* **19** (2012) 1018–1023.
- [3.415] FAIRBAIRN, N., MUNSON, C., KHAN, Z.A., BUTTERWORTH, M., The role of hybrid SPECT–CT for lymphatic mapping in patients with melanoma, *J. Plast. Reconstr. Aesthet. Surg.* **66** (2013) 1248–1255.
- [3.416] VUTHALURU, S., et al., Sentinel lymph node biopsy in malignant eyelid tumor: Hybrid single photon emission computed tomography/computed tomography and dual dye technique, *Am. J. Ophthalmol.* **156** (2013) 43–49.
- [3.417] STOFFELS, I., et al., Cost-effectiveness of preoperative SPECT–CT combined with lymphoscintigraphy vs. lymphoscintigraphy for sentinel lymph node excision in patients with cutaneous malignant melanoma, *Eur. J. Nucl. Med. Mol. Imaging* **41** (2014) 1723–1731.
- [3.418] ZENDER, C., GUO, T., WENG, C., FAULHABER, P., REZAEI, R., Utility of SPECT–CT for periparotid sentinel lymph node mapping in the surgical management of head and neck melanoma, *Am. J. Otolaryngol.* **35** (2014) 12–18.
- [3.419] DOEPKER, M.P., et al., Comparison of single-photon emission computed tomography–computed tomography (SPECT–CT) and conventional planar lymphoscintigraphy for sentinel node localization in patients with cutaneous malignancies, *Ann. Surg. Oncol.* **24** (2017) 355–361.
- [3.420] MURER, K., HUBER, G.F., HAILE, S.R., STOECKLI, S.J., Comparison of morbidity between sentinel node biopsy and elective neck dissection for treatment of the n0 neck in patients with oral squamous cell carcinoma, *Head Neck* **33** (2011) 1260–1264.
- [3.421] KLODE, J., et al., Advantages of preoperative hybrid SPECT–CT in detection of sentinel lymph nodes in cutaneous head and neck malignancies, *J. Eur. Acad. Dermatol. Venereol.* **25** (2011) 1213–1221.
- [3.422] VERMEEREN, L., et al., SPECT–CT for sentinel lymph node mapping in head and neck melanoma, *Head Neck* **33** (2011) 1–6.

- [3.423] BROGLIE, M.A., HAERLE, S.K., HUBER, G.F., HAILE, S.R., STOECKLI, S.J., Occult metastases detected by sentinel node biopsy in patients with early oral and oropharyngeal squamous cell carcinomas: Impact on survival, *Head Neck* **35** (2013) 660–666.
- [3.424] DEN TOOM, I.J., et al., Additional non-sentinel lymph node metastases in early oral cancer patients with positive sentinel lymph nodes, *Eur. Arch. Otorhinolaryngol.* **274** (2017) 961–968.
- [3.425] TRINH, B.B., et al., SPECT–CT adds distinct lymph node basins and influences radiologic findings and surgical approach for sentinel lymph node biopsy in head and neck melanoma, *Ann. Surg. Oncol.* **25** (2018) 1716–1722.
- [3.426] SMITH, V.A., LENTSCH, E.J., Sentinel node biopsy in head and neck desmoplastic melanoma: An analysis of 244 cases, *Laryngoscope* **122** (2012) 116–120.
- [3.427] HAERLE, S.K., HANY, T.F., STROBEL, K., SIDLER, D., STOECKLI, S.J., Is there an additional value of SPECT–CT over planar lymphoscintigraphy for sentinel node mapping in oral/oropharyngeal squamous cell carcinoma? *Ann. Surg. Oncol.* **16** (2009) 3118–3124.
- [3.428] DEN TOOM, I.J., et al., The added value of SPECT-CT for the identification of sentinel lymph nodes in early stage oral cancer, *Eur. J. Nucl. Med. Mol. Imaging* **44** (2017) 998–1004.
- [3.429] TARTAGLIONE, G., et al., Sentinel node in oral cancer: The nuclear medicine aspects. A survey from the sentinel European node trial, *Clin. Nucl. Med.* **41** (2016) 534–542.
- [3.430] MEERWEIN, C.M., et al., Multi-slice SPECT–CT vs. lymphoscintigraphy and intraoperative gamma ray probe for sentinel node mapping in HNSCC, *Eur. Arch. Otorhinolaryngol.* **274** (2017) 1633–1642.
- [3.431] DÍAZ-FEIJOO, B., et al., Change in clinical management of sentinel lymph node location in early stage cervical cancer: The role of SPECT–CT, *Gynecol. Oncol.* **120** (2011) 353–357.
- [3.432] HOOGEN DAM, J.P., et al., Preoperative sentinel node mapping with ^{99m}Tc-nanocolloid SPECT-CT significantly reduces the intraoperative sentinel node retrieval time in robot assisted laparoscopic cervical cancer surgery, *Gynecol. Oncol.* **129** (2013) 389–394.
- [3.433] KLAPDOR, R., et al., Value and advantages of preoperative sentinel lymph node imaging with SPECT–CT in cervical cancer, *Int. J. Gynecol. Cancer* **24** (2014) 295–302.
- [3.434] COLLARINO, A., DONSWIJK, M.L., VAN DRIEL, W.J., STOKKEL, M.P., VALDÉS OLMOS, R.A., The use of SPECT–CT for anatomical mapping of lymphatic drainage in vulvar cancer: Possible implications for the extent of inguinal lymph node dissection, *Eur. J. Nucl. Med. Mol. Imaging* **42** (2015) 2064–2071.
- [3.435] KLAPDOR, R., LÄNGER, F., GRATZ, K.F., HILLEMANN, P., HERTEL, H., SPECT–CT for SLN dissection in vulvar cancer: Improved SLN detection and dissection by preoperative three-dimensional anatomical localisation, *Gynecol. Oncol.* **138** (2015) 590–596.

- [3.436] SAHBAI, S., et al., Pericervical injection of ^{99m}Tc -nanocolloid is superior to peritumoral injection for sentinel lymph node detection of endometrial cancer in SPECT-CT, *Clin. Nucl. Med.* **41** (2016) 927–932.
- [3.437] SAHBAI, S., et al., Sentinel lymph node mapping using SPECT-CT and gamma probe in endometrial cancer: An analysis of parameters affecting detection rate, *Eur. J. Nucl. Med. Mol. Imaging* **44** (2017) 1511–1519.
- [3.438] NAAMAN, Y., et al., The added value of SPECT-CT in sentinel lymph nodes mapping for endometrial carcinoma, *Ann. Surg. Oncol.* **23** (2016) 450–455.
- [3.439] NAUMANN, C.M., et al., Evaluation of the diagnostic value of preoperative sentinel lymph node (SLN) imaging in penile carcinoma patients without palpable inguinal lymph nodes via single photon emission computed tomography/computed tomography (SPECT-CT) as compared to planar scintigraphy, *Urol. Oncol.* **36** (2018) 92.e17–92.e24.
- [3.440] KOPKA, K., BENEŠOVÁ, M., BAŘINKA, C., HABERKORN, U., BABICH, J., Glu-Ureido-based inhibitors of prostate-specific membrane antigen: Lessons learned during the development of a novel class of low-molecular-weight theranostic radiotracers, *J. Nucl. Med.* **58** Suppl. 2 (2017) 17S–26S.
- [3.441] HILLIER, S.M., et al., Preclinical evaluation of novel glutamate-urea-lysine analogues that target prostate-specific membrane antigen as molecular imaging pharmaceuticals for prostate cancer, *Cancer Res.* **69** (2009) 6932–6940.
- [3.442] HILLIER, S.M., et al., ^{99m}Tc -labeled small-molecule inhibitors of prostate-specific membrane antigen for molecular imaging of prostate cancer, *J. Nucl. Med.* **54** (2013) 1369–1376.
- [3.443] SANTOS-CUEVAS, C., et al., ^{99m}Tc -labeled PSMA inhibitor: Biokinetics and radiation dosimetry in healthy subjects and imaging of prostate cancer tumors in patients, *Nucl. Med. Biol.* **52** (2017) 1–6.
- [3.444] FRIGERIO, B., et al., Full preclinical validation of the ^{123}I -labeled anti-PSMA antibody fragment ScFvD2B for prostate cancer imaging, *Oncotarget* **8** (2017) 10919–10930.
- [3.445] ROBU, S., et al., Preclinical evaluation and first patient application of ^{99m}Tc -PSMA-I&S for SPECT imaging and radioguided surgery in prostate cancer, *J. Nucl. Med.* **58** (2017) 235–242.
- [3.446] GOFFIN, K.E., et al., Phase 2 study of ^{99m}Tc -Trofolostat SPECT-CT to identify and localize prostate cancer in intermediate- and high-risk patients undergoing radical prostatectomy and extended pelvic LN dissection, *J. Nucl. Med.* **58** (2017) 1408–1413.
- [3.447] SCHMIDKONZ, C., et al., SPECT-CT with the PSMA ligand ^{99m}Tc -MIP-1404 for whole-body primary staging of patients with prostate cancer, *Clin. Nucl. Med.* **43** (2018) 225–231.
- [3.448] SU, H.-C., et al., The value of ^{99m}Tc -PSMA SPECT-CT-guided surgery for identifying and locating lymph node metastasis in prostate cancer patients, *Ann. Surg. Oncol.* **26** (2019) 653–659.
- [3.449] REINFELDER, J., et al., First experience with SPECT-CT using a ^{99m}Tc -labeled inhibitor for prostate-specific membrane antigen in patients with biochemical recurrence of prostate cancer, *Clin. Nucl. Med.* **42** (2017) 26–33.

- [3.450] SU, H.-C., et al., Evaluation of ^{99m}Tc -labeled PSMA-SPECT-CT imaging in prostate cancer patients who have undergone biochemical relapse, *Asian J. Androl.* **19** (2017) 267–271.
- [3.451] SCHMIDKONZ, C., et al., ^{99m}Tc -MIP-1404-SPECT-CT for the detection of PSMA-positive lesions in 225 patients with biochemical recurrence of prostate cancer, *Prostate* **78** (2018) 54–63.
- [3.452] LIU, C., et al., Relationship between PSA kinetics and Tc- 99m HYNIC PSMA SPECT-CT detection rates of biochemical recurrence in patients with prostate cancer after radical prostatectomy, *Prostate* **78** (2018) 1215–1221.
- [3.453] SCHMIDKONZ, C., et al., PSMA SPECT-CT with ^{99m}Tc -MIP-1404 in biochemical recurrence of prostate cancer: Predictive factors and efficacy for the detection of PSMA-positive lesions at low and very-low PSA levels, *Ann. Nucl. Med.* **33** (2019) 891–898.
- [3.454] LAWAL, I.O., et al., Diagnostic sensitivity of Tc- 99m HYNIC PSMA SPECT-CT in prostate carcinoma: A comparative analysis with Ga-68 PSMA PET-CT, *Prostate* **77** (2017) 1205–1212.
- [3.455] GARCÍA-PEREZ, F.O., et al., Head to head comparison performance of ^{99m}Tc -EDDA/HYNIC-iPSMA SPECT-CT and ^{68}Ga -PSMA-11 PET-CT a prospective study in biochemical recurrence prostate cancer patients, *Am. J. Nucl. Med. Mol. Imaging* **8** (2018) 332–340.
- [3.456] RATHKE, H., et al., Intra-individual comparison of Tc- 99m -MDP bone scan and the PSMA-ligand Tc- 99m -MIP-1427 in patients with osseous metastasized prostate cancer, *J. Nucl. Med.* **59** (2018) 1373–1379.
- [3.457] SCHMIDKONZ, C., et al., Assessment of treatment response by ^{99m}Tc -MIP-1404 SPECT-CT: A pilot study in patients with metastatic prostate cancer, *Clin. Nucl. Med.* **43** (2018) e250–e258.
- [3.458] SCHMIDKONZ, C., et al., ^{99m}Tc -MIP-1404 SPECT-CT for patients with metastatic prostate cancer: Interobserver and intraobserver variability in treatment-related longitudinal tracer uptake assessments of prostate-specific membrane antigen-positive lesions, *Clin. Nucl. Med.* **45** (2020) 105–112.
- [3.459] VAN LEEUWEN, F.W.B., et al., Minimal-invasive robot-assisted image-guided resection of prostate-specific membrane antigen-positive lymph nodes in recurrent prostate cancer, *Clin. Nucl. Med.* **44** (2019) 580–581.
- [3.460] VIOLET, J., et al., Dosimetry of ^{177}Lu -PSMA-617 in metastatic castration-resistant prostate cancer: Correlations between pretherapeutic imaging and whole-body tumor dosimetry with treatment outcomes, *J. Nucl. Med.* **60** (2019) 517–523.
- [3.461] JACKSON, P.A., HOFMAN, M.S., HICKS, R.J., SCALZO, M., VIOLET, J., Radiation dosimetry in ^{177}Lu -PSMA-617 therapy using a single posttreatment SPECT-CT scan: A novel methodology to generate time- and tissue-specific dose factors, *J. Nucl. Med.* **61** (2020) 1030–1036.
- [3.462] GÖTZ, T.I., et al., Particle filter de-noising of voxel-specific time-activity-curves in personalized ^{177}Lu therapy, *Z. Med. Phys.* **30** (2020) 116–134.

- [3.463] NOVIKOV, S.N., et al., Axillary lymph node staging in breast cancer: Clinical value of single photon emission computed tomography–computed tomography (SPECT-CT) with ^{99m}Tc -methoxyisobutylisonitrile, *Ann. Nucl. Med.* **29** (2015) 177–183.
- [3.464] KURATA, S., et al., Assessment of ^{99m}Tc -MIBI SPECT/(CT) to monitor multidrug resistance-related proteins and apoptosis-related proteins in patients with ovarian cancer: A preliminary study, *Ann. Nucl. Med.* **29** (2015) 643–649.
- [3.465] COLLARINO, A., et al., Experimental validation of absolute SPECT–CT quantification for response monitoring in breast cancer, *Med. Phys.* **45** (2018) 2143–2153.
- [3.466] DENECKE, T., et al., Planning transarterial radioembolization of colorectal liver metastases with Yttrium 90 microspheres: Evaluation of a sequential diagnostic approach using radiologic and nuclear medicine imaging techniques, *Eur. Radiol.* **18** (2008) 892–902.
- [3.467] HAMAMI, M.E., et al., SPECT–CT with ^{99m}Tc -MAA in radioembolization with ^{90}Y microspheres in patients with hepatocellular cancer, *J. Nucl. Med.* **50** (2009) 688–692.
- [3.468] LAUENSTEIN, T.C., et al., Radioembolization of hepatic tumors: Flow redistribution after the occlusion of intrahepatic arteries, *RöFo* **183** (2011) 1058–1064.
- [3.469] AHMADZADEHFAR, H., et al., The significance of bremsstrahlung SPECT–CT after yttrium-90 radioembolization treatment in the prediction of extrahepatic side effects, *Eur. J. Nucl. Med. Mol. Imaging* **39** (2012) 309–315.
- [3.470] BURGMANS, M.C., et al., Computed tomography hepatic arteriography has a hepatic falciform artery detection rate that is much higher than that of digital subtraction angiography and ^{99m}Tc -MAA SPECT–CT: Implications for planning ^{90}Y radioembolization? *Eur. J. Radiol.* **81** (2012) 3979–3984.
- [3.471] PADIA, S.A., et al., Comparison of positron emission tomography and bremsstrahlung imaging to detect particle distribution in patients undergoing yttrium-90 radioembolization for large hepatocellular carcinomas or associated portal vein thrombosis, *J. Vasc. Interv. Radiol.* **24** (2013) 1147–1153.
- [3.472] ZADE, A.A., et al., ^{90}Y microsphere therapy: Does ^{90}Y PET–CT imaging obviate the need for ^{90}Y Bremsstrahlung SPECT–CT imaging? *Nucl. Med. Commun.* **34** (2013) 1090–1096.
- [3.473] VAN DEN HOVEN, A.F., et al., Identifying aberrant hepatic arteries prior to intra-arterial radioembolization, *Cardiovasc. Interv. Radiol.* **37** (2014) 1482–1493.
- [3.474] GATES, V.L., SINGH, N., LEWANDOWSKI, R.J., SPIES, S., SALEM, R., Intraarterial hepatic SPECT–CT imaging using ^{99m}Tc -macroaggregated albumin in preparation for radioembolization, *J. Nucl. Med.* **56** (2015) 1157–1162.
- [3.475] ILHAN, H., et al., Systematic evaluation of tumoral ^{99m}Tc -MAA uptake using SPECT and SPECT–CT in 502 patients before ^{90}Y radioembolization, *J. Nucl. Med.* **56** (2015) 333–338.
- [3.476] SPREAFICO, C., et al., Intrahepatic flow redistribution in patients treated with radioembolization, *Cardiovasc. Interv. Radiol.* **38** (2015) 322–328.

- [3.477] THEYSOHN, J.M., et al., Radioembolization with Y-90 glass microspheres: Do we really need SPECT-CT to identify extrahepatic shunts? *PLoS One* **10** (2015) e0137587.
- [3.478] ERXLEBEN, C., et al., Hepatopulmonary shunting after surgical, interventional and systemic therapy in patients with liver malignancies scheduled for radioembolization, *Acta Radiol.* **57** (2016) 908–913.
- [3.479] YUE, J., et al., Comparison of quantitative Y-90 SPECT and non-time-of-flight PET imaging in post-therapy radioembolization of liver cancer, *Med. Phys.* **43** (2016) 5779.
- [3.480] BORRELLI, P., et al., Contribution of SPECT–CT for sentinel node localization in patients with ipsilateral breast cancer relapse, *Eur. J. Nucl. Med. Mol. Imaging* **44** (2017) 630–637.
- [3.481] DITTMANN, H., et al., A prospective study of quantitative SPECT–CT for evaluation of lung shunt fraction prior to SIRT of liver tumors, *J. Nucl. Med.* **59** (2018) 1366–1372.
- [3.482] FEINGOLD, D.L., et al., Does hemodynamic instability predict positive technetium-labeled red blood cell scintigraphy in patients with acute lower gastrointestinal bleeding? A review of 50 patients, *Dis. Colon Rectum* **48** (2005) 1001–1004.
- [3.483] SCHILLACI, O., et al., SPECT–CT with a hybrid imaging system in the study of lower gastrointestinal bleeding with technetium-99m red blood cells, *Q. J. Nucl. Med. Mol. Imaging* **53** (2009) 281–289.
- [3.484] WANG, Z.G., et al., Technological value of SPECT–CT fusion imaging for the diagnosis of lower gastrointestinal bleeding, *Genet. Mol. Res.* **14** (2015) 14947–14955.
- [3.485] OTOMI, Y., et al., The diagnostic ability of SPECT–CT fusion imaging for gastrointestinal bleeding: A retrospective study, *BMC Gastroenterol.* **18** (2018) 183.
- [3.486] DAM, H.Q., et al., The SNMMI procedure standard/EANM practice guideline for gastrointestinal bleeding scintigraphy 2.0, *J. Nucl. Med. Technol.* **42** (2014) 308–317.
- [3.487] GRADY, E., Gastrointestinal bleeding scintigraphy in the early 21st century, *J. Nucl. Med.* **57** (2016) 252–259.
- [3.488] SPOTTSWOOD, S.E., et al., SNMMI and EANM practice guideline for Meckel diverticulum scintigraphy 2.0, *J. Nucl. Med. Technol.* **42** (2014) 163–169.
- [3.489] GELFAND, M.J., LEMEN, L.C., PET–CT and SPECT–CT dosimetry in children: The challenge to the pediatric imager, *Semin. Nucl. Med.* **37** (2007) 391–398.
- [3.490] DEMIRCI, E., HAS SIMSEK, D., KABASAKAL, L., MÜLAZIMOĞLU, M., Abdominal splenosis mimicking peritoneal metastasis in prostate-specific membrane antigen PET–CT, confirmed with selective spleen SPECT–CT, *Clin. Nucl. Med.* **42** (2017) e504–e505.
- [3.491] BUDAK, E., ORAL, A., YAZICI, B., GULER, E., OMUR, O., Splenosis of the liver capsule, *Clin. Nucl. Med.* **43** (2018) e460–e462.
- [3.492] ANDERSEN, J.B., MORTENSEN, J., BECH, B.H., HØJGAARD, L., BORGWARDT, L., First experiences from Copenhagen with paediatric single photon emission computed tomography/computed tomography, *Nucl. Med. Commun.* **32** (2011) 356–362.

- [3.493] MATTHAY, K.K., et al., Criteria for evaluation of disease extent by ¹²³I-metaiodobenzylguanidine scans in neuroblastoma: A report for the International Neuroblastoma Risk Group (INRG) Task Force, *Br. J. Cancer* **102** (2010) 1319–1326.
- [3.494] LIU, B., SERVAES, S., ZHUANG, H., SPECT–CT MIBG imaging is crucial in the follow-up of the patients with high-risk neuroblastoma, *Clin. Nucl. Med.* **43** (2018) 232–238.
- [3.495] ČERNÝ, I., PRÁŠEK, J., KAŠPÁRKOVÁ, H., Superiority of SPECT–CT over planar ¹²³I-MIBG images in neuroblastoma patients with impact on Curie and SIOPEN score values, *Nuklearmedizin* **55** (2016) 151–157.
- [3.496] FUKUOKA, M., TAKI, J., MOCHIZUKI, T., KINUYA, S., Comparison of diagnostic value of I-123 MIBG and high-dose I-131 MIBG scintigraphy including incremental value of SPECT–CT over planar image in patients with malignant pheochromocytoma/paraganglioma and neuroblastoma, *Clin. Nucl. Med.* **36** (2011) 1–7.
- [3.497] FRANZIUS, C., et al., Whole-body PET–CT with ¹¹C-meta-hydroxyephedrine in tumors of the sympathetic nervous system: Feasibility study and comparison with ¹²³I-MIBG SPECT–CT, *J. Nucl. Med.* **47** (2006) 1635–1642.
- [3.498] PICCARDO, A., et al., Diagnosis, treatment response, and prognosis: The role of ¹⁸F-DOPA PET–CT in children affected by neuroblastoma in comparison with ¹²³I-mIBG scan: The first prospective study, *J. Nucl. Med.* **61** (2020) 367–374.
- [3.499] ISHIGUCHI, H., et al., Diagnostic performance of ¹⁸F-FDG PET–CT and whole-body diffusion-weighted imaging with background body suppression (DWIBS) in detection of lymph node and bone metastases from pediatric neuroblastoma, *Ann. Nucl. Med.* **32** (2018) 348–362.
- [3.500] WAGNER, L.M., et al., Detection of lymph node metastases in pediatric and adolescent/young adult sarcoma: Sentinel lymph node biopsy versus fludeoxyglucose positron emission tomography imaging — a prospective trial, *Cancer* **123** (2017) 155–160.
- [3.501] KUO, P.H., et al., Whole-body lymphangioscintigraphy and SPECT–CT in children with lymphatic complications after surgery for complex congenital heart disease, *Lymphology* **52** (2019) 157–165.
- [3.502] KIM, H.-Y., GELFAND, M.J., SHARP, S.E., SPECT–CT imaging in children with papillary thyroid carcinoma, *Pediatr. Radiol.* **41** (2011) 1008–1012.
- [3.503] LIU, L., HUANG, F., LIU, B., HUANG, R., Detection of distant metastasis at the time of ablation in children with differentiated thyroid cancer: The value of pre-ablation stimulated thyroglobulin, *J. Pediatr. Endocrinol. Metab.* **31** (2018) 751–756.
- [3.504] BAE, S., KANG, Y., SONG, Y.S., LEE, W.W., K-SPECT GROUP, Maximum standardized uptake value of foot SPECT–CT using Tc-99m HDP in patients with accessory navicular bone as a predictor of surgical treatment, *Medicine* **98** (2019) e14022.
- [3.505] YAMANE, T., KUJI, I., SETO, A., MATSUNARI, I., Quantification of osteoblastic activity in epiphyseal growth plates by quantitative bone SPECT–CT, *Skelet. Radiol.* **47** (2018) 805–810.

- [3.506] LEHMAN, V.T., MURPHY, R.C., MAUS, T.P., ^{99m}Tc-MDP SPECT–CT of the spine and sacrum at a multispecialty institution: Clinical use, findings, and impact on patient management, *Nucl. Med. Commun.* **34** (2013) 1097–1106.
- [3.507] BROWNE, L.P., et al., Optimal imaging strategy for community-acquired *Staphylococcus aureus* musculoskeletal infections in children, *Pediatr. Radiol.* **38** (2008) 841–847.
- [3.508] SHARMA, P., et al., ^{99m}Tc-Methylene diphosphonate SPECT–CT as the one-stop imaging modality for the diagnosis of osteoid osteoma, *Nucl. Med. Commun.* **35** (2014) 876–883.
- [3.509] SHARMA, P., et al., SPECT-CT in routine clinical practice: Increase in patient radiation dose compared with SPECT alone, *Nucl. Med. Commun.* **33** (2012) 926–932.
- [3.510] LASSMANN, M., TREVES, S.T., Paediatric radiopharmaceutical administration: Harmonization of the 2007 EANM paediatric dosage card (version 1.5.2008) and the 2010 North American consensus guidelines, *Eur. J. Nucl. Med. Mol. Imaging* **41** (2014) 1036–1041.
- [3.511] HOU, X., BIRKENFELD, B., PIWOWARSKA-BILSKA, H., CELLER, A., Patient-specific dosimetry of ^{99m}Tc-HYNIC-Tyr³-Octreotide in children, *Eur. J. Nucl. Med. Mol. Imaging Phys.* **4** (2017) 24.

4. INCIDENTAL FINDINGS ON CT

As a consequence of the increase in the use of hybrid imaging, the authors came across several significant incidental and unexpected radiological findings while reviewing these studies. An incidental finding can be defined as an unsuspected finding that is not related to the clinical indication for performing the diagnostic test [4.1]. The reporting clinician should be aware of the incidental findings seen in the CT component of the study. They should be categorized appropriately and communicated to the referring clinicians. In general, incidental findings are categorized as major, moderate and minor. Major incidental findings must be investigated further, and the clinical team should be informed accordingly. Moderate incidental findings may often require further investigation. Minor incidental findings rarely require further investigation and are less likely, or unlikely, to have an adverse outcome. The management of incidental findings is extensively reported in papers published by the United Kingdom’s Royal College of Radiologists and the American College of Radiology, among others [4.1–4.14]. Yap et al. reviewed 2447 SPECT–CT studies and reported the overall prevalence of potentially significant incidental and unexpected findings to be 8.7% [4.12] (Table 4.1).

TABLE 4.1. INCIDENTAL FINDINGS ON CT
(adapted from Refs [4.1–4.14])

Minor	Moderate	Major
<i>Head and neck region</i>		
Parathyroid adenoma	Thyroid incidentalomas	Brain masses ^a Orbital mass Cervical masses, including parotid masses and ear, nose and throat masses
<i>Chest region</i>		
Calcified pleural plaques	Emphysema	Breast nodule
Left-sided inferior vena cava	Bronchiectasis	Pneumothorax
Calcified pulmonary nodule	Cardiomegaly	Pulmonary embolism ^a
	Pericardial effusion	Solid pulmonary mass
	Pleural effusion	
	Pulmonary parenchymal opacity	
<i>Abdomen</i>		
Gallstones in gallbladder	Gallstone in common bile duct	Solid liver mass
Hepatic cysts	Pancreatic cystic lesion	Solid renal mass
Diverticulosis	Hepato-splenomegaly	Gall bladder mass
Renal calculus	Abdominal wall hernia	Bilateral small kidneys
Renal cysts	Absent kidney	Gastric mass
Appendicolith	Adrenal mass	Colon or small bowel mass
Fatty liver	Bowel inflammation	Oesophageal mass
Renal atrophy	Irregular nodular margin liver	Solid pancreatic mass
Umbilical hernia	Air in the biliary tree	Indeterminate liver, splenic and pancreatic lesions
Hiatus hernia	Adrenal adenoma	Ascites
	Adrenal mass with benign appearance	Indeterminate retroperitoneal masses
	Hydronephrosis	Complex renal cyst
		Atypical adrenal mass
<i>Pelvic region</i>		

TABLE 4.1. INCIDENTAL FINDINGS ON CT
(adapted from Refs [4.1–4.14]) (cont.)

Minor	Moderate	Major
Lipoma	Uterine enlargement	Undescended testis
Bladder diverticulum	Pelvic kidney	Ovarian cyst >5 cm
Simple ovarian cyst	Ureteric calculus	Uterine mass
Uterine fibroids	Scrotal hydrocoele	Ovarian solid or mixed mass
Bladder stone	Prostate enlargement	Bladder mass
Uterine calcifications		
Bartholin's cysts		
<i>Vascular system</i>		
Left-sided vena cava	Pulmonary artery dilatation	Deep vein thrombosis ^a
Retroaortic left renal vein	Signs of portal venous hypertension	Aortic aneurysm >5 cm
	Atherosclerosis	Aortic dissection ^a
	Coronary artery calcification	Vascular stenosis ^a
<i>Musculoskeletal system</i>		
Muscle atrophy	n.a. ^b	Vertebral body destruction
Bone infarct		Lytic bone lesions
Degenerative spine changes		Indeterminate sclerotic bone lesion
<i>Reticuloendothelial system</i>		
n.a. ^b	Splenomegaly	Cervical, thoracic and abdominal lymph node >1 cm

^a Particularly evident in contrast-enhanced CT.

^b n.a.: not applicable.

REFERENCES TO SECTION 4

- [4.1] MUNDEN, R.F., et al., Managing incidental findings on thoracic CT: Mediastinal and cardiovascular findings. A white paper of the ACR Incidental Findings Committee, *J. Am. Coll. Radiol.* **15** (2018) 1087–1096.
- [4.2] HUNOLD, P., SCHMERMUND, A., SEIBEL, R.M., GRÖNEMEYER, D.H., ERBEL, R., Prevalence and clinical significance of accidental findings in electron-beam tomographic scans for coronary artery calcification, *Eur. Heart J.* **22** (2001) 1748–1758.

- [4.3] OSMAN, M.M., COHADE, C., FISHMAN, E.K., WAHL, R.L., Clinically significant incidental findings on the unenhanced CT portion of PET–CT studies: Frequency in 250 patients, *J. Nucl. Med.* **46** (2005) 1352–1355.
- [4.4] BRUZZI, J.F., et al., Incidental findings on integrated PET–CT that do not accumulate ¹⁸F-FDG, *Am. J. Roentgenol.* **187** (2006) 1116–1123.
- [4.5] GOETZE, S., PANNU, H.K., WAHL, R.L., Clinically significant abnormal findings on the ‘nondiagnostic’ CT portion of low-amperage-CT attenuation-corrected myocardial perfusion SPECT–CT studies, *J. Nucl. Med.* **47** (2006) 1312–1318.
- [4.6] BEATTY, J.S., et al., Incidental PET–CT findings in the cancer patient: How should they be managed? *Surgery* **146** (2009) 274–281.
- [4.7] HUSMANN, L., et al., Prevalence of noncardiac findings on low dose 64-slice computed tomography used for attenuation correction in myocardial perfusion imaging with SPECT, *Int. J. Cardiovasc. Imaging* **25** (2009) 859–865.
- [4.8] BERLAND, L.L., et al., Managing incidental findings on abdominal CT: White paper of the ACR incidental findings committee, *J. Amer. Coll. Radiol.* **7** (2010) 754–773.
- [4.9] LUMBRERAS, B., DONAT, L., HERNÁNDEZ-AGUADO, I., Incidental findings in imaging diagnostic tests: A systematic review, *Br. J. Radiol.* **83** (2010) 276–289.
- [4.10] CHOPRA, A., FORD, A., DE NORONHA, R., MATTHEWS, S., Incidental findings on positron emission tomography/CT scans performed in the investigation of lung cancer, *Br. J. Radiol.* **85** (2012) e229–e237.
- [4.11] FRANK, L., QUINT, L.E., Chest CT incidentalomas: Thyroid lesions, enlarged mediastinal lymph nodes, and lung nodules, *Cancer Imaging* **12** (2012) 41–48.
- [4.12] YAP, K.K., et al., Prevalence of incidental or unexpected findings on low-dose CT performed during routine SPECT–CT nuclear medicine studies, *J. Med. Imaging Radiat. Oncol.* **59** (2015) 26–33.
- [4.13] COWARD, J., NIGHTINGALE, J., HOGG, P., The clinical dilemma of incidental findings on the low-resolution CT images from SPECT–CT MPI studies, *J. Nucl. Med. Technol.* **44** (2016) 167–172.
- [4.14] PORT, S., Incidental findings on hybrid SPECT-CT and PET-CT scanners: Is it time for new training and reporting guidelines? *J. Nucl. Cardiol.* **26** (2019) 1694–1696.

ABBREVIATIONS

CAC	coronary artery calcification
CAD	coronary artery disease
CCTA	cardiac computed tomography angiography
CIED	cardiac implantable electronic device
CT	computed tomography
CTPA	computed tomography pulmonary angiography
DOPA	dihydroxyphenylalanine
FDG	fluorodeoxyglucose
GEP-NET	gastroenteropancreatic neuroendocrine tumour
GI	gastrointestinal
HPT	hyperparathyroidism
HU	Hounsfield unit
MDP	methylene diphosphonate
mIBG	metaiodobenzylguanidine
MPI	myocardial perfusion imaging
NEN	neuroendocrine neoplasm
NPV	negative predictive value
PET	positron emission tomography
PPV	positive predictive value
PSA	prostate-specific antigen
PSMA	prostate-specific membrane antigen
PTA	parathyroid adenoma
Q	lung perfusion scintigraphy
SLN	sentinel lymph node
SPECT	single-photon emission computed tomography
SSA	somatostatin analogue
SUV	standardized uptake value
TKA	total knee arthroplasty
V/Q	ventilation and perfusion scintigraphy
WBS	whole body scintigraphy

CONTRIBUTORS TO DRAFTING AND REVIEW

Angel Quenguan, P.	International Atomic Energy Agency
Biassoni, L.	Great Ormond Street Hospital for Children, United Kingdom
Brink, A.	Red Cross War Memorial Children's Hospital/ University of Cape Town, South Africa
Bucheli Pabon, J.C.	International Atomic Energy Agency
De Palma, D.	Circolo Hospital, ASST-Settelaghi, Italy
Dondi, M.	International Atomic Energy Agency
El-Haj, N.	International Atomic Energy Agency
Estrada Lobato, E.	International Atomic Energy Agency
Giammarile, F.	International Atomic Energy Agency
Gnanasegaran, G.	Royal Free Hospital, United Kingdom
Israel, O.	Rappaport Faculty of Medicine, Israel
Knoll, P.	International Atomic Energy Agency
Kuwert, T.	Friedrich-Alexander University Erlangen–Nürnberg, Germany
Lafougère, C.	University of Tübingen, Germany
Mariani, G.	University of Pisa, Italy
Massalha, S.	University of Ottawa Heart Institute, Canada
Nadel, H.R.	Lucile Packard Children's Hospital, Stanford University, United States of America
Orellana, P.	International Atomic Energy Agency
Paez, D.	International Atomic Energy Agency
Pellet, O.	International Atomic Energy Agency



IAEA

International Atomic Energy Agency

No. 26

ORDERING LOCALLY

IAEA priced publications may be purchased from the sources listed below or from major local booksellers.

Orders for unpriced publications should be made directly to the IAEA. The contact details are given at the end of this list.

NORTH AMERICA

Bernan / Rowman & Littlefield

15250 NBN Way, Blue Ridge Summit, PA 17214, USA

Telephone: +1 800 462 6420 • Fax: +1 800 338 4550

Email: orders@rowman.com • Web site: www.rowman.com/bernan

REST OF WORLD

Please contact your preferred local supplier, or our lead distributor:

Eurospan Group

Gray's Inn House

127 Clerkenwell Road

London EC1R 5DB

United Kingdom

Trade orders and enquiries:

Telephone: +44 (0)176 760 4972 • Fax: +44 (0)176 760 1640

Email: eurospan@turpin-distribution.com

Individual orders:

www.eurospanbookstore.com/iaea

For further information:

Telephone: +44 (0)207 240 0856 • Fax: +44 (0)207 379 0609

Email: info@eurospangroup.com • Web site: www.eurospangroup.com

Orders for both priced and unpriced publications may be addressed directly to:

Marketing and Sales Unit

International Atomic Energy Agency

Vienna International Centre, PO Box 100, 1400 Vienna, Austria

Telephone: +43 1 2600 22529 or 22530 • Fax: +43 1 26007 22529

Email: sales.publications@iaea.org • Web site: www.iaea.org/publications

Single photon emission computed tomography (SPECT) has been used in routine diagnostic applications and in research since the 1980s. In the following decades, as the clinical application of hybrid imaging has grown, SPECT-computed tomography (SPECT-CT) has demonstrated improved patient management and become fully integrated in the routine diagnostic approach to a variety of clinical indications, including both oncologic and non-oncologic diseases. This IAEA Human Health Series publication presents a review of the published data from recent applications of SPECT-CT across nine different clinical scenarios, including oncology, neurology, orthopaedics, endocrinology and cardiology, to demonstrate the variety of hybrid imaging in nuclear medicine and support decision making when allocating resources in the healthcare system. It provides a relevant source of information for nuclear medicine physicians, radiologists and clinical practitioners.

IAEA HUMAN HEALTH SERIES

INTERNATIONAL ATOMIC ENERGY AGENCY

VIENNA

ISBN 978-92-0-111522-5

ISSN 2075-3772